Spring 5-4-2019

Development of Local Drug Delivery Systems for Periodontal Disease

Yosif Hassan Almoshari
University of Nebraska Medical Center

DEVELOPMENT OF LOCAL DRUG DELIVERY SYSTEMS FOR PERIODONTAL DISEASE

by

Yosif H, Almoshari

A DISSERTATION

Presented to the Faculty of

the University of Nebraska Graduate College

in Partial Fulfillment of the Requirements

for the Degree of Doctor of Philosophy

Department of Pharmaceutical Sciences

Under the Supervision of Professor Dong Wang

University of Nebraska Medical Center

Omaha, Nebraska

May, 2019

Supervisory Committee:

Dong Wang, Ph.D.

Richard A. Reinhardt, D.D.S., Ph.D.

Geoffrey M. Thiele, Ph.D.

Yazen Alnouti, Ph.D.

(وَقُلْ رَبِّ زِدْنِي عِلْمًا)

هذه الرسالة التي منحتني درجة الدكتوراه في العلوم الصيدلانية

بتأريخ 12 شعبان 1440 الموافق 18 أبريل 2019

أُهديها بِكلِ إجلالٍ واشتياق إلى أُمي و أُبي، وبِكل مودةٍ وحُب إلى زوجتي وطفلي، وبِكل احترامٍ وتقدير إلى إِخوتي وأَخواتي، وبِكل اعتزاز وفخر إلى موطِني بلادِ الحرمين

This dissertation is dedicated with all love and gratitude to my family

'I will love you forever'

TABLE OF CONTENTS

ACKNOWLEDGMENTS

I would like first to acknowledge my mentor, Dr. Dong Wang, for his dedicated guidance and support during my journey towards this degree. Despite the challenges students may face through this journey, he has always been kind, reasonable and supportive, even in my personal life. Thanks for the inspiration, critical thinking learning and positive criticism that inspire me to be a good future academic scientist. Truly, he is a scientist whom I am glad and proud of being his mentee.

I would also like to thank my committee members, Dr. Richard Reinhardt, Dr. Geoffrey Thiele, and Dr. Yazen Alnouti for their time and mentoring throughout my study. I would also like to thank people who helped me here at the University of Nebraska Medical Center. My colleagues in Dr. Wang's lab, especially Dr. Jia and Dr. Ren for their help in the chemical syntheses. Dr. Joseph Vetro's lab for using their instruments and Dr. Subodh Lele for histological evaluations. I also would thank Jazan University for providing a scholarship and financial support to complete my graduate study.

Finally, I would like to express my sincere gratitude to my family for continued love, encouragement, and support throughout my abroad study. My parents, wife, brothers, and sisters have always believed in me to accomplish what I have set out to achieve. I am grateful to my wife for being a supportive, patient, and loving partner. Without her, my life here in the United States would not be this easy. My acknowledgment would be incomplete without thanking my baby-son who has made my life wonderful and provided nice and fun moments every day.

ABSTRACT

DEVELOPMENT OF LOCAL DRUG DELIVERY SYSTEMS FOR THE TREATMENT OF PERIODONTAL DISEASE

Yosif H. Almoshari, Ph.D.

University of Nebraska Medical Center, 2019

Supervisor: Dong Wang, Ph.D.

Periodontitis is an inflammatory disease induced by complex interactions between the host immune system and pathogens that affect the integrity of teeth-supporting tissues. To prevent disease progression and thus preserve the alveolar bone structure, simultaneous anti-inflammatory and osteogenic intervention is essential. Hence, simvastatin (SIM) and a glycogen synthase kinase 3 beta inhibitor (BIO) were selected as anti-inflammatory and osteogenic agents.

First, SIM is a HMG-CoA reductase inhibitor widely prescribed for hypercholesterolemia. It has been reported to ameliorate inflammation and promote osteogenesis. Its clinical applications on these potential secondary indications, however, have been hampered by its lack of osteotropicity and poor water solubility. To address this challenge, we proposed to design and evaluate the therapeutic efficacy of a novel simvastatin prodrug with better water solubility and bone affinity. The prodrug (SIM-PPi) was synthesized by directly conjugating a SIM trimer to a pyrophosphate (PPi). It was characterized and evaluated *in vitro* for its water solubility, osteotropicity, toxicity, anti-inflammatory, and osteoinductive properties. It was then tested for anti-inflammatory and osteoinductive properties

in vivo by three weekly injections into gingiva of a ligature-induced experimental periodontitis rat model**.** *In vitro* studies showed that SIM-PPi has greatly improved water-solubility of SIM and shows strong binding to hydroxyapatite (HA). In macrophage culture, SIM-PPi inhibited LPS-induced pro-inflammatory cytokines (IL-1β, IL-6). In osteoblast culture, it was found to significantly increase alkaline phosphatase (ALP) activity with accelerated mineral deposition, confirming the osteogenic potential of SIM-PPi. When tested *in vivo* on an experimental periodontal bone-loss model, SIM-PPi exhibited a superior prophylactic effect compared to dose equivalent SIM in reducing inflammatory cells and in preserving the alveolar bone structure, as shown in the histological and micro-CT data.

Second, a glycogen synthase kinase 3 beta inhibitor (BIO) is a potent inflammation modulator and osteogenic agent. However, its lack of osteotropicity, poor water solubility, and potential long-term side effects have hampered its clinical applications. To address these limitations, pyrophosphorylated Pluronic F127 was synthesized to prepare a novel, injectable and thermosensitive hydrogel (PF127) that could effectively release BIO to exert its therapeutic effects locally. Comparing to F127 hydrogel, PF127 hydrogels exhibited strong binding to hydroxyapatite (HA) discs as a function of PPi content. Additionally, BIO's solubility in PF127 solution compared to F127 was greatly improved and proportionally to the polymer concentration. When tested *in vivo* on an experimental periodontal bone-loss rat model, PF127-BIO hydrogel exhibited a superior prophylactic effect in preserving alveolar bone structure and preventing periodontal inflammation, as shown by the micro-CT and histological data, respectively.

Altogether, these two delivery strategies (SIM-PPi prodrug and PF127 hydrogel) with excellent bone binding may have the potential to be further developed for better clinical management of bone loss associated with periodontitis.

LIST OF FIGURES

LIST OF TABLES

LIST OF SCHEMES

LIST OF ABBREVIATIONS

ABC: Alveolar bone crest

ALP: Alkaline phosphatase

BMP-2: Bone morphogenetic protein-2

CEJ: Cementoenamel junction

EDTA: Ethylenediaminetetraacetic acid

GCF: Gingival crevicular fluid

HA: Hydroxyapatite

HMG-CoA: 3-Hydroxy-3-methyl-glutaryl-coenzyme A

LPS: Lipopolysaccharide

M1: First molar

M2: Second molar

MCP-1: Monocyte chemoattractant protein-1

MMPs: Matrix metalloproteinases

MTT: 3-(4,5-Dimethyl- thiazol-2yl)-2,5- diphenyltetrazoliumbromide

OPG: Osteoprotegerin

PPi: Pyrophosphate

RANK: Receptor activator of nuclear factor-kappa B

RANKL: Receptor activator of nuclear factor-kappa B ligand

ROI: Region of interest

SIM: Simvastatin

SIM-PPi: Simvastatin-pyrophosphate

Tb.N: Trabecular number

Tb.Sp: Trabecular spacing or separation

Tb.Th: Trabecular thickness

μ-CT: Micro-computed tomography

SRP: Scaling and root planning

PD: Probing depth

CAL: Clinical attachment level

ONJ: Osteonecrosis of the jaw

COX-1: Cyclooxygenase-1

COX-2: Cyclooxygenase-2

PGE2: Prostaglandin E2

HPMC: Hydroxypropyl methylcellulose

PLGA: Poly(lactic-co-glycolic acid)

GTR: Guided Tissue Regeneration

GSK3β: Glycogen synthase kinase 3 beta

PEO: Ethylene oxide

PPO: Polypropylene oxide

PF127: Pyrophosphorylated F127

CCK-8: Cell Counting Kit-8

LCGT: Lower critical gelation temperature

UCGT: Upper critical gelation temperature

CMC: Critical micellar concentration

CHAPTER 1.

INTRODUCTION

1.1 Periodontal diseases: definitions and classifications

Periodontal or gum diseases are a group of inflammatory disorders that compromise the supporting tissues of teeth and share common clinical manifestations. Based on the progressive nature of periodontal diseases, they can be divided into two main stages. First, gingivitis which is an early and non-destructive inflammatory disease that occurs when dental plaque accumulates around teeth and affects soft tissues surrounding the teeth. It causes gum swelling with a tendency to bleed upon slight provocation(1).

Second, periodontitis, the focus of this dissertation, is the destructive stage of periodontal disease that is associated with bleeding upon probing, increased probing depth, and may cause gingival recession. It can present in a localized or generalized form and characterize by periodontal inflammation of soft and hard tissues leading to periodontal attachment and alveolar bone loss(2). Periodontitis can be classified based on its progression into chronic and aggressive. The chronic form is most prevalent in adults and characterized by slow and progressive attachment and bone loss, while aggressive form results in rapid and severe attachment loss and bone destruction(3).

The disease afflicts 45.9 % of adults in the United States, confirming the high burden of periodontitis(4). Men are more likely to have gum disease than women, and teenagers rarely develop periodontitis, but they can develop gingivitis. Furthermore, the harmful health impact of periodontitis is not only limited to the local tissue destruction and alveolar bone resorption, but it may also affect systemic health by increasing the incidence risk of systemic inflammatory diseases, atherosclerosis, and cancer(5).

1.2 Risk factors

1.2.1 Smoking

It has been clinically established and demonstrated that a positive correlation between cigarette smoking and a higher risk for periodontal disease and alveolar bone loss is clear(6). Nicotine is one of the most pharmacologically active compounds in cigarette smoke. It has been shown to promote collagen breakdown and to inhibit gingival fibroblast growth and production of fibronectin and collagen *in vitro*, which are vital components to a healthy periodontium(7). Furthermore, it has been shown that when periodontal cells exposed to nicotine, the growth and protein content were decreased. Also, damaged cell membranes and atypical shapes were observed(8). Nicotine also has been evidenced to stimulate osteoclast differentiation and the resorption of calcium phosphate which may illustrate the severity of alveolar bone loss and refractory disease incidence

in smokers(9). Nicotine has also been shown to delay apoptosis which would allow for osteoclasts to persist the resorptive process(10).

1.2.2 Diabetes

Both type 1 and type 2 diabetes mellitus has been confirmed as a major risk factor for periodontal diseases(11–13). The risk of periodontitis is increased by approximately threefold in diabetics compared with non-diabetic individuals, and higher risk with poor glycemic control(14). When glucose is elevated in saliva, harmful bacteria grow in saliva and combine with food to form a soft plaque. In a study of 350 diabetic children (6–18 years old) vs 350 non-diabetic controls, the proportion of periodontal disease was greater in the children with diabetes (>20% vs 8% of sites, respectively)(15). The mechanisms by which diabetes affects periodontal health are complicated and still not solely defined. It has been proposed that upregulated pro-inflammatory cytokines, the formation of advanced glycation end-products (AGEs), and reactive oxygen species (ROS) are mechanisms that affect periodontal tissues. It has been reported that the level of pro-inflammatory cytokines PGE2 and IL-1β is higher in GCF of diabetics when compared to non-diabetics(16). AGEs bind to their receptor (RAGE), which is overexpressed in diabetics(17), and stimulate pro-inflammatory cytokines(18,19) and also induce osteoblast apoptosis(20). As oxidative stress is increased in diabetes, superoxide is increased in the mitochondria which lead to greater inflammation(17,21).

1.3 Pathogenesis

The disease initiates with gingivitis which is considered a significant risk factor for developing periodontitis, an irreversible immune reaction. It characterized by the loss of teeth-attached soft tissues and severe alveolar bone resorption which may lead to teeth loss. It has been reported that gingivitis does not always develop into periodontitis, indicating that in addition to plaque accumulation, host susceptibility is necessary to develop periodontitis(5). Once periodontitis is established, a pro-inflammatory cytokine cascade would initiate the destruction of soft and hard tissues. It is well reported that pro-inflammatory cytokines secreted by monocytes, lymphocytes, and some resident fibroblasts are responsible for the disease progression(22). Interleukin-1β (IL-1β) is considered one of the most potent inducers of bone resorption and is reported to be elevated in inflamed gingival tissues and gingival crevicular fluid (GCF) promoting connective tissues destruction through inducing matrix metalloproteinases (MMPs)(22). Subsequently, interleukin-6 (IL-6) is secreted in response to bone resorbing inducers including IL-1β(22). This inflammatory cascade promotes osteoclastogenesis by disrupting the balance between receptor activator of nuclear factor kappa-B ligand (RANKL) and its decoy receptor osteoprotegerin (OPG). The RANKL will be overexpressed to interact with receptor activator of nuclear factor kappa-B (RANK) receptor expressed on the osteoclast precursor cells, promoting osteoclast activation and initiating alveolar bone resorption(23,24).

1.4 Conventional treatment

1.4.1 Mechanical therapy

Scaling and root planing (SRP) is the non-surgically based therapy that is aimed at reducing the levels and proportions of periodontal pathogens and increasing the proportions of beneficial species(25). SRP is the nonsurgical-based therapy and performed to remove dental biofilm and calculus from periodontal pockets and smoothing the tooth root to eliminate bacterial toxins, thereby reducing the host inflammatory response. While scaling means the removal of plaque, calculus, and stains on the crown or root surface, root planing indicates the removal of cementum or surface dentin that is rough or contaminated with bacterial toxins. The beneficial outcomes following SRP therapy have been reported as decreases in the probing depth (PD) and increases in the clinical attachment level (CAL)(26).

1.4.2 Antimicrobial agents

Due to the difficulty in adequately reducing bacteria using mechanical debridement alone, antibiotics such as tetracyclines, doxycycline, metronidazole, amoxicillin, ciprofloxacin, and azithromycin may be used as adjunctive therapy(27). Systemic administration has been shown to be effective as adjunctive therapy in the treatment of chronic and aggressive periodontitis(28). These agents accumulate in connective tissue, saliva, and gingival crevicular fluid. Local delivery is another route of administration using different delivery systems by which drug is placed into the periodontal pocket and sustainably released over time aiming at affecting periodontal pathogens at the site of injection.

1.4.3 Host modulation agents

Host modulation is another approach for treating periodontal disease. This therapy aims at affecting the host's response to the bacterial challenge through ameliorating inflammation or inducing osteogenesis, thereby preventing the progression of the disease.

1.4.3.1 Non-steroidal anti-inflammatory agents (NSAIDs)

NSAIDs have been used as adjunctive therapy to SRP therapy. They work by inhibiting cyclooxygenase (COX-1 and/or COX-2) and thus prostaglandin synthesis, including PGE2. Non-selective NSAIDs (i.e. COX-1 and COX-2 inhibitors) that have been used in periodontal research include; aspirin, flurbiprofen, ibuprofen, naproxen, and piroxicam. Whereas, selective NSAIDs (i.e. COX-2 inhibitors) include; meloxicam, nimesulide, etodolac, and celecoxib. Long-term use of NSAIDs was shown to reduce alveolar bone loss in patients with periodontitis(29). A review study on the effects of NSAIDs concluded that although some results were promising, no data from long-term, multicenter prospective clinical trials are available for determining whether these therapeutic effects can be retained on a long-term basis(30). Furthermore, chronic use of non-selective NSAIDs is associated with potential side effects to the liver, kidney, and gastrointestinal system.

1.4.3.2 Subantimicrobial dose doxycycline (SDD)

SDD, known commercially as Periostat®, is a 20-mg capsule of doxycycline hyclate taken orally twice a day for a period of three to nine months. Due to this prolonged dosage scheduling, patient compliance and the cost are considered as disadvantages of this therapy. It is the first FDA approved systemic drug for host modulation as an adjunct to mechanical therapy in the treatment of periodontitis(31). Its clinical efficacy has been shown to be partially through its ability to inhibit collagenolytic matrix metalloproteinases (MMPs) in gingival tissues and fluid, specifically MMP-8 and MMP-13(32) Long-term periodontal treatment with SDD has proven to exert no antimicrobial effect on the periodontal microflora associated with chronic periodontitis(33). It has been shown that when SDD is used in addition to SRP in patients with chronic periodontitis, clinical parameters of periodontitis such as CAL and PDs were significantly improved compared to SRP therapy alone(34).

1.4.3.3 Bisphosphonates

Bisphosphonates are a class of molecules known to chelate with calcium ions in the bone and considered as potent inhibitors of bone resorption. They have been effectively used in bone targeting and bone loss-related disorders such as osteoporosis and periodontal disease. Specifically, alendronate acts as a potent inhibitor of bone resorption and has been used

widely in periodontitis management. Several studies have shown that local application of alendronate to oral bone preserve or stimulate bone growth(35–43). However, the long-term clinical use of bisphosphonates has been associated with higher incident rates of osteonecrosis of the jaw (ONJ) and atypical fracture which limit their use(44,45).

1.4.3.4 Statins

Statins are a class of anti-hyperlipidemic agents that have gained research interest in the treatment of periodontal disease. They act mainly through hepatic 3-hydroxy-3-methylglutaryl (HMG)-CoA reductase inhibition, thereby affecting the metabolic pathway that produces cholesterol(46). Researchers have found that statins, such as simvastatin (SIM) and lovastatin, induce the expression of bone morphogenic protein-2 (BMP-2) leading to substantial osteogenic effects(47,48). Furthermore, SIM has been reported as a potent antimicrobial agent against both *A. actinomycetemcomitans* and *P. gingivalis*(49), and an anti-inflammatory agent that reduces the expression of cytokines such as IL-6, IL-8, and MCP-1, both *in vitro* and *in vivo* by inhibiting the activation of NF-κB that regulates the expression of diverse inflammatory cytokines(50,51). Due to these unique therapeutic properties, statins have been considered as potential therapeutic candidates for periodontitis. The translation of this therapeutic potential into clinical practice, however, has been largely hampered by the statins' lack of tissue specificity, especially to the bone.

Systemic administration of SIM has been investigated for effects on periodontitis-associated alveolar bone loss and has exhibited a limited impact on periodontal bone due to its hepatotropicity resulting in very limited drug concentration at the skeletal tissues(52). However, local delivery of simvastatin as an adjunct to mechanical periodontal treatment (SRP) has been shown to improve bone regeneration in chronic(53,54) and aggressive periodontitis(55). Meta-analysis has confirmed simvastatin as an effective adjunct to SRP for creating bone fill(56). Yet, SIM's water solubility and osteotropicity remain challenging.

1.5 Local drug delivery systems for the treatment of periodontitis

Even though mechanical management (SRP) removes plaque which contains microorganisms, its effectiveness is limited due to lack of accessibility to bacteria in deeper periodontal pockets. Surgical therapy may be useful but cannot be done in medically compromised individuals. Therefore, therapeutic agents are recommended as adjunctive therapy to prevent disease progression. These agents (antimicrobials and host modulators) mostly are administered systemically which exposes the body to large dose causing antibiotic resistance, adverse drug reaction, and side effects, making them less patient compliant(57,58). Additionally, high concentration of the drug in GCF cannot be achieved when given systemically as drug distributes during circulation to other organs of the body(59). Alternatively, local drug delivery in the form of intra-pocket administration proven to be more advantageous than systemic administration(58,60). When antibiotics and other

therapeutic agents are delivered locally, a high concentration of drug inside periodontal pockets can be attained with reduced systemic distribution, thereby minimizing side effects, and high potential acceptability. However, rapid drug clearance from periodontal pockets requires repeated applications which could reduce patient compliance and be indicative of a low clinical translation potential. Hence, local drug delivery systems have been developed to overcome all such limitations. These systems were aimed at achieving sustained/controlled drug release, maintaining therapeutic concentrations at the periodontal site over a period of time, thereby reducing dosing frequency, and improving patient adherence. In this section, the main local drug delivery systems developed for drug administration to the periodontal pocket and their effectiveness in the periodontal therapy will be discussed. They include; fibers, films, gels, microparticles, nanoparticles, and others.

1.5.1 Fibers

Fiber-based drug delivery systems are described as slender, elongated thread-like polymeric structures with the ability to enhance drug solubility and the sustainable release of therapeutic agents at the target site. They are placed into the periodontal pocket and secured with periodontal dressing to ensure a sustained release of the entrapped drug into the pocket. Several polymers have been utilized such as poly(e-caprolactone) (PCL), polyurethane, polypropylene, cellulose acetate propionate, ethyl vinyl acetate (EVA), alginate, collagen, nylon, and chitosan. There are two types of fibers that have been used in periodontal

drug delivery; hollow and monolithic fibers. Hollow fibers are comprised of drug reservoirs loaded with drug molecules. These fibers release therapeutic agent by simple diffusion through the reservoir wall(61). When these hollow fibers of cellulose acetate filled with tetracycline are locally delivered into periodontal pockets, a dramatic reduction in the periodontal microflora and clinical signs of disease were shown by these fibers loaded with less than 1/1000 tetracycline dose that would have been used for systemic therapy(62). However, due to simple diffusion, the release of the tetracycline from the cellulose acetate hollow fibers was very rapid with approximately 95% of the drug released in the first two hours. Hence, an effective drug concentration for long periods with a single application could not be obtained. In another study, when these fibers containing 20% (v/v) chlorhexidine were delivered into periodontal pockets, a prompt and significant reduction in signs and symptoms of periodontitis was exhibited(63).

To improve fiber delivery efficiency, monolithic fibers were developed by loading drug into the molten polymers, spinning it at high temperature followed by rapid cooling(64). Several *in vitro* and *in vivo* studies showed that these fibers were effective in slowly releasing the encapsulated drug. In one study, EVA monolithic fibers loaded with 25% tetracycline hydrochloride were delivered locally into the periodontal pocket of 10 patients as an adjunct to mechanical therapy and oral hygiene. The fibers reduced the total count of pocket microflora to a level near the limit of dark field microscopy, reduced bleeding on probing, decreased pocket depth probing, and increased attachment levels(65). Furthermore, chitosan-based

fiber containing tetracycline treatment as an adjunct to mechanical periodontal therapy in moderate to advanced periodontitis patients was effective in regard to probing pocket depth reduction and bleeding on probing, while fiber treatment only did not exhibit any beneficial effect on gain of clinical attachment level(66). Periodontal Plus AB™ (Advanced Biotech Products, Chennai, India) is biodegradable tetracycline-impregnated fibrillar collagen that contains 25 mg pure fibrillar collagen with approximately 2 mg of tetracycline hydrochloride. It is commercially available and has been introduced for the treatment of gingival and periodontal diseases(67). Moreover, ciprofloxacin and diclofenac sodium have been formulated into fibers comprised of alginate and glycerol crosslinked with barium cations, and resulted in growth inhibition of *E. coli*, *E. faecalis*, and *S. mutans* over 10 days *in vitro*(68). Also, gentamicin sulfate was incorporated in gravity-spun polycaprolactone (PCL) fibers that can be used for periodontal disease, and growth of *Staphylococcus epidermidis* was suppressed up to 2 weeks *in vitro*(69). Another nylon-based fiber loaded with amoxicillin trihydrate was prepared for periodontal infections and found to be very effective *in vitro* in the controlled delivery of amoxicillin and can be an alternative to systemic administration(70). Nanofibers also have been recently studied, as delivery systems, for local application due to their special structure, which resembles the extracellular matrix. Several antibiotics include tetracycline hydrochloride(71), doxycycline(72), amoxicillin(73), metronidazole(73,74), and metronidazole benzoate(75) have been incorporated into nanofibers. To conclude, though the clinical efficacy of these fibers demonstrated by well conducted and well-controlled

studies, their placement has been challenging as patients experience discomfort during fiber placement and various degrees of gingival redness were observed at fiber removal. The intricacies of winding a fiber into place, and then the removal of it after several days may limit its wide acceptance in clinical settings(76).

1.5.2 Films

Films or chips are implantable polymeric matrix drug delivery devices, where drug molecules are distributed throughout the polymer. Polymeric films have been made for the sustained release of therapeutic agents at the site of action. The ease of application with minimal pain, high drug loading, and controlled size of the films make them an ideal device to be used in periodontal pockets for drug delivery. The thickness of the film should not exceed 400 μm and should possess adhesive property to ensure stability during oral hygiene practice. Drug release occurs by diffusion and/or matrix dissolution or erosion. The release mechanism depends on the type of polymer used to make the chip. When water-insoluble non-degradable polymers are used to prepare films, drug release is mediated through diffusion alone. Those prepared with soluble or biodegradable polymers release drug by diffusion and matrix erosion or dissolution mechanisms(77).

Non-biodegradable ethyl cellulose has been used to prepare films for the delivery of chlorhexidine gluconate/diacetate(78), metronidazole(79–81), tetracycline(82,83), and minocycline(84) and showed greater improvements in the incidence of bleeding on probing, probing depths and attachment levels compared to traditional periodontal therapy. It was noticed that the use of chloroform as the

casting solvent significantly slowed the release rate compared to ethanol. However, when polyethylene glycol was added into the films, the release rate of the drugs increased(85).

On the other hand, degradable polymers (natural or synthetic)-based films have been utilized for drug delivery. They erode or dissolve in the placement site so that removal after placement is not required. Periodontal application of these films resulted in a significant improvement in clinical parameters. Among natural biopolymers, atelocollagen, a pepsin-solubilized type I collagen, has been investigated as a potential carrier for anti-bacterial agents in periodontal disease. Glutaraldehyde cross-linked atelocollagen prolonged tetracycline concentration in GCF for at least ten days(83). Gelatin, another natural polymer obtained from fish, was cross-linked and utilized for the delivery of chlorhexidine diacetate or chlorhexidine hydrochloride. *In vitro* data showed a varied sustained drug release kinetic from 4 to 80 hours, depending on the drug concentration and cross-linking degree of the polymer(86). Moreover, a chip that weighs approximately 6.9 mg and contains 2.5 mg of chlorhexidine gluconate in a biodegradable matrix of hydrolyzed gelatin cross-linked with glutaraldehyde has been developed and commercially available under the trade name Periochip®. It showed an initial burst release in the first 24 hours, followed by a constant slower release over about seven days. Due to its adhesive nature, it remains inside the pocket with no additional aids for retention which is an advantage compared to other biodegradable films. Chitosan film has also been utilized with taurine (antioxidant agent). Taurine augments the

wound healing ability of chitosan showing great potential to be used in inflammatory diseases such as periodontitis(87).

Synthetic biodegradable polymers have also been used for sustained release of drug in the periodontal pocket. In one study, amoxicillin and metronidazole were combined into PLGA and showed a synergistic effect against *E. limosum*, which had been reported to be resistant to metronidazole(88). The films showed a sustained *in vitro* release over 16 days and drug concentrations *in vivo* were maintained above the MIC value. By contrast, PLGA films loaded with tetracycline hydrochloride showed very short residence time in the periodontal pockets with incomplete release of tetracycline(89). This might be explained due to the hydrophobic nature of PLGA matrix and the difference in physicochemical properties of the drugs. In another study, the water-soluble polymer Eudragit S1 and non-water-soluble polymer Eudragit L1 were used to prepare films for the delivery of clindamycin(90). Another group also showed that minocycline embedded in PCL achieved sustained release of the drug within the periodontal pocket for seven days and concluded that this film would be a useful tool for periodontal disease treatment(84). Lastly, a clinico-laboratory study was performed for the treatment of periodontal disease using chlorhexidine-loaded Diplen-Denta films(91). This treatment was shown to be highly effective in individuals diagnosed with catarrhal gingivitis or generalized periodontitis. Overall, periodontal inserts, particularly biodegradable that do not need to be removed after

intra-pocket insertion, would be superior to non-biodegradable films and fiber delivery systems.

1.5.3 Injectable gels

Gels are semisolid formulations used in numerous biomedical pharmaceutical applications. They are crosslinked polymer-based systems in which therapeutic agents can be physically or chemically incorporated to provide a sustained-release kinetic. Several hydrogels and oleogels receive intensive attention for the localized delivery of therapeutics into periodontal pockets since they are easy to prepare and administer and also their bio-adhesive property enhances the retention time in the periodontal pocket.

Chitosan, a novel biodegradable natural polymer, in a gel form (1%, w/w) with or without 15% metronidazole, was effective in the treatment of chronic periodontitis(92). Elyzol® 25% is a dental gel contained metronidazole benzoate (40%) in a mixture of glyceryl monooleate (GMO) and triglyceride (sesame oil) developed for periodontitis treatment. A study compared the clinical and microbiological parameters after repeated local applications of 1% metronidazole or 1% chlorhexidine gels in periodontal pockets treated by scaling and root planing and obtained similar positive findings with both gels at 1% concentration(93). Chlo-Site, a xanthan-based gel with 1.5% chlorhexidine, was evaluated following scaling and root planing in 30 patients of both genders having chronic periodontitis. Its clinical effects after topical subgingival application as an adjunct to scaling and root planing appeared to cause significant improvement compared with scaling and root

planing alone in individuals with chronic periodontitis(94). Furthermore, local delivery of 1% alendronate gel into the periodontal pocket has been utilized to prevent bone destruction associated with periodontitis. When locally delivered into periodontal pockets of patients with type 2 diabetes mellitus and chronic periodontitis as an adjunct to scaling and root planning, it resulted in a significant increase in the probing depth reduction, clinical attachment level gain, and improved bone fill compared to control (free gel)(42,95). Also, local simvastatin gel was applied locally in a 60-patient study as an adjunct to scaling and root planing and showed a greater decrease in the gingival index and probing depth and a clinical attachment level gain with a significant decrease in mean intrabony defect when compared to control group (SRP plus placebo)(53,96). Another study evaluated the effect of locally delivered atorvastatin (2% w/v) containing chitosan gel in the treatment of periodontitis in rats. Significant alveolar bone healing with anti-inflammatory effect was observed(97).

Thermosensitive hydrogel systems have been utilized extensively in drug delivery, controlled release, and cell encapsulation applications. Their unique thermal reversible gelation property makes them an attractive delivery vehicle for regenerative applications in dentistry. They exist in solution form at room temperature and then rapidly convert to hydrogel at physiological temperature holding encapsulated drugs in their crosslinked structures. They can be an ideal intra-pocket delivery system as they can easily pass through into periodontal pocket where they solidify *in situ* and then deliver the therapeutic agent for a prolonged period. Atridox® is an injectable thermosensitive biodegradable gel

composed of 10% doxycycline hyclate dissolved in Atrigel® delivery system, which is a bioabsorbable, polymeric formulation composed of 36.7% poly (D-lactide) (PLA) dissolved in 63.3% N-methyl-2-pyrrolidone (NMP). Doxycycline concentrations in GCF reached nearly 1500 µg/mL two hours following treatment with Atridox® and maintained at 140 µg/mL at day 7. In another study, Atrigel® containing 5% sanguinarine was superior to the control in the treatment of adult periodontitis and the findings have been confirmed in a clinical trial(98). A study demonstrated a significant reduction in the clinical and microbiological parameters after using Elyzol® and Atridox®(99). Another thermosensitive hydrogel system composed of Poloxamer 407 and Carbopol 934P and containing propolis extract has been designed for periodontal disease treatment(100). The release of the propolis was controlled by the relaxation of polymer chains, and the greatest mucoadhesive property was achieved when using a 60:1 ratio of Poloxamer 407: Carbopol 934P. Recently, several poloxamer 407-based thermosensitive gel systems have been formulated, characterized, and evaluated *in vitro* for their potential application in periodontal disease treatment. An *in situ* gel using poloxamer 407 (20% w/v) and chitosan (0.5%, 1%, 1.5%, 2.0% 2.5% w/v) containing two antibiotics: levofloxacin and metronidazole was formulated with syringeable, thermo-responsive, and mucoadhesive properties(101). Other researchers developed a poloxamer 407-based hydrogel with the addition of Carbopol 934P to make it a pH-sensitive and mucoadhesive for the buccal delivery of curcumin to study its anti-inflammatory properties. The prepared hydrogel was easily syringeable and effective in terms of the reduction of the probing depth,

bleeding index and amount of plaque(102). The same hydrogel was also used to develop a dual-controlled release periodontal system containing ciprofloxacin and the anti-inflammatory enzyme serratiopeptidase(103). In another study, a thermosensitive mucoadhesive gel composed of poloxamer 407 (21% w/v), poloxamer 188 (2% w/v), and hydroxypropyl methylcellulose (HPMC) (0.5% w/v) was developed and characterized for the buccal delivery of the moxifloxacin. The formulation exhibited sustained drug release and showed a promising antibacterial efficacy against *Aggregatibacter actinomycetemcomitans* and *Streptococcus mutans* which are involved in periodontal infections(104). Moreover, an injectable antimicrobial delivery system for periodontal treatment based on chitosan/gelatin/*β*-glycerolphosphate hydrogel has been developed and showed no cytotoxic effects(105). Another recent study prepared and characterized a minocycline-loaded hydrogel composed of PLGA and N-methylpyrrolidone (NMP) as a promising treatment for periodontitis(106). Together, semi-solid formulations have been extensively investigated as a local delivery system for therapeutic agents in periodontal disease. Particularly, thermosensitive gels are attractive since their administration can be easily and rapidly performed with even distribution in the pocket. However, their mechanical strength and retention time are major concerns.

1.5.4 Microparticulate system

This system consists of polymeric micro-sized particles into which drug molecules incorporated either physically or chemically for controlled release at the

target site. It is a highly stable system for the delivery of an optimum concentration of the drug in the periodontal pocket. Non-biodegradable as well as biodegradable polymers have been investigated for the preparation of microparticles. These materials include natural polymers, modified natural materials, and synthetic polymers. Among biodegradable polymers, PLGA is the most common one utilized for microparticles development. The drug release from PLGA-based microparticles depends upon the polymer (lactide: glycolide) ratio, molecular weight, crystallinity and pH of the medium. Arestin®, 1 mg minocycline PLGA microspheres, is an approved microparticles delivery system for periodontal disease as an adjunct to mechanical therapy. When administered to treat chronic periodontitis, it was concluded that Arestin® combined with SRP is more effective and safer than SRP alone in reducing the signs of chronic periodontitis(107). However, a recent randomized clinical trial study concluded that the use of minocycline microspheres did not result in an additional benefit over SRP alone(108). PLGA-based microparticles containing tetracycline has been also designed for periodontal disease therapy(109). These particles have been also suspended in Pluronic F127 to form a thermosensitive hydrogel at body temperature and hold the microcapsules in the periodontal pocket for the duration of treatment. Furthermore, PLGA microparticles loaded with chlorhexidine free base, chlorhexidine digluconate were prepared with single emulsion, solvent evaporation technique(110). Recently, doxycycline microspheres were prepared by w/o/w double emulsion technique. The formulation achieved controlled delivery of doxycycline for up to 11 days and was also effective with respect to microbiological

and clinical parameters for up to three months(111). However, the retention of such formulations in the periodontal pocket needs more investigation and clarification.

1.5.5 Nanoparticulate system

Recently, intensive research has been done worldwide utilizing nanotechnology to improve the effectiveness of drugs and minimizing their side effects. Nanoparticles provide several advantages compared to microparticles including high dispersibility in an aqueous medium, slow release rate, and high stability. Due to their nanosize, they can distribute deeply into regions that may be inaccessible to other delivery systems, such as the deep periodontal pockets. Hence, the frequency of administration would be reduced and a uniform distribution of the drug molecules over an extended period of time would be obtained(61). Formulating drugs into nanoparticles led to a dramatic change in their pharmacokinetic parameters and a subsequent reduction in drug dose(112). Nanoparticles (liposomes, micelles, or polymeric) have been used for periodontal drug delivery resulting in powder materials with a particle size in the range of 50–180 nm. Several liposomal formulations of different therapeutic agents have been developed, characterized, and evaluated *in vitro* and *in vivo* for local treatment of periodontal disease and showed promising outcomes(113–115). However, liposomes have some limitations including physical and chemical stability, drug leakage, and difficulties in scaling up which might limit their use. Furthermore, recent PEG-based simvastatin micelles were developed for periodontitis(116). The study concluded that three weekly injections of these nanoparticles decreased

alveolar bone loss and inflammation in rats. Minocycline-loaded poly(ethylene glycol)-poly(lactic acid) nanoparticles were also prepared and evaluated in beagles(117). Effective minocycline concentrations were maintained in GCF for 12 days [48]. In another study, triclosan-loaded polymeric (PLGA, poly-lactic-acid and cellulose acetate phthalate) nanoparticles were prepared by emulsification–diffusion process and were tested *in vivo* in a periodontitis dog model, as a preliminary study. It was found that triclosan-loaded nanoparticles penetrated through the junctional epithelium(118). Moreover, Harungana madagascariensis leaf extract (HLE)-loaded PLGA nanoparticles were prepared using interfacial polymer deposition following the solvent diffusion method and its bactericidal activity was investigated *in vitro*. Formulating HLE into a nanoparticle system improved its antibacterial performance and reduced the bactericidal concentration(119). In another study, a multi-component release system composed of biodegradable nanoparticles which have bioadhesive properties encapsulated within a moisture sensitive microparticle was patented. The positively charged surfactant entrapped on the particle surface mediates the bio-adhesive properties of the nanoparticles. This system can be formulated into any oral hygiene product including gels, chewing gums, toothpaste and mouthwash for the treatment and prevention of periodontal disease(120). In addition, antisense oligonucleotide- loaded chitosan-tripolyphosphate (TPP) nanoparticles were prepared by adding TPP after the formation of chitosan/oligonucleotide complex. The nanoparticles sustainably released oligonucleotides and have the potential to be used in periodontal diseases(121). Furthermore, nanoparticles can be

employed to counter the emergence and increase of bacterial resistance to multiple antibiotics. Antimicrobial enzymes can be conjugated to nanoparticles to produce an antibiotic-free treatment for microbial infections(122).

1.5.6 Miscellaneous

Other local drug delivery systems have been developed for periodontium regeneration. In a study where the effects of local delivery of a simvastatin–alendronate–β-cyclodextrin (SIM–ALN–CD) conjugate for preventing experimental periodontitis bone loss was investigated, it was concluded that such a conjugate system has the potential to prevent periodontitis-associated alveolar bone loss(123).

1.6 Summary

Periodontal disease is a major public health concern and the development of effective therapies to prevent the disease or treat/regenerate periodontal tissues is an ultimate goal. Its management has traditionally focused on the use of mechanical procedures plus systemic antimicrobial agents to reduce pathogen load and to prevent disease progression. However, the constant unraveling of pathogenesis behind periodontal diseases has shifted the route of drug administration in periodontal therapy, from systemic to intra-pocket-targeted delivery systems. These local systems have been successful and shown positive outcomes in a large number of clinical studies in terms of overall periodontal

health. However, concerted efforts in developing ideal intra-pocket drug delivery systems are still needed. Most of the currently available formulations, which focused only on delivering anti-microbial agents, suffer from several limitations including lack of osteotropicity or tooth binding, the removal of non-biodegradable delivery systems, lack of penetration into deeper regions of periodontal pocket and poor patient compliance, indicative of a low clinical translation potential. Therefore, and as will be discussed in the next two chapters, the work of this thesis focused on developing novel intra-pocket delivery systems of bone anabolic and host modulation agents for the treatment of periodontal diseases, in consideration of abovementioned limitations.

References

1. Murakami S, Mealey BL, Mariotti A, Chapple ILC. Dental plaque–induced gingival conditions. J Clin Periodontol. 2018;

2. Tatakis DN, Kumar PS. Etiology and pathogenesis of periodontal diseases. Dent Clin North Am. 2005;49(3 SPEC. ISS.):491–516.

3. Wiebe CB, Putnins EE. The periodontal disease classification system of the American Academy of Periodontology - An update. Journal of the Canadian Dental Association. 2000.

4. Eke PI, Dye BA, Wei L, Slade GD, Thornton-Evans GO, Borgnakke WS, et al. Update on Prevalence of Periodontitis in Adults in the United States: NHANES 2009 to 2012. J Periodontol [Internet]. 2015 May [cited 2017 Dec 22];86(5):611–22. Available from: http://www.ncbi.nlm.nih.gov/pubmed/25688694

5. Hajishengallis G. Periodontitis: from microbial immune subversion to systemic inflammation. Nat Rev Immunol [Internet]. 2014;15(1):30–44. Available from: http://www.ncbi.nlm.nih.gov/pubmed/25534621

6. Grossi SG, Genco RJ, Machtet EE, Ho AW, Koch G, Dunford R, et al. Assessment of Risk for Periodontal Disease. II. Risk Indicators for Alveolar Bone Loss. J Periodontol. 2010;

7. Tipton DA, Dabbous MK. Effects of Nicotine on Proliferation and Extracellular Matrix Production of Human Gingival Fibroblasts In Vitro. J

Periodontol. 2012;

8. Alpar B, Leyhausen G, Sapotnick A, Günay H, Geurtsen W. Nicotine-induced alterations in human primary periodontal ligament and gingiva fibroblast cultures. Clin Oral Investig. 1998;

9. Henemyre CL, K. Scales D, Hokett SD, Cuenin MF, Peacock ME, Parker MH, et al. Nicotine Stimulates Osteoclast Resorption in a Porcine Marrow Cell Model. J Periodontol. 2005;

10. Wright SC, Zhong J, Zheng H, Larrick JW. Nicotine inhibition of apoptosis suggests a role in tumor promotion. FASEB J. 2018;

11. Khader YS, Dauod AS, El-Qaderi SS, Alkafajei A, Batayha WQ. Periodontal status of diabetics compared with nondiabetics: A meta-analysis. J Diabetes Complications. 2006;

12. Chávarry NGM, Vettore MV, Sansone C, Sheiham A. The relationship between diabetes mellitus and destructive periodontal disease: a meta-analysis. Oral Health Prev Dent. 2009;

13. G.E. S, B. C-B, N.P. L. Effects of diabetes mellitus on periodontal and peri-implant conditions: Update on associations and risks. J Clin Periodontol. 2008;

14. Mealey BL. Periodontal disease and diabetes. J Am Dent Assoc. 2014;137(October):S26–31.

15. Lalla E, Cheng B, Lal S, Kaplan S, Softness B, Berg EG, et al. Diabetes

mellitus promotes periodontal destruction in children. J Clin Periodontol. 2007;

16. Salvi GE, Yalda B, Collins JG, Jones BH, Smith FW, Arnold RR, et al. Inflammatory Mediator Response as a Potential Risk Marker for Periodontal Diseases in Insulin-Dependent Diabetes Mellitus Patients. J Periodontol. 2012;

17. Pitocco D, Zaccardi F, Di Stasio E, Romitelli F, Santini SA, Zuppi C, et al. Oxidative Stress, Nitric Oxide, and Diabetes. Rev Diabet Stud [Internet]. 2010 [cited 2018 Apr 26];7(1):15–25. Available from: http://www.ncbi.nlm.nih.gov/pubmed/20703435

18. Kayal RA, Siqueira M, Alblowi J, McLean J, Krothapalli N, Faibish D, et al. TNF-α mediates diabetes-enhanced chondrocyte apoptosis during fracture healing and stimulates chondrocyte apoptosis Through FOXO1. J Bone Miner Res [Internet]. 2010 Feb 8 [cited 2018 Apr 26];25(7):1604–15. Available from: http://www.ncbi.nlm.nih.gov/pubmed/20200974

19. Ackermann PW, Hart DA. Influence of Comorbidities: Neuropathy, Vasculopathy, and Diabetes on Healing Response Quality. Adv wound care [Internet]. 2013 Oct [cited 2018 Apr 19];2(8):410–21. Available from: http://online.liebertpub.com/doi/abs/10.1089/wound.2012.0437

20. Orasanu G, Plutzky J. The pathologic continuum of diabetic vascular disease. J Am Coll Cardiol [Internet]. 2009 Feb 3 [cited 2018 Apr 19];53(5 Suppl):S35-42. Available from:

http://www.ncbi.nlm.nih.gov/pubmed/19179216

21. Ip TP, Leung J, Kung AWC. Management of osteoporosis in patients hospitalized for hip fractures. Osteoporos Int [Internet]. 2010 Dec [cited 2018 Apr 19];21(Suppl 4):S605-14. Available from: http://www.ncbi.nlm.nih.gov/pubmed/21058000

22. Yucel-Lindberg T, Båge T. Inflammatory mediators in the pathogenesis of periodontitis. Expert Rev Mol Med [Internet]. 2013;15(August):e7. Available from: http://www.ncbi.nlm.nih.gov/pubmed/23915822

23. Graves DT, Li J, Cochran DL. Inflammation and uncoupling as mechanisms of periodontal bone loss. Crit Rev Oral Biol Med [Internet]. 2011;90(2):143–53. Available from: http://www.pubmedcentral.nih.gov/articlerender.fcgi?artid=3144100&tool=pmcentrez&rendertype=abstract

24. Hienz SA, Paliwal S, Ivanovski S. Mechanisms of bone resorption in periodontitis. J Immunol Res. 2015;2015.

25. Socransky SS, Haffajee AD. Dental biofilms: Difficult therapeutic targets. Periodontol 2000. 2002;

26. Cobb CM. Clinical significance of non-surgical periodontal therapy: an evidence-based perspective of scaling and root planing. J Clin Periodontol. 2002;

27. Prakasam A, Elavarasu Ss, Natarajan R. Antibiotics in the management of

aggressive periodontitis. J Pharm Bioallied Sci. 2014;

28. Sgolastra F, Gatto R, Petrucci A, Monaco A. Effectiveness of Systemic Amoxicillin/Metronidazole as Adjunctive Therapy to Scaling and Root Planing in the Treatment of Chronic Periodontitis: A Systematic Review and Meta-Analysis. J Periodontol. 2012;83(10):1257–69.

29. Williams RC, Jeffcoat MK, Howard Howell T, Rolla A, Stubbs D, Teoh KW, et al. Altering the Progression of Human Alveolar Bone Loss With the Non-Steroidal Anti-Inflammatory Drug Flurbiprofen. J Periodontol. 2010;

30. Salvi G, Lang N. The Effects of Non-Steroidal Anti-Inflammatory Drugs (Selective and Non-Selective) on the Treatment of Periodontal Diseases. Curr Pharm Des. 2005;

31. Golub LM, McNamara TF, Ryan ME, Kohut B, Blieden T, Payonk G, et al. Adjunctive treatment with subantimicrobial doses of doxycycline: Effects on gingival fluid collagenase activity and attachment loss in adult periodontitis. J Clin Periodontol. 2001;

32. Golub LM, Lee HM, Greenwald RA, Ryan ME, Sorsa T, Salo T, et al. A matrix metalloproteinase inhibitor reduces bone-type collagen degradation fragments and specific collagenases in gingival crevicular fluid during adult periodontitis. Inflamm Res. 1997;

33. Walker C, Thomas J, Nangó S, Lennon J, Wetzel J, Powala C. Long-Term Treatment With Subantimicrobial Dose Doxycycline Exerts No Antibacterial Effect on the Subgingival Microflora Associated With Adult Periodontitis. J

Periodontol. 2005;

34. Caton JG, Ciancio SG, Blieden TM, Bradshaw M, Crout RJ, Hefti AF, et al. Treatment With Subantimicrobial Dose Doxycycline Improves the Efficacy of Scaling and Root Planing in Patients With Adult Periodontitis. J Periodontol. 2005;71(4):521–32.

35. Yaffe A, Iztkovich M, Earon Y, Alt I, Lilov R, Binderman I. Local Delivery of an Amino Bisphosphonate Prevents the Resorptive Phase of Alveolar Bone Following Mucoperiosteal Flap Surgery in Rats. J Periodontol. 2012;

36. Meraw SJ, Reeve CM, Wollan PC. Use of Alendronate in Peri-Implant Defect Regeneration. J Periodontol. 2005;

37. Meraw SJ, Reeve CM. Qualitative Analysis of Peripheral Peri-Implant Bone and Influence of Alendronate Sodium on Early Bone Regeneration. J Periodontol. 2005;

38. Binderman I, Adut M, Yaffe A. Effectiveness of Local Delivery of Alendronate in Reducing Alveolar Bone Loss Following Periodontal Surgery in Rats. J Periodontol. 2005;

39. Srisubut S, Teerakapong A, Vattraphodes T, Taweechaisupapong S. Effect of local delivery of alendronate on bone formation in bioactive glass grafting in rats. Oral Surgery, Oral Med Oral Pathol Oral Radiol Endodontology. 2007;

40. Komatsu K, Shimada A, Shibata T, Shimoda S, Oida S, Kawasaki K, et al.

Long-term effects of local pretreatment with alendronate on healing of replanted rat teeth. J Periodontal Res. 2008;

41. Küük D, Ay S, Kara MI, Avunduk MC, Gümus C. Comparison of local and systemic alendronate on distraction osteogenesis. Int J Oral Maxillofac Surg. 2011;

42. Pradeep AR, Sharma A, Rao NS, Bajaj P, Naik SB, Kumari M. Local Drug Delivery of Alendronate Gel for the Treatment of Patients With Chronic Periodontitis With Diabetes Mellitus: A Double-Masked Controlled Clinical Trial. J Periodontol. 2012;

43. Pulikkotil SJ, Nath S. Letter to the Editor: Re: 1% Alendronate Gel as Local Drug Delivery in the Treatment of Class II Furcation Defects: A Randomized Controlled Clinical Trial. J Periodontol. 2014;

44. Durie BGM, Katz M, Crowley J. Osteonecrosis of the Jaw and Bisphosphonates. N Engl J Med [Internet]. 2005 Jul 7 [cited 2017 Nov 6];353(1):99–102. Available from: http://www.ncbi.nlm.nih.gov/pubmed/16000365

45. Kennel KA, Drake MT. Adverse effects of bisphosphonates: implications for osteoporosis management. Mayo Clin Proc [Internet]. 2009 Jul [cited 2017 Nov 6];84(7):632–7; quiz 638. Available from: http://www.ncbi.nlm.nih.gov/pubmed/19567717

46. Bellosta S, Bernini F, Ferri N, Quarato P, Canavesi M, Arnaboldi L, et al. Direct vascular effects of HMG-CoA reductase inhibitors. Atherosclerosis

[Internet]. 1998 Apr [cited 2017 Aug 23];137 Suppl:S101-9. Available from: http://www.ncbi.nlm.nih.gov/pubmed/9694549

47. Mundy G, Garrett R, Harris S, Chan J, Chen D, Rossini G, et al. Stimulation of bone formation in vitro and in rodents by statins. Science [Internet]. 1999;286(5446):1946–9. Available from: http://www.ncbi.nlm.nih.gov/pubmed/10583956

48. Garrett IR, Mundy GR. The role of statins as potential targets for bone formation. Arthritis Res [Internet]. 2002 [cited 2017 Aug 23];4(4):237. Available from: http://www.ncbi.nlm.nih.gov/pubmed/12106493

49. Emani S, Gunjiganur G, Mehta D. Determination of the antibacterial activity of simvastatin against periodontal pathogens, Porphyromonas gingivalis and Aggregatibacter actinomycetemcomitans: An in vitro study. Contemp Clin Dent [Internet]. 2014 Jul [cited 2017 Apr 27];5(3):377. Available from: http://www.ncbi.nlm.nih.gov/pubmed/25191077

50. Lazzerini PE, Lorenzini S, Selvi E, Capecchi PL, Chindamo D, Bisogno S, et al. Simvastatin inhibits cytokine production and nuclear factor-kB activation in interleukin 1??-stimulated synoviocytes from rheumatoid arthritis patients. Clin Exp Rheumatol. 2007;25(5):696–700.

51. Pereira MC, Cardoso PRG, Da Rocha LF, Rêgo MJBM, Gonçalves SMC, Santos FA, et al. Simvastatin inhibits cytokines in a dose response in patients with rheumatoid arthritis. Inflamm Res. 2014;63(4):309–15.

52. Cunha-Cruz J, Saver B, Maupome G, Hujoel PP. Statin Use and Tooth

Loss in Chronic Periodontitis Patients. J Periodontol [Internet]. 2006 Jun [cited 2017 Nov 5];77(6):1061–6. Available from: http://www.ncbi.nlm.nih.gov/pubmed/16734582

53. Pradeep AR, Thorat MS. Clinical Effect of Subgingivally Delivered Simvastatin in the Treatment of Patients With Chronic Periodontitis: A Randomized Clinical Trial. J Periodontol [Internet]. 2010 Feb [cited 2017 Nov 6];81(2):214–22. Available from: http://www.ncbi.nlm.nih.gov/pubmed/20151799

54. Agarwal S, Chaubey K, Chaubey A, Agarwal V, Madan E, Agarwal M. Clinical efficacy of subgingivally delivered simvastatin gel in chronic periodontitis patients. J Indian Soc Periodontol [Internet]. 2016 [cited 2018 May 25];20(4):409. Available from: http://www.ncbi.nlm.nih.gov/pubmed/28298823

55. Priyanka N, Abhilash A, Saquib S, Malgaonkar N, Kudyar N, Gupta A, et al. Clinical Efficacy of Subgingivally Delivered 1.2 mg Simvastatin in the Treatment of Patients with Aggressive Periodontitis: A Randomized Controlled Clinical Trial. Int J Periodontics Restorative Dent [Internet]. [cited 2018 May 25];37(2):e135–41. Available from: http://www.ncbi.nlm.nih.gov/pubmed/28196160

56. Akram Z, Vohra F, Javed F. Efficacy of statin delivery as an adjunct to scaling and root planing in the treatment of chronic periodontitis: A meta-analysis. J Investig Clin Dent [Internet]. 2018 May [cited 2018 May

25];9(2):e12304. Available from: http://www.ncbi.nlm.nih.gov/pubmed/29119729

57. Walker CB. Selected antimicrobial agents: Mechanisms of action, side effects and drug interactions. Periodontol 2000. 1996;

58. Southard GL, Godowski KC. Subgingival controlled release of antimicrobial agents in the treatment of periodontal disease. Int J Antimicrob Agents. 1998;

59. Goodson JM. Antimicrobial strategies for treatment of periodontal diseases. Periodontol 2000. 1994;

60. Schwach-Abdellaoui K, Vivien-Castioni N, Gurny R. Local delivery of antimicrobial agents for the treatment of periodontal diseases. European Journal of Pharmaceutics and Biopharmaceutics. 2000.

61. Pragati S, Ashok S, Kuldeep S. Recent advances in periodontal drug delivery systems. Int J Drug Deliv. 2011;1(1):1–14.

62. Goodson JM, Haffajee A, Socransky SS. Periodontal therapy by local delivery of tetracycline. J Clin Periodontol. 1979;6(2):83–92.

63. Greenstein G. Local drug delivery in the treatment of periodontal diseases: assessing the clinical significance of the results. J Periodontol [Internet]. 2006 Apr [cited 2017 Aug 23];77(4):565–78. Available from: http://www.joponline.org/doi/10.1902/jop.2006.050140

64. Goodson JM, Holborow D, Dunn RL, Hogan P, Dunham S. Monolithic

Tetracycline-containing Fibers for Controlled Delivery to Periodontal Pockets. J Periodontol. 2010;54(10):575–9.

65. Tonetti MS, Pini-Prato G, Cortellini P. Principles and clinical applications of periodontal controlled drug delivery with tetracycline fibers. Int J Periodontics Restorative Dent. 1994;

66. Yalcin F, Demirel K, Onan U. Evaluation of adjunctive tetracycline fiber therapy with scaling and root planing: short-term clinical results3. Periodontal Clin Investig. 1999.

67. Sachdeva S, Agarwal V. Evaluation of commercially available biodegradable tetracycline fiber therapy in chronic periodontitis. J Indian Soc Periodontol. 2011;

68. Johnston D, Choonara YE, Kumar P, Du Toit LC, Van Vuuren S, Pillay V. Prolonged delivery of ciprofloxacin and diclofenac sodium from a polymeric fibre device for the treatment of peridontal disease. Biomed Res Int. 2013;

69. Chang HI, Lau YC, Yan C, Coombes AGA. Controlled release of an antibiotic, gentamicin sulphate, from gravity spun polycaprolactone fibers. J Biomed Mater Res - Part A. 2008;

70. Ahuja A, Ali J, Shareef A, Khar RK. Formulation and development of targeted retentive device for the treatment of periodontal infections with amoxycillin trihydrate. Indian J Pharm Sci. 2006;

71. Kenawy ER, Bowlin GL, Mansfield K, Layman J, Simpson DG, Sanders

EH, et al. Release of tetracycline hydrochloride from electrospun poly(ethylene-co-vinylacetate), poly(lactic acid), and a blend. J Control Release. 2002;

72. Feng K, Sun H, Bradley MA, Dupler EJ, Giannobile W V., Ma PX. Novel antibacterial nanofibrous PLLA scaffolds. J Control Release. 2010;

73. Chen DWC, Lee FY, Liao JY, Liu SJ, Hsiao CY, Chen JK. Preclinical experiments on the release behavior of biodegradable nanofibrous multipharmaceutical membranes in a model of four-wall intrabony defect. Antimicrob Agents Chemother. 2013;

74. Xue J, He M, Liang Y, Crawford A, Coates P, Chen D, et al. Fabrication and evaluation of electrospun PCL–gelatin micro-/nanofiber membranes for anti-infective GTR implants. J Mater Chem B. 2014 Sep;2(39):6867–77.

75. Zamani M, Morshed M, Varshosaz J, Jannesari M. Controlled release of metronidazole benzoate from poly ε-caprolactone electrospun nanofibers for periodontal diseases. Eur J Pharm Biopharm. 2010;

76. Goodson JM, Cugini MA, Kent RL, Armitage GC, Cobb CM, Fine D, et al. Multicenter evaluation of tetracycline fiber therapy: II. Clinical response. J Periodontal Res. 1991 Jul;26(4):371–9.

77. Langer R, Peppas NA. Advances in Biomaterials, Drug Delivery, and Bionanotechnology. In: AIChE Journal. 2003.

78. Ikinci G, Şenel S, Akincibay H, Kaş S, Erciş S, Wilson CG, et al. Effect of

chitosan on a periodontal pathogen Porphyromonas gingivalis. Int J Pharm. 2002;

79. Labib GS, Aldawsari HM, Badr-Eldin SM. Metronidazole and Pentoxifylline films for the local treatment of chronic periodontal pockets: preparation, in vitro evaluation and clinical assessment . Expert Opin Drug Deliv. 2014;

80. El-Kamel AH, Ashri LY, Alsarra IA. Micromatricial metronidazole benzoate film as a local mucoadhesive delivery system for treatment of periodontal diseases. AAPS PharmSciTech. 2007;

81. Shifrovitch Y, Binderman I, Bahar H, Berdicevsky I, Zilberman M. Metronidazole-Loaded Bioabsorbable Films as Local Antibacterial Treatment of Infected Periodontal Pockets. J Periodontol. 2009;

82. Minabe M, Takeuchi K, Nishimura T, Hori T, Umemoto T. Therapeutic effects of combined treatment using tetracycline???immobilized collagen film and root planing in periodontal furcation pockets. J Clin Periodontol. 1991;

83. MINABE M, UEMATSU A, NISHIJIMA K, TOMOMATSU E, TAMURA T, YAMASHITA O, et al. Application of a local drug delivery system to periodontal therapy. I. Development of the collagen preparations immobilized tetracycline. Nihon Shishubyo Gakkai Kaishi (Journal Japanese Soc Periodontol. 2011;

84. Kyun KD, Yun KS, Young JS, Pyoung CC, Heui SS. [Development of minocycline containing polycaprolactone film as a local drug delivery].

Taehan Chikkwa Uisa Hyophoe Chi. 1990;

85. Golomb G, Friedman M, Soskolne A, Stabholz A, Sela MN. Sustained Release Device Containing Metronidazole for Periodontal Use. J Dent Res. 1984 Sep;63(9):1149–53.

86. Steinberg D, Friedman M, Soskolne A, Sela MN. A New Degradable Controlled Release Device for Treatment of Periodontal Disease: In Vitro Release Study. J Periodontol. 2012;

87. Özmeriç N, Özcan G, Haytaç CM, Alaaddinoğlu EE, Sargon MF, Şenel S. Chitosan film enriched with an antioxidant agent, taurine, in fenestration defects. J Biomed Mater Res. 2000;

88. Ahuja A, Ali J, Rahman S. Biodegradable periodontal intrapocket device containing metronidazole and amoxycillin: Formulation and characterisation. Pharmazie. 2006;

89. Agarwal RK, Robinson DH, Maze GI, Reinhardt RA. Development and characterization of tetracycline-poly(lactide/glycolide) films for the treatment of periodontitis. J Control Release. 1993 Feb;23(2):137–46.

90. HIGASHI K, MATSUSHITA M, MORISAKI K, HAYASHI S, MAYUMI T. Local drug delivery systems for the treatment of periodontal disease. J Pharmacobiodyn. 2011;

91. Dedeian VR, Solov'eva NI, Ezikian TI, Medvedeva IA. [The treatment of periodontal diseases using Diplen-Denta films with chlorhexidine (a clinico-

laboratory study)]. Stomatologiia (Mosk). 1997;

92. Akincibay H, Şenel S, Ay ZY. Application of chitosan gel in the treatment of chronic periodontitis. J Biomed Mater Res - Part B Appl Biomater. 2007;

93. Perinetti G, Paolantonio M, Cordella C, D'Ercole S, Serra E, Piccolomini R. Clinical and microbiological effects of subgingival administration of two active gels on persistent pockets of chronic periodontitis patients. J Clin Periodontol. 2004;

94. Jain M, Dave D, Jain P, Manohar B, Yadav B, Shetty N. Efficacy of xanthan based chlorhexidine gel as an adjunct to scaling and root planing in treatment of the chronic periodontitis. J Indian Soc Periodontol. 2013 Jul;17(4):439.

95. Pradeep AR, Kumari M, Rao NS, Naik SB. 1% Alendronate Gel as Local Drug Delivery in the Treatment of Class II Furcation Defects: A Randomized Controlled Clinical Trial. J Periodontol. 2013 Mar;84(3):307–15.

96. Rao NS, Pradeep AR, Bajaj P, Kumari M, Naik SB. Simvastatin local drug delivery in smokers with chronic periodontitis: A randomized controlled clinical trial. Aust Dent J. 2013;

97. Özdoğan AI, İlarslan YD, Kösemehmetoğlu K, Akca G, Kutlu HB, Comerdov E, et al. In vivo evaluation of chitosan based local delivery systems for atorvastatin in treatment of periodontitis. Int J Pharm. 2018;550(1–2):470–6.

98. Poison AM, Stoller NH, Hanes PJ, Bandt CL, Garrett S, Southard G. 2 multi-center trials assessing the clinical efficacy of 5% sanguinarine in a biodegradable drug delivery system. J Clin Periodontol. 2005;

99. Salvi GE, Mombelli A, Mayfield L, Rutar A, Suvan J, Garrett S, et al. Local antimicrobial therapy after initial periodontal treatment. J Clin Periodontol. 2002;

100. Bruschi ML, Jones DS, Panzeri H, Gremião MPD, De Freitas O, Lara EHG. Semisolid systems containing propolis for the treatment of periodontal disease: In vitro release kinetics, syringeability, rheological, textural, and mucoadhesive properties. J Pharm Sci. 2007;

101. Bansal M, Mittal N, Yadav SK, Khan G, Gupta P, Mishra B, et al. Periodontal thermoresponsive, mucoadhesive dual antimicrobial loaded in-situ gel for the treatment of periodontal disease: Preparation, in-vitro characterization and antimicrobial study. J Oral Biol Craniofacial Res. 2018;

102. Nasra MMA, Khiri HM, Hazzah HA, Abdallah OY. Formulation, in-vitro characterization and clinical evaluation of curcumin in-situ gel for treatment of periodontitis. Drug Deliv. 2017;

103. Pathak K, Sharma V, Singh K, Chhabra G. Thermosensitive periodontal sol of ciprofloxacin hydrochloride and serratiopeptidase: Pharmaceutical and mechanical analysis. Int J Pharm Investig. 2014;4(1):5.

104. Sheshala R, Quah SY, Tan GC, Meka VS, Jnanendrappa N, Sahu PS.

Investigation on solution-to-gel characteristic of thermosensitive and mucoadhesive biopolymers for the development of moxifloxacin-loaded sustained release periodontal in situ gels. Drug Deliv Transl Res. 2018;

105. Pakzad Y, Ganji F. Thermosensitive hydrogel for periodontal application: In vitro drug release, antibacterial activity and toxicity evaluation. J Biomater Appl. 2016;30(7):919–29.

106. Wang X, Ma J, Zhu X, Wang F, Zhou L. Minocycline-loaded in situ hydrogel for periodontitis treatment. Curr Drug Deliv. 2017;14:664–71.

107. Gopinath V, Ramakrishnan T, Emmadi P, Ambalavanan N, Mammen B, Vijayalakshmi. Effect of a controlled release device containing minocycline microspheres on the treatment of chronic periodontitis: A comparative study. J Indian Soc Periodontol. 2009;

108. Killeen AC, Harn JA, Erickson LM, Yu F, Reinhardt RA. Local Minocycline Effect on Inflammation and Clinical Attachment During Periodontal Maintenance: Randomized Clinical Trial. J Periodontol. 2016;87(10):1149–57.

109. Liu DZ, Chen WP, Lee CP, Wu SL, Wang YC, Chung TW. Effects of alginate coated on PLGA microspheres for delivery tetracycline hydrochloride to periodontal pockets. J Microencapsul. 2004;21(6):643–52.

110. Yue IC, Poff J, Cortés ME, Sinisterra RD, Faris CB, Hildgen P, et al. A novel polymeric chlorhexidine delivery device for the treatment of periodontal disease. Biomaterials. 2004;

111. Rao SK, Setty S, Acharya AB, Thakur SL. Efficacy of locally-delivered doxycycline microspheres in chronic localized periodontitis and on Porphyromonas gingivalis. J Investig Clin Dent. 2011;3(2):128–34.

112. Patravale VB, Date AA, Kulkarni RM. Nanosuspensions: a promising drug delivery strategy. J Pharm Pharmacol. 2004;

113. Petelin M, Pavlica Z, Ivanuša T, Šentjurc M, Skalerič U. Local delivery of liposome-encapsulated superoxide dismutase and catalase suppress periodontal inflammation in beagles. J Clin Periodontol. 2000;

114. Liu D, Yang PS. Minocycline hydrochloride nanoliposomes inhibit the production of TNF-α in LPS-stimulated macrophages. Int J Nanomedicine. 2012;

115. Sugano M, Negishi Y, Endo-Takahashi Y, Hamano N, Usui M, Suzuki R, et al. Gene delivery to periodontal tissue using Bubble liposomes and ultrasound. J Periodontal Res. 2014;

116. Bradley AD, Zhang Y, Jia Z, Zhao G, Wang X, Pranke L, et al. Effect of Simvastatin Prodrug on Experimental Periodontitis. J Periodontol [Internet]. 2016 May [cited 2017 Apr 2];87(5):577–82. Available from: http://www.ncbi.nlm.nih.gov/pubmed/26799395

117. Yao W, Xu P, Pang Z, Zhao J, Chai Z, Li X, et al. Local delivery of minocycline-loaded PEG-PLA nanoparticles for the enhanced treatment of periodontitis in dogs. Int J Nanomedicine. 2014;

118. Piñón-Segundo E, Ganem-Quintanar A, Alonso-Pérez V, Quintanar-Guerrero D. Preparation and characterization of triclosan nanoparticles for periodontal treatment. Int J Pharm. 2005;

119. Moulari B, Lboutounne H, Chaumont JP, Guillaume Y, Millet J, Pellequer Y. Potentiation of the bactericidal activity of Harungana madagascariensis Lam. ex Poir. (Hypericaceae) leaf extract against oral bacteria using poly (D, L-lactide-co-glycolide) nanoparticles: In vitro study. Acta Odontol Scand. 2006;64(3):153–8.

120. Ahmad F, Iqbal Z, Jain N, Jain G, Talegaonkar S, Ahuja A, et al. Dental Therapeutic Systems. Recent Pat Drug Deliv Formul. 2008;

121. Dung TH, Lee S-R, Han S-D, Kim S-J, Ju Y-M, Kim M-S, et al. Chitosan-TPP nanoparticle as a release system of antisense oligonucleotide in the oral environment. J Nanosci Nanotechnol. 2007 Nov;7(11):3695–9.

122. Satishkumar R, Vertegel A. Charge-directed targeting of antimicrobial protein-nanoparticle conjugates. Biotechnol Bioeng. 2008;100(3):403–12.

123. Price U, Le HOT, Powell SE, Schmid MJ, Marx DB, Zhang Y, et al. Effects of local simvastatin-alendronate conjugate in preventing periodontitis bone loss. J Periodontal Res. 2013;48(5):541–8.

CHAPTER 2.

Local Application of Pyrophosphorylated Simvastatin Prevents Experimental Periodontitis

2.1 INTRODUCTION

As discussed in Chapter 1, periodontitis is an oral inflammatory disease that affects the integrity of tooth-supporting tissues including gingiva, periodontal ligament, cementum, and alveolar bone. The pathogenic bacterial population and host immune response are considered as keystones in the emergence and persistence of the disease(1). Non-surgical treatment options are limited to plaque (biofilm) removal which aim to reduce inflammation(2) followed by administration of local and systemic antibiotics to minimize bacterial load in the periodontal pocket(3,4). Additionally, nonsteroidal anti-inflammatory medications, sub-antimicrobial doses of doxycycline, and growth factors have all been utilized as host modulation agents to reduce disease progression(5,6). However, their effect on the inflammation-induced alveolar bone loss is limited. Hence, there is an urgent need for the development of a therapeutic strategy that can prevent/regenerate alveolar bone loss.

As discussed in Chapter 1, statins are a class of anti-hyperlipidemic agents which have been found to ameliorate inflammation and to induce the expression of bone morphogenic protein-2 (BMP-2) leading to substantial osteogenic effects(7,8). They have been considered as potential therapeutic candidates for periodontal disease. However, their aqueous solubility and osteotropicity are

major limitations. Local delivery systems of SIM have been developed to enhance solubility and provide a sustained release, and have shown potential protection of the periodontal tissues (9,10).

In this chapter, a novel strategy to address the limitations associated with the clinical utility of SIM for periodontal disease is discussed. A SIM prodrug was developed by conjugating a SIM trimer to osteotropic pyrophosphate (PPi). The prodrug (SIM-PPi) was fully characterized, and its therapeutic efficacy was evaluated *in vitro* and in an experimental periodontitis rat model.

2.2 METHODS AND MATERIALS

2.2.1 Materials

Simvastatin was purchased from Zhejiang Ruibang Laboratories (Wenzhou, Zhejiang, China) Hydroxyapatite microparticles (HA, DNA grade Bio-Gel HTP gel) were purchased from Bio-Rad (Hercules, CA, USA). Mouse macrophage RAW 264.7 cells, osteoblast MC3T3-L1 cells, and Dulbecco's Modified Eagle Medium (DMEM) were originally purchased from ATCC (Manassas, VA, USA). Minimum Essential Media (alpha-MEM) and trypsin-EDTA were purchased from Gibco (Grand Island, NY, USA). Fetal bovine serum (FBS) was obtained from Gemini BenchMark (West Sacramento, CA). Silver nitrate was purchased from RICCA Chemical Company (Arlington, TX). Sodium thiosulfate was purchased from Alfa Aesar (Haverhill, MA). All other reagents and solvents, if not specified, were obtained from either Fisher Scientific (Pittsburgh, PA, USA) or Acros Organics (Morris Plains, NJ, USA).

2.2.2 Synthesis of the simvastatin-pyrophosphate prodrug (SIM-PPI)

Synthesis of compound 1

Simvastatin (6.27g, 15 mmol), butane-1,4-diol (27.3g, 300 mmol) and *p*-toluenesulfonic acid monohydrate ($TsOH \cdot H_2O$, 285 mg, 1.5mmol) were dissolved in anhydrous CH_2Cl_2 (30 mL). The solution was stirred at room temperature for 3 hr. $NaHCO_3$ (saturated solution, 15 mL) and ethyl acetate (100 mL) were added

and then washed with brine (80 mL×3). The organic phase was dried over Na_2SO_4 and then the solvent was removed. The residue was purified by flash column chromatography (ethyl acetate/hexanes = 3/1) to give compound 1 (5.76 g), yield: 75.6%.

^{1}H NMR (500 MHz, $CDCl_3$): δ (ppm) = 5.97 (d, *J* = 9.7 Hz, 1H), 5.78 (dd, *J* = 9.7 Hz, 6.3 Hz, 1H), 5.49 (s, 1H), 5.38 (d, *J* = 2.5 Hz, 1H), 4.26 (d, *J* = 3.8 Hz, 1H), 4.20 (s, 1H), 4.16 (t, *J* = 6.5 Hz, 2H), 3.83 (s, 1H), 3.78 (br, 1H), 3.67 (t, *J* = 6.0 Hz, 2H), 2.49 (s, 1H), 2.48 (s, 1H), 2.43 (m, 1H), 2.39 (s, 1H), 2.36 (dd, *J* = 12.3 Hz, 6.2Hz, 1H), 2.24 (d, *J* = 10.6 Hz, 1H), 1.95 (m, 2H), 1.76 (m, 2H), 1.60-1.70 (m, 4H), 1.45-1.60 (m, 5H), 1.26 (m, 1H), 1.19 (m, 1H), 1.12 (s, 3H), 1.11 (s, 3H), 1.08 (d, *J* = 7.4 Hz, 3H), 0.87 (d, *J* = 7.0 Hz, 3H), 0.83 (t, *J* = 7.5 Hz, 3H).

^{13}C NMR (125 MHz, $CDCl_3$): δ (ppm) = 178.14, 172.27, 133.04, 131.54, 129.45, 128.20, 72.15, 68.95, 68.08, 64.50, 61.96, 42.90, 42.29, 41.94, 37.61, 36.19, 34.74, 32.93, 32.89, 30.42, 28.94, 27.19, 24.98, 24.70, 24.59, 24.14, 23.00, 13.79, 9.21.

MS (ESI): m/z = 531.1 ($M + Na^+$), calculated MW = 508.3.

Synthesis of compound 2

Compound 1 (6.5 g, 12.8 mmol) and imidazole (1.74 g, 25.6 mmol) were dissolved in anhydrous CH_2Cl_2 (30 mL) and cooled to 0 °C. *t*-Butyldimethylsilyl chloride (TBSCl, 2.10 g, 14 mmol) was added. The solution was stirred at 0 °C for 3 hr. Ethyl acetate (100 mL) were added and then washed with brine (80 mL×3). The organic phase was dried over Na_2SO_4 and then the solvent was removed. The

residue was purified by flash column chromatography (ethyl acetate/hexanes = 1/1) to give compound 1 (7.18 g), yield: 90.2%.

^{1}H NMR (500 MHz, $CDCl_3$): δ (ppm) = 5.93 (d, *J* = 9.7 Hz, 1H), 5.73 (dd, *J* = 9.7 Hz, 6.3Hz, 1H), 5.44 (s, 1H), 5.34 (d, *J* = 2.6 Hz, 1H), 4.21, (br, 1H), 4.09 (t, *J* = 6.6 Hz, 2H), 4.07 (s, 1H), 3.79, (s, 1H), 3.73 (br, 1H), 3.59 (t, *J* = 6.2 Hz, 2H), 2.44 (s, 1H), 2.43 (s, 1H), 2.39 (m, 1H), 2.33 (dd, *J* = 11.4 Hz, 6.1Hz), 2.19 (d, *J* = 10.6 Hz, 1H), 1.90 (br, 2H), 1.65 (m, 2H), 1.53 (m, 9H), 1.21 (m, 1H), 1.14 (m, 1H), 1.08 (s, 3H), 1.07 (s, 3H), 1.04 (d, *J* = 7.4 Hz, 3H), 0.85 (s, 9H), 0.82 (s, d, *J* = 7.0 Hz, 3H), 0.78 (t, *J* = 7.5 Hz, 3H), 0.01 (s, 6H).

^{13}C NMR (125 MHz, $CDCl_3$): δ (ppm) = 177.81, 172.18, 132.93, 131.50, 129.28, 128.14, 72.02, 68.81, 67.92, 64.47, 62.32, 42.76, 42.27, 41.71, 37.52, 36.13, 34.69, 32.82, 30.34, 28.96, 27.12, 25.76, 25.01, 24.62, 24.51, 24.10, 22.92, 18.10, 13.71, 9.13, -5.50

MS (ESI): m/z = 645.5 ($M + Na^+$), calculated MW = 622.4.

Synthesis of compound 3

Compound 2 (5.35 g, 7 mmol), triethylamine (2.12 g, 3 mmol) and 4-dimethylaminopyridine (DMAP, 170 mg, 1.4 mmol) were dissolved in anhydrous CH_2Cl_2 (20 mL) and cooled to 0 °C. Ac_2O (1.78 g, 17.5 mmol) was added. The solution was stirred at 0 °C for 0.5 hr. Ethyl acetate (70 mL) was added and washed with HCl (25 mL, 1 M) and brine (100 mL). The organic phase was dried over Na_2SO_4 and then the solvent was removed to give crude product compound 3 (4.90 g). It was used directly in the next reaction without further purification.

^{1}H NMR (500 MHz, $CDCl_3$): δ (ppm) = 5.93 (d, *J* = 9.7 Hz, 1H), 5.73 (dd, *J* = 9.7 Hz, 6.3Hz, 1H), 5.45 (s, 1H), 5.30 (d, *J* = 2.6Hz, 1H), 5,19 (pent, *J* = 6.2 Hz), 4.84 (m, 1H), 4.06 (t, *J* = 6.6 Hz, 2H), 3.60 (t, *J* = 6.2 Hz, 2H), 2.57 (s, 1H), 2.56 (s, 1H), 2.39 (m, 1H), 2.33 (dd, *J* = 11.4Hz, 6.1Hz), 2.19 (d, *J* = 11.7 Hz, 1H), 2.02 (s, 3H), 1.96 (s, 3H), 1.93 (m, 3H), 1.82 (m, 1H), 1.60-1.70 (m, 4H), 1.40-1.60 (m, 5H), 1.31 (m, 1H), 1.14 (m, 1H), 1.08 (s, 3H), 1.07 (s, 3H), 1.04 (d, *J* = 7.4 Hz, 3H), 0.85 (s, 9H), 0.82 (d, *J* = 7.0 Hz, 3H), 0.78 (t, *J* = 7.5 Hz, 3H), 0.01 (s, 6H).

^{13}C NMR (125 MHz, $CDCl_3$): δ (ppm) = 177.32, 170.33, 169.87, 169.81, 132.68, 131.41, 129.53, 128.26, 70.95, 67.73, 67.63, 64.51, 62.34, 42.74, 38.58, 37.57, 37.39, 36.25, 32.81, 32.72, 30.99, 30.35, 28.96, 27.14, 25.78, 25.05, 24.59, 24.53, 23.24, 22.89, 21.03, 20.88, 18.14, 13.64, 9.14, -5.48

MS (ESI): m/z = 729.7 ($M + Na^+$), calculated MW = 706.5.

Synthesis of compound 4

Compound 3 (4.90g, 6.9 mmol) was dissolved in a mixture solution (MeOH/CH_2Cl_2 = 1/1, 20 mL) and cooled to 0 °C. TsOH monohydrate (133 mg, 0.7 mmol) was added. The solution was stirred at 0 °C for 1 hr. Ethyl acetate (100 mL) was added and then washed with brine (80 mL×3). The organic phase was dried over Na_2SO_4 and then the solvent was removed. The residue was purified by flash column chromatography (ethyl acetate/hexanes = 1/1) to give compound 4 (3.69 g), yield: 89.0% for two steps.

^{1}H NMR (500 MHz, $CDCl_3$): δ (ppm) = 5.88 (d, *J* = 9.7 Hz, 1H), 5.66 (dd, *J* = 9.7 Hz, 6.3Hz, 1H), 5.40 (s, 1H), 5.23 (d, *J* = 2.6Hz, 1H), 5.13 (pent, *J* = 6.2 Hz), 4.77

(m, 1H), 4.06 (m, 2H), 3.60 (t, *J* = 6.2 Hz, 2H), 2.514 (s, 1H), 2.510 (s, 1H), 2.50 (t, *J* = 3.8 Hz, 1H), 2.33 (m, 1H), 2.26 (dd, *J* = 11.4Hz, 6.1Hz, 1H), 2.19 (d, *J* = 11.7Hz, 1H), 1.96 (s, 3H), 1.93 (s, 3H), 1.86 (m, 3H), 1.76 (m, 1H), 1.45-1.65 (m, 9H), 1.26 (m, 1H), 1.06 (m, 1H), 1.02 (s, 3H), 1.01 (s, 3H), 0.98 (d, *J* = 7.4 Hz, 3H), 0.77 (d, *J* = 7.0 Hz, 3H), 0.73 (t, *J* = 7.5 Hz, 3H).

^{13}C NMR (125 MHz, $CDCl_3$): δ (ppm) = 177.34, 170.38, 169.86, 169.78, 132.54, 131.25, 129.40, 128.13, 70.90, 67.64, 67.59, 64.34, 61.67, 42.63, 38.53, 37.48, 37.23, 36.12, 32.67, 32.56, 30.91, 30.22, 28.74, 27.00, 24.80, 24.46, 24.39, 23.14, 22.76, 20.90, 20.75, 13.50, 9.02

MS (ESI): m/z = 615.4 ($M + Na^+$), calculated MW = 592.4.

Synthesis of compound 5

Compound 2 (2.50 g, 4.0 mmol), succinic anhydride (1.6 g, 16 mmol), triethyl amine (2.0 g, 20 mmol) and DMAP (146 mg, 1.2 mmol) were dissolved in anhydrous CH_2Cl_2 (20 mL). The solution was stirred overnight. Ethyl acetate (70 mL) was added and then washed with HCl (25 mL, 1 M) and brine (100 mL). The organic phase was dried over Na_2SO_4 and then the solvent was removed. The residue was purified by flash column chromatography (ethyl acetate/hexanes = 1/1 and trace amount of acetic acid) to give compound 5 (2.89 g), yield: 87.8%.

^{1}H NMR (500 MHz, $CDCl_3$): δ (ppm) = 10.79 (br, 2H), 5,96 (d, *J* = 9.7 Hz, 1H), 5.75 (dd, *J* = 9.7 Hz, 6.3Hz, 1H), 5.48 (s, 1H), 5.35 (d, *J* = 2.6 Hz, 1H), 5,23 (pent, *J* = 6.2 Hz), 4.89 (m, 1H), 4.08 (t, *J* = 6.6 Hz, 2H), 3.63 (t, *J* = 6.2 Hz, 2H), 2.55-2.75 (m , 10H), 2.42 (s, 1H), 2.34 (dd, *J* = 11.4 Hz, 6.1Hz, 1H), 1.94 (m, 1H), 1.87

(s, 3H), 1.84 (m, 1H), 1.60-1.70 (m, 4H), 1.40-1.60 (m, 5H), 1.34 (m, 1H), 1.105 (s, 3H), 1.098 (s, 3H), 1.06 (d, *J* = 7.4 Hz, 3H), 0.85 (s, 9H), 0.81 (d, *J* = 7.0 Hz, 3H), 0.80 (t, *J* = 7.5 Hz, 3H), 0.05 (s, 6H).

^{13}C NMR (125 MHz, $CDCl_3$): δ (ppm) = 178.11, 177.32, 176.71, 171.66, 171.17, 170.07, 132.79, 131.43, 129.57, 128.26, 71.55, 68.12, 68.04, 64.62, 62.57, 42.92, 38.43, 37.73, 37.47, 36.13, 32.86, 31.10, 30.35, 29.02, 28.93, 28.79, 27.16, 25.85, 25.03, 24.60, 24.58, 23.60, 22.97, 18.23, 13.69, 9.19, -5.42.

MS (ESI): m/z = 845.0 ($M + Na^+$), calculated MW = 822.4.

Synthesis of compound 6

Compound 5 (1.65 g, 2.0 mmol) and DMAP (73 mg, 0.6 mmol) were dissolved in anhydrous CH_2Cl_2 (20 mL) and cooled to 0 °C. *N,N'*-Dicyclohexylcarbodiimide (DCC, 1.24 g, 6.0 mmol) in anhydrous CH_2Cl_2 (5 mL) was added and then compound 4 (2.48 g, 4.6 mmol) was added. The solution was stirred at 0 °C for 1 hr. Dichloromethane (70 mL) was added and filtered to remove the solid. The filtrate was then concentrated. The residue was purified by column chromatography (ethyl acetate/hexanes = 1/2 to 1/1) to give compound 6 (3.53 g), yield: 89.6%.

^{1}H NMR (500 MHz, $CDCl_3$): δ (ppm) = 5,93 (d, *J* = 9.7 Hz, 3H), 5.73 (dd, *J* = 9.7 Hz, 6.3Hz, 3H), 5.45 (s, 3H), 5.29 (d, *J* = 2.6 Hz, 3H), 5,18 (pent, *J* = 6.1 Hz, 3H), 4.83 (m, 3H), 4.08 (m, 10H), 3.58 (t, *J* = 6.2 Hz, 2H), 2.59 (s, 3H), 2. 56 (m, 14H), 2.34 (dd, *J* = 11.4 Hz, 6.1Hz, 1H), 2.21 (d, *J* = 11.7 Hz, 1H), 2.02 (s, 6H), 1.98 (s, 6H), 1.94 (m, 9H), 1.87 (m, 3H), 1.40-1.70 (m, 27H), 1.31 (m, 3H), 1.14 (m, 3H),

1.07 (s, 9H), 1.06 (s, 9H), 1.03 (d, *J* = 7.4 Hz, 9H), 0.84 (s, 9H), 0.82 (d, *J* = 7.0 Hz, 9H), 0.78 (t, *J* = 7.5 Hz, 9H), 0.01 (s, 6H).

^{13}C NMR (125 MHz, $CDCl_3$): δ (ppm) = 177.28, 177.23, 171.98, 171.85, 171.59, 171.12, , 170.29, 169.78, 169.76, 169.74, 132.68, 132.62, 131.39, 131.36, 129.49, 129.46, 128.21, 71.34, 70.89, 67.91, 67.64, 67.58, 64.46, 63.94, 63.93, 63.87, 63.85, 62.31, 60.12, 42.69, 38.51, 38.29, 37.57, 37.33, 36.20, 32.76, 32.67, 30.96, 30.30, 28.99, 28.92, 28.76, 28.72, 27.09, 25.75, 25.01, 24.55, 24.51, 24.48, 23.40, 23.21, 22.84, 20.99, 20.83, 18.10, 14.02, 13.63, 13.60, 9.11, 05.51

MS (ESI): m/z = 1994.9 ($M + Na^+$), calculated MW = 1971.4.

Synthesis of compound 7

Compound 6 (3.13 g, 1.59 mmol) was dissolved in a mixture solution (methanol/CH_2Cl_2 = 1/1, 20 mL) and cooled to 0 °C. TsOH monohydrate (60.4 mg, 0.32 mmol) was added. The solution was stirred at 0 °C for 1 hr. Ethyl acetate (100 mL) was added and then washed with brine (80 mL×3). The organic phase was dried over Na_2SO_4 and then the solvent was removed. The residue was purified by flash column chromatography (ethyl acetate/hexanes = 1/1) to give compound 7 (2.59 g), yield: 87.8%.

^{1}H NMR (500 MHz, $CDCl_3$): δ (ppm) = 5.97 (d, *J* = 9.7Hz, 3H), 5.77 (dd, *J* = 9.7 Hz, 6.3Hz, 3H), 5.50 (s, 3H), 5.33(d, *J* = 2.6Hz, 3H), 5.23 (pent, *J* = 6.1 Hz, 3H), 4.87 (m, 3H), 4.11 (m, 10H), 3.66 (t, *J* = 6.2 Hz, 2H), 2.61 (m, 14H), 2.43 (s, 3H), 2.34 (dd, *J* = 11.4 Hz, 6.1Hz, 3H), 2.21 (d, *J* = 11.7 Hz, 3H), 2.06 (s, 6H), 2.04 (s, 6H), 1.94 (m, 9H), 1.85 (m, 3H), 1.50-1.70 (m, 24H), 1.46 (m, 3H), 1.33 (m, 3H),

1.13 (m, 3H), 1.11 (s, 9H), 1.10 (s, 9H), 1.07 (d, *J* = 7.4 Hz, 9H), 0.86 (s, 9H), 0.82 (d, *J* = 7.0 Hz, 9H), 0.82 (t, , *J* = 7.4 Hz, 9H).

^{13}C NMR (125 MHz, $CDCl_3$): δ (ppm) = 177.45, 172.15, 172.09, 171.78, 171.26, 170.47, 169.94, 169.84, 177.45, 172.15, 172.09, 171.78, 171.26, 170.47, 169.94, 169.84, 132.74, 131.45, 129.63, 128.30, 71.43, 71.00, 68.08, 67.75, 67.71, 64.50, 64.06, 64.00, 62.07, 42.81, 38.61, 38.47, 37.66, 37.43, 36.29, 32.87, 32.86, 32.76, 31.16, 31.06, 30.40, 29.09, 29.03, 28.86, 28.80, 27.19, 25.09, 24.98, 24.66, 24.64, 24.61, 24.58, 23.54, 23.31, 22.94, 21.10, 20.95, 13.73, 13.69, 9.21, 9.20

MS (ESI): m/z = 1880.6 ($M + Na^+$), calculated MW = 1857.4

Synthesis of compound 8

Compound 7 (386 mg, 0.21 mmol) and DMAP (5.1 mg, 0.04 mmol) were dissolved in anhydrous dichloromethane (20 mL) and cooled to 0 °C. DCC (65g, 0.315mmol) in anhydrous dichloromethane (3 mL) was added and then bromoacetic acid (38.4 mg, 0.27 mmol) was added. The solution was stirred at 0 °C for 1 hr. Dichloromethane (70 mL) was added and filtered to remove the solid. The filtrate was then concentrated. The residue was purified by column chromatography (ethyl acetate/hexanes = 1/2) to give compound 8 (336 mg, 0.172 mmol), yield: 82.1%.

^{1}H NMR (500 MHz, $CDCl_3$): δ (ppm) = 5.97 (d, *J* = 9.7Hz, 3H), 5.77 (dd, *J* = 9.7Hz, 6.3Hz, 3H), 5.50 (s, 3H), 5.33(d, *J* = 2.6 Hz, 3H), 5.23 (pent, *J* = 6.1 Hz, 3H), 4.87 (m, 3H), 4.20 (t, 5.8 Hz, 2H), 4.11 (m, 10H), 3.85 (s, 2H), 3.65 (t, *J* = 6.2 Hz, 2H), 2.63 (s, 6H), 2.63 (s, 6H), 2.61 (s, 4H), 2.59 (s, 4H), 2.43 (s, 3H), 2.34 (dd, *J* =

11.4 Hz, 6.1 Hz, 3H), 2.22 (d, *J* = 11.7Hz, 3H), 2.06 (s, 6H), 2.04 (s, 6H), 1.94 (m, 9H), 1.85 (m, 3H), 1.50-1.70 (m, 24H), 1.46 (m, 3H), 1.33 (m, 3H), 1.13 (m, 3H), 1.11 (s, 9H), 1.10 (s, 9H), 1.07 (d, *J* = 7.4 Hz, 9H), 0.86 (d, *J* = 7.0Hz, 9H), 0.82 (t, , *J* = 7.4Hz, 9H).

^{13}C NMR (125 MHz, $CDCl_3$): δ (ppm) = 177.39, 177.35, 172.06, 171.94, 171.71, 171.20, 170.40, 169.87, 169.77, 167.07, 132.70, 131.42, 129.59, 128.27, 71.38, 70.96, 67.95, 67.71, 67.67, 65.52, 64.02, 64.00, 63.98, 63.94, 63.89, 42.77, 38.58, 38.35, 37.67, 37.62, 37.40, 36.26, 32.84, 32.82, 32.73, 31.07, 31.02, 30.37, 29.05, 28.98, 28.82, 28.76, 27.15, 25.68, 25.06, 24.95, 24.63, 24.61, 24.58, 24.55, 23.50, 23.28, 22.90, 21.07, 20.91, 13.70, 13.66, 9.16.

Synthesis of compound 9

Compound 8 (300 mg, 0.154 mmol) was dissolved in anhydrous acetonitrile (5 mL) and cooled to 0°C. Tris(tetrabutylammonium) hydrogen pyrophosphate (277 mg, 0.308 mmol) was added. The solution was stirred at 0 °C for 1 hr. The organic solvent was removed. The residue was then dissolved in water and the solution went through the sodium resin to exchange the cation to sodium. The elution was then lyophilized. The residue was then purified by cellulose column chromatography (isopropanol/acetonitrile/H_2O = 1:1:2) to give product compound 9 (176 mg), yield: 54.1%.

^{1}H NMR (500 MHz, DMSO): δ (ppm) = 5.95 (d, *J* = 9.7 Hz, 3H), 5.77 (dd, *J* = 9.7 Hz, 6.3Hz, 3H), 5.50 (s, 3H), 5.2 (s, 3H), 5.11 (pent, *J* = 6.1 Hz, 3H), 4.76 (m, 3H), 4.35 (d, 6.1 Hz, 2H), 4.09 (s, 2H), 4.03 (s, 8H), 2.63 (m, 6H), 2.56 (m, 12H), 2.47

(s, 3H), 2.38 (dd, *J* = 11.4 Hz, 6.1Hz, 3H), 2.24 (d, *J* = 11.7 Hz, 3H), 1.98 (s, 6H), 1.97 (s, 6H), 1.94 (m, 9H), 1.85 (m, 3H), 1.50-1.70 (m, 24H), 1.46 (m, 3H), 1.33 (m, 3H), 1.13 (m, 3H), 1.04 (s, 9H), 1.02 (s, 9H), 1.01 (d, *J* = 7.4 Hz, 9H), 0.81 (d, *J* = 7.0 Hz, 9H), 0.76 (t, , *J* = 7.4Hz, 9H).

^{31}P NMR (202.5MHz, DMSO): δ (ppm) = -9.46, -10.67.

2.2.3 Comparing aqueous solubility of SIM-PPi and SIM

This experiment was conducted to compare the aqueous solubility of SIM-PPi and free SIM. The solubility values of SIM-PPi and SIM were obtained by measuring equilibrium solubility after adding the analyte to the testing medium for a predetermined period of time(11,12). Briefly, SIM-PPi and SIM, (1 mg/mL) each, were added to either deionized water or phosphate buffer in microcentrifuge tubes. The suspensions were agitated on a rotor at 22 ± 2 °C for 48 hr to reach the equilibrium. The mixtures were then centrifuged (2,000 rpm, 5 min) to settle the undissolved drug. The supernatants (saturated solutions) were obtained by filtering through 0.2 µm syringe filters, and then the SIM-PPi and SIM concentrations were measured using a UV spectrophotometer (SpectraMax M2, Molecular Devices, Sunnyvale, CA, USA) at 230 nm.

2.2.4 In vitro hydroxyapatite (HA) binding assay

To predict the binding of SIM-PPi to HA, which is the primary inorganic component of natural hard tissues, an *in vitro* binding test was performed using HA particles (Bio-Gel HTP, particle size is a range of 10-90 um, Bio-Rad). Briefly, SIM-PPi (1 mg/mL) was dissolved in 4 mL 25% isopropyl alcohol (1 mL of isopropyl alcohol diluted in 3 mL of 1.3× PBS to achieve final concentration of 1× PBS composed of 11.9 mM phosphates, 137 mM sodium chloride, and 2.7 mM potassium chloride). HA (100 mg) was then added to the solution. The PBS solution of alendronate (ALN) and SIM acid were separately prepared and mixed with HA (100 mg) for the binding analysis. All binding media contained 11.9 mM phosphates, 137 mM sodium chloride, and 2.7 mM potassium chloride. All three suspensions were agitated in micro-centrifuge tubes on a rotary mixer for varying lengths of time (30 min, 2 hr and 6 hr). At the end of each time point, the HA was spun down by centrifuging at 85 ×g for 5 min. The binding affinity was assessed by measuring the relative concentration of SIM-PPi, SIM, and ALN in the supernatants. The concentrations of SIM-PPi and SIM was detected by measuring the absorbance at 230 nm using a UV spectrophotometer (SpectraMax M2, Molecular Devices, Sunnyvale, CA, USA). The concentration of ALN was measured using the ninhydrin assay(13). The relative HA binding was calculated according to the following formula:

$$\text{HA binding } (\%) = \frac{(X - Y)}{X} \times 100$$

where X is the initial concentration (1 mg/mL) and Y is the concentration in the supernatant after incubation with HA.

2.2.5 Cell culture

Cell viability assay

Mouse macrophage RAW 264.7 and osteoblast MC3T3-L1 cell lines were cultured in Dulbecco's modified Eagle Medium (DMEM) and Minimum Essential Media (MEM), respectively. Each medium was supplemented with 10% fetal bovine serum (FBS) and 1% penicillin/streptomycin (basal growth mediums). Cells were incubated at 37 °C in 5% CO_2 to 90% confluence. Cellular toxicity of SIM-PPI was evaluated using the 3-(4,5-dimethyl-thiazol-2yl)-2,5- diphenyltetrazoliumbromide (MTT) assay. Briefly, RAW 264.7 and MC3T3-L1 cells were seeded in 96 well plates (1×10^4 cells/well) and treated with various concentrations of SIM-PPi, free SIM (0.01 nM to 1 mM, SIM equivalent), and free PPi (PPi in SIM-PPi equivalent), and then incubated for 24, 48 and 72 hr. Following each time point, 10 µL of MTT reagent were added to each well and further incubated for 4 hr at 37 °C. MTT detergent reagent (100 µL) was added to each well to solubilize deposited formazan, then incubated in the dark at room temperature for 2 hr. The

absorbance of each well was recorded at 570 nm using a microplate reader (SpectraMax M2, Molecular Devices, Sunnyvale, CA, USA).

Measurement of LPS-induced cytokine

LPS-induced pro-inflammatory cytokines were measured to investigate whether SIM-PPi retains the anti-inflammatory property of SIM. RAW 264.7 cells were seeded into 24-well plate (2×10^5 cells/well) in 1 mL medium and incubated overnight. The cells were pre-treated with 100 nM SIM or its equivalent SIM-PPi or PPi (PPi in SIM-PPi equivalent) for 1 hr before LPS challenge (1 μg/mL); the cells were then incubated in a 37 °C, 5% CO_2 incubator for 24 hr. Supernatants were collected and centrifuged, then stored at -80 °C until assayed for IL-6 and IL-1β concentrations using ELISA kits according to the manufacturer's protocols (Invitrogen).

Measurement of alkaline phosphatase (ALP) activity

Intracellular ALP was measured using *p-nitrophenyl phosphate as a substrate* to investigate whether SIM-PPi retains the osteoinductive property of SIM. *Briefly,* MC3T3-L1 cells were seeded in 24-well plates at a density of 4×10^4 cells/well in the basal growth medium. At 80% confluence, 100 nM SIM or its equivalent of SIM-PPi or PPi (PPi in SIM-PPi equivalent) were added to the basal growth medium supplemented with 4 mM inorganic phosphate as a phosphate ions source, and the incubation was continued with medium changed every 72 hr. A

negative control group (con-) was cultured in only basal growth medium to observe any spontaneous differentiation. Also, a positive control group (con+) was included and cultured in an osteogenic medium which was composed of basal growth medium, 4 mM inorganic phosphate, and osteoinductive supplements (0.28 mM ascorbic acid and 100 nM dexamethasone). After 3, 7, and 14 days, the culture medium was removed, and cell lysate was prepared according to the assay protocol. The cells were washed twice with ice-cold phosphate buffered saline (PBS) followed by scraping the cells with 100 µl of ice-cold lysis buffer. The cells were homogenized with the lysis buffer and centrifuged at high speed (13,000×g for 3 min); the supernatants were frozen at -20 °C until assayed for the ALP activity using a commercial ALP assay kit (BioVision Incorporated, Milpitas, CA).

Alizarin red S staining and quantification

To visualize calcium deposition by differentiated osteoblasts, MC3T3-L1 cells in a 24-well plate were stained with Alizarin red S (ARS) after 28 days of culture with medium change every 72 hr. Briefly, after washing the cellular monolayer with PBS, cells were fixed with 10% formalin for 30 min at room temperature, washed twice with DI water, and then stained with 2% ARS solution (pH 4.3) at room temperature in the dark for 45 min. Cells were then washed five times with DI water and observed for the presence of calcium deposition as identified by red color presence. ARS staining was quantified using the method described by Gregory CA., et al (14). Briefly, following cells staining and washing, the plate was

placed in the freezer overnight to dry samples, and then 0.2 mL of 10% acetic acid in each well was added, and the plate was incubated at room temperature with shaking for 30 min. Cells with acetic acid were then scrapped and collected in a micro-centrifuge tube, and vortexed for 30 seconds, followed by heating for 10 min at 85 °C, and then cooling in an ice bath. After centrifugation at 20,000 ×g for 15 min, supernatants were collected, and adjusted pH to 4.3 with 10% ammonium hydroxide (75 µL). Lastly, each sample (50 µL) was placed in an opaque-walled 96-well plate with clear bottom and absorbance measured at 405 nm using a microplate reader (SpectraMax M2, Molecular Devices, Sunnyvale, CA, USA).

von Kossa staining

To further visualize and confirm the mineralized *nodules*, cells were stained with von Kossa stain after 28 days in culture with medium change every 72 hr; wherein silver ions replace calcium and react with phosphate under strong light to be seen as metallic silver. Cells were washed and fixed in 10% formalin for 30 min, washed with DI water, and then incubated with 5% silver nitrate solution (RICCA Chemical company) at room temperature under bright light for 45 minutes or until mineral deposits turned black or dark brown. After that, cells were washed 3 times with DI water, followed by incubating with 5% sodium thiosulfate (Alfa Aesar) for 5 min to remove unreacted silver. After washing with ID water five times, wells were photographed and visually examined for calcium deposits.

2.2.6 Evaluation of SIM-PPi's therapeutic efficacy on an experimental periodontitis rat model

Sprague Dawley rats (female, 10-month-old, retired breeders) were purchased from Envigo. The animals were acclimated for one week prior to any experimental procedure. Rats were divided randomly into four groups: experimental periodontitis with saline injection; experimental periodontitis with SIM treatment; experimental periodontitis with PPi treatment; experimental periodontitis with SIM-PPi treatment (Table I). A power analysis was performed to determine the number of animals needed to show a 30% difference in bone area stimulated by simvastatin prodrug compared to a control. This analysis used data from previous studies(15,16). In order to detect a greater than 30% change in bone 80% of the time when testing at the 5% level of significance (assuming normality of the data), at least 5 animals would be needed in each group. Since 8 rats/group was used in a previous study testing the same ligature-induced periodontitis model(9), we used the same animal group size. Silk ligatures were used to induce the experimental periodontitis as previously described(9). Briefly, each rat was anesthetized using a chamber attached to isoflurane vaporizer (1- 4% isoflurane and 100% oxygen), followed by body weight measurement. To maintain anesthesia during experimental procedures, a nose cone (0.5% - 2% isoflurane and 100% oxygen) was applied throughout the entire experimental procedure. Experimental periodontitis was induced in all groups by gently tightening a 4-0 silk ligature around the maxillary 2nd molars in both sides. All animals were monitored and checked weekly to monitor the progression of periodontitis. Post-procedure

analgesic (flunixin 2.5 mg/kg, *s.c.* every 12 hr) was given when signs of pain were observed. After 2 weeks, ligatures were removed. Different treatments including SIM-PPi (dissolved in 25% isopropyl alcohol as described in the HA binding study, 2.56 mg, equivalent to 1.5mg SIM), SIM acid (dissolved in PBS, 1.56 mg, equivalent to 1.5 mg of SIM), and PPi (dissolved in PBS, 0.26 mg, equivalent to the PPi content in SIM-PPi) were locally injected (10µL) into the palatal gingiva between the maxillary first molar (M1) and second molar (M2) on the first day of week 1, 2 and 3 after ligature placement. In the treatment of human periodontitis, this local delivery would be accompanied by scaling and root planing, but lack of long-term root contamination imprecise root planing with the rat model have led to its omission in most recent local drug-delivery studies(17–19). At week 4, all animals were euthanized using CO_2 asphyxiation followed by dissecting the entire palate including all three molars and placed in 10% formalin for µ-CT and histological evaluations. All animal procedures were approved by the Institutional Animal Care and Use Committee (IACUC) of University of Nebraska Medical Center (UNMC).

2.2.7 Micro-computed tomography (µ-CT) analysis

At the end-point, palates including all three molars on both sides were collected and fixed in 10% formalin. All samples were scanned using a micro-CT imaging system (Bruker SkyScan1172, Kontich, Belgium), as described in previous studies (9,10). The voltage and current of X-ray source were set at 70 kV and 141 µA,

respectively, with a pixel size of 8.6 µm and a 0.5 mm-thick aluminum filter was used. The exposure time was 580 ms, and X-ray projections were obtained at 0.7° intervals with a scanning angular rotation of 180°, and 8 frames were averaged for each rotation. To generate three-dimensional (3D) images, scans were reconstructed using the system-reconstruction software (NRecon; Skyscan). Sagittal sections were obtained using the Skyscan DataViewer software, then the linear distance from the cementoenamel junction (CEJ) to the alveolar bone crest (ABC) was measured in millimeters using the Skyscan CT-Analyzer software. For each sample, the linear distance was measured from two points: distopalatal of M1 and mesiopalatal of M2. Longer distance means more bone loss and vice versa. Coronal sections obtained using the Skyscan DataViewer were used to measure bone volume (BV), trabecular thickness (Tb.Th), trabecular number (Tb.N) and trabecular separation (Tb.Sp) using the CT Analyzer. A rectangular region of interest (ROI, excluding the roots) was selected, with its length extended from the distopalatal of M1 to the mesiopalatal of M2, width from the palatal side to the midline of M1 and M2, and height 130 slices below CEJ of M1 and M2. The sample analysis was performed by two examiners independently to ensure accurate assessment.

2.2.8 Histological evaluation

After completing the µ-CT analysis, all specimens were decalcified in 14% ethylenediaminetetraacetic acid (EDTA) solution for one month. After decalcification, samples were embedded in paraffin. Sagittal sections (5µm) were obtained in a mesiodistal direction with roots aligned in one plane and then stained

with hematoxylin and eosin for microscopic observation. To evaluate connective tissues between M1 and M2 for inflammatory cell infiltrate and alveolar crest for osteoclasts, a pathologist (SML) who was blind to experimental groups qualitatively assessed samples using a light microscope (Olympus System Microscope Model BX53) under 200× magnification. Neutrophils and lymphocytic infiltrate were evaluated qualitatively in the gingival tissues above the alveolar crest using a scoring system(20,21) (Table II). Osteoclasts lining the surface of alveolar crest were also qualitative assessed using a scoring system(22) (Table III).

2.2.9 Statistical analysis

All the obtained data were presented as the mean ± standard deviation (SD). Statistical analysis was performed using SPSS 22.0 software (SPSS Inc., Chicago, IL, USA) and Prism 7.0 software (GraphPad, San Diego, CA). Continous outcomes among more than three groups were compared using the one-way Analysis of Variance (ANOVA) for one variable data and two-way ANOVA for two variable data. Tukey's post-hoc multiple comparisons was conducted in case a significant difference among the group means was found. *P*-value < 0.05 was considered statistically significant.

2.3 RESULTS

2.3.1 Aqueous solubility of SIM-PPi

The aqueous solubility of SIM-PPi at 22 ± 2 °C and pH 7 was analyzed and compared to SIM. The solubility of SIM-PPi was determined to be 0.899 mg/mL (equivalent to 0.53 mg/mL of SIM) after being equilibrated for 48 hr in deionized water and 0.969 mg/mL (equivalent to 0.57 mg/mL of SIM) in phosphate buffer. For SIM, its solubility was determined to be 0.0025 mg/mL in deionized water and 0.0073 mg/mL in phosphate buffer. Clearly, conjugating PPi to SIM trimer has greatly improved SIM's water solubility.

2.3.2 SIM-PPi binding to hydroxyapatite (HA)

HA binding assay was performed to assess the bone affinity of SIM-PPi (Fig. 1). After 30 min incubation, SIM-PPi showed significantly higher (23%) binding to HA when compared to SIM alone which did not show any binding. As the HA incubation time extended to 2 hr, SIM-PPi's binding to HA increased to 50% and reached the plateau. After 6 hr of incubation, SIM-PPi's binding to HA remained at 51%. During the entire binding study, SIM exhibited minimum binding to HA. As a strong osteotropic agent and a positive control for the HA binding experiment, ALN showed very strong binding to HA (77%) as expected.

2.3.3 Cell viability

To evaluate the *in vitro* safety of SIM-PPi, both RAW264.7 and MC3T3-L1 cells were treated with wide range of concentrations of SIM-PPi (1 nM to 1mM, SIM equivalent) for 24, 48 and 72 hr and the cell viability was determined using the MTT assay (Figure 2). For both cell lines, they almost shared the same toxicity profile. The viability of RAW 264.7 cells treated with more than 100 μM of SIM-PPi (SIM equivalent) was substantially decreased over the three days, the viability was less than 60% after 72 hr. The viability of MC3T3-L1 cells treated with more than 250 μM of SIM-PPi (SIM equivalent) was decreased dramatically after three days (less than 40%). However, when both cell lines treated with more than 100 nM of free SIM, the viability was reduced over the three days, indicating that SIM has narrower toxicity range than SIM-PPi. Free PPi increased cell populations and did not show any signs of toxicity for 72 hr. Hence, 100 nM of SIM-PPi (SIM equivalent) was used in the following experiments as non-toxic concentration to evaluate both anti-inflammatory and osteogenic effects on macrophages RAW 264.7 and osteoblasts MC3T3-L1, respectively.

2.3.4 Effect of SIM-PPi on LPS-induced cytokines

The concentrations of IL-6 and IL-1β were detected in the culture supernatants of RAW 264.7 cells using ELISA kits (Fig. 3). LPS challenged cells showed a tremendous increase in both cytokines comparing to the control group (medium only). SIM-PPi treated group showed a significant reduction in IL-6 ($P < 0.05$) and

IL-1β ($P < 0.0001$) when compared to the LPS group. The SIM-treated group exhibited the lowest concentration of both IL-6 and IL-1β.

2.3.5 ALP activity measurement

The ALP activity in the control and experimental groups are shown in Figure 4B. The cells in the negative control culture did not show any significant activity of ALP after 3, 7, and 14 days, as expected. As anticipated, in the positive control culture, the cells expression of ALP was increased significantly over 14 days. Among all the tested samples, free SIM culture showed the highest level of ALP after 3, 7, and 14 days ($P < 0.0001$). At day 7, ALP activity increased significantly for SIM-PPi and PPi cultures compared to the negative control ($P < 0.0001$). After 14 days, SIM-PPi culture continued to express a substantial level of ALP as compared to the negative control ($P < 0.0001$), while PPi culture showed a slight decrease in the ALP activity.

2.3.6 Alizarin red S (ARS) and von Kossa staining

To evaluate calcium deposit and mineralized nodules, ARS and von Kossa staining assays were used. As shown in Figure 4A&C, the two stains showed similar observations, and they were both in agreement with the ALP findings. The negative control group showed very little calcium deposit and ARS quantity, while positive control and SIM treated groups exhibited significant ARS quantity ($P < 0.0001$) with the highest mineralized nodules when compared to negative control (con-), as expected. And most importantly, SIM-PPi treated group showed

significantly higher ARS quantity ($P < 0.01$) when compared to negative control and PPi groups, with more mineralized nodules formation. PPi group has the lowest ARS quantity and calcium deposit among all tested groups except the negative control.

2.3.7 Micro-computed tomography (μ-CT) analysis

As shown in Figure 5A, it is obvious that the SIM-PPi treated group preserved alveolar bone crest compared to other treated groups. The linear distance of CEJ to ABC, representing alveolar crest height, indicated that the SIM-PPi treated group had significantly shorter distance when compared to saline-treated group (0.98 mm vs. 1.32 mm, $P > 0.05$). SIM and PPi treated groups did not exhibit statistically significant differences when compared to the saline-treated group as presented in Figure 5B. For further validation of alveolar bone loss, different bone volumetric parameters, as shown in Figure 6, were quantified. The SIM-PPi treated group demonstrated significantly ($P > 0.05$) different values in bone volume (BV, 0.85 mm^3 vs. 0.38 mm^3), trabecular thickness (Tb.Th, 0.78 mm vs. 0.62 mm), trabecular number (Tb.N, 2.86 mm^{-1} vs. 1.69 mm^{-1}) and trabecular separation (Tb.Sp, 0.35 mm vs. 0.47 mm) than the saline group. In contrast, when comparing SIM and PPi treated groups to the saline group, none of the above parameters produced statistically significant differences.

2.3.8 Histological evaluation

To evaluate the effect of the different treatments on the inflammatory infiltrate and osteoclasts, H&E stained sections were assessed qualitatively. Histology scores of neutrophils and lymphocytes were shown in Figure 7B-C, based on the grading criteria in Table II. SIM-PPi treated group earned the lowest score of neutrophils ($P < 0.01$) and lymphocytes ($P < 0.0001$) when compared to saline group, while neutrophils of SIM-treated group did not exhibit statistically significant difference when compared to the saline group. Osteoclast scores of the SIM-PPi-treated group were the lowest among all the treatment groups and were significantly lower than the saline-treated group (Figure 7D, $P < 0.05$).

2.4 DISCUSSION

Simvastatin (SIM) has been reported to have osteogenic (7,8) and anti-inflammatory properties (23,24), making it a promising candidate for therapeutic intervention for periodontal diseases. Local application of SIM has been explored in periodontitis treatment (25–28). The lack of osteotropicity and its poor water solubility have limited the clinical applications of SIM in managing periodontitis. To overcome these limitations, alternatives technologies for local delivery of SIM have been developed to enhance solubility and to provide a sustained release; and have shown potential protection of the periodontal tissues. In a previous study, local application of SIM (0.5 mg)/alendronate-β-cyclodextrin complex (SIM–ALN–CD) was tested on an LPS-induced periodontitis as a preventative agent against a future episode of periodontitis. It was concluded that the locally applied SIM–ALN–CD has the potential to prevent periodontitis associated bone loss(10). A concern with this formulation is the use of ALN (a bisphosphonate) as the bone-homing moiety. It has been well recognized that the long-term clinical use of bisphosphonates has been associated with higher incident rates of osteonecrosis of the jaw (ONJ) and atypical fracture (29,30). Another previous study aimed to examine the effect of a locally delivered SIM prodrug in a ligature-induced periodontitis rat model(9). The amphiphilic macromolecular prodrug of SIM (1.5 mg) was designed and prepared by conjugating SIM trimer to a polyethylene glycol monomethylether (mPEG) molecule. The study concluded that three weekly injections of the macromolecular SIM prodrug (SIM-PEG) decreased alveolar bone

loss and inflammation in rats. While the SIM-PEG design solubilizes SIM in water by forming micelles, a limitation of this prodrug is its lack of osteotropicity and the relatively low drug loading.

To provide SIM with better water solubility and osteotropicity but also to avoid potential long-term side effects associated with bisphosphonates (e.g. ONJ), we have developed a novel SIM prodrug by conjugating SIM trimer directly to a pyrophosphate (PPi) (Scheme 1). This design was built upon the findings of our previous studies(9,10). The three SIMs are chemically conjugated via ester bonds which can be hydrolyzed *in vivo* in the presence of esterases. One of the three SIMs conjugated to PPi is in the active SIM acid form, and the other two are in the lactone form, which would be activated upon exposure to the *in vivo* environment (e.g. esterase, water, low pH, and elevated temperature). Pyrophosphate (PPi) is a water-soluble and calcium-binding molecule. It is known for decades in the food industry as a leavening agent. Due to its high affinity to enamel, dentin, and tarter (31), it has been used widely in dental and oral care products (32–34). PPi is biodegradable (via phosphatase) with phosphate as its degradation product, which has a much better safety profile than the bisphosphonates (29,30). Therefore, we proposed to conjugate PPi to SIM-trimer to improve SIM's water solubility and to provide osteotropicity. The findings of the present study validate these design objectives and confirm the anti-inflammatory and periodontal bone preservation/regeneration capacity of the SIM-PPi design on an experimental periodontitis rat model.

Conjugating PPi to SIM trimer increased its water solubility over 200-fold. The binding experiment (Figure 1) showed that SIM-PPi has stronger binding to HA than free SIM, confirming that SIM-PPi as a bone-specific prodrug is a viable strategy for local delivery of SIM to the skeletal tissues. In Raw 264.7 culture, SIM-PPi was found to effectively inhibited LPS-induced interleukin-1β (IL-1β), which is considered as one of the most potent inducers of bone resorption, and interleukin-6 (IL-6), which is secreted in response to bone resorbing inducers including IL-1β(35). These findings suggest that SIM-PPi may reduce periodontal inflammation by attenuating the pro-inflammatory cytokines secreted by the inflammatory cells. The data also showed that SIM-PPi could significantly increase ALP activity in MC3T3-E1 culture after 7 and 14 days when compared to negative control (Figure 4B). In addition, ARS and Von Kossa staining data indicated that SIM-PPi significantly increased calcium deposits and mineralized nodules formation in MC3T3-E1 when compared to negative control (Figure 4A&C). Taken together, these *in vitro* data confirm that SIM-PPi retains the well-established SIM-mediated anti-inflammatory (23,24) and osteoinductive (36) activities after conjugating with PPi. It is important to note that due to its prodrug nature, SIM-PPi showed lower *in vitro* activity than SIM (SIM-PPi needs to be activated by exposing to an *in vivo* inflammatory condition: esterase, acidic pH, and elevated temperature).

When evaluated *in vivo* using a ligature-induced periodontitis rat model, micro-CT analysis of alveolar bone showed that the SIM-PPi treatment was the most effective treatment among all groups in preserving alveolar bone integrity (Figures 5&6). It significantly prevented alveolar crest loss (Figure 5) and maintained bone

volumetric parameters (BV, Tb.Th, Tb.N, and Tb.Sp) (Figure 6) when compared to saline control. Also, in accordance with the micro-CT findings, histological evaluation revealed a superior anti-inflammatory effect of SIM-PPi. It significantly reduced both inflammatory cell infiltrate (neutrophil and lymphocyte) and osteoclast score when compared to control (Figure 7). PPi itself did not show any significant protective effects against bone loss indicating that it did not contribute to preserving alveolar bone integrity. Ideally, a local treatment for periodontal bone loss should be given when developing periodontitis lesions are identified. Therefore, to make the treatment more clinically relevant, the weekly SIM-PPi injections was initiated at the time of ligature placement and continued for 3 weeks.

Overall, the weekly administration of SIM-PPi was found to be more effective in preventing periodontitis-induced alveolar bone loss when compared to dose equivalent SIM treatment. We believe that SIM-PPi's retention after local administration in combination with its gradual activation and releasing of simvastatin acid provide a rational explanation of the superior therapeutic effect of SIM-PPi over free SIM in prevention of alveolar bone loss associated with periodontitis. Furthermore, the weekly SIM-PPi administration schedule, possibly using pocket irrigation, would be easily adapted into current dental preventive care practice, indicative of a high clinical translation potential.

2.5 CONCLUSION

In this study, we report the design and synthesis of a novel osteotropic simvastatin (SIM) prodrug by conjugating three SIMs to a pyrophosphate (PPi). This prodrug design not only enhanced SIM solubility but also exhibited affinity to hydroxyapatite (HA), with retained bone anabolic and anti-inflammatory properties of SIM. When tested on an experimental periodontitis rat model, SIM-PPi was found to be effective in preserving periodontal bone. Upon further optimization, we believe this novel simvastatin prodrug may have the potential to be developed into a novel clinical management of periodontal diseases.

Table I. In vivo experimental design.

Group	Number	Side	Week 1*	Week 2*	Week 3*	Week 4
1	8	Left	Ligatures, SIM-PPi	SIM-PPi	Remove Ligatures, SIM-PPi	Euthanized
		Right	Ligatures, PPi	PPi	Remove Ligatures, PPi	Euthanized
2	8	Left	Ligatures, SIM	SIM	Remove Ligatures, SIM	Euthanized
		Right	Ligatures, Saline	Saline	Remove Ligatures, Saline	Euthanized

*Doses: SIM-PPi (2.56 mg, equiv. 1.5mg SIM), SIM acid (1.56mg, equiv. 1.5mg SIM), PPi (0.26 mg equivalent to PPi content in SIM-PPi). (10 µL injection volume).

Table II. Description of histological scores of neutrophils and lymphocytes.

Score	Evaluation
0	Normal (no inflammatory cells).
1	Few inflammatory cells (lining < 30 % of the affected tissues above the alveolar crest and between M1 & M2).
2	Some inflammatory cells (lining 30 - 60 % of the affected tissues above the alveolar crest and between M1 & M2).
3	Many inflammatory cells (lining > 60 % of the affected tissues above the alveolar crest and between M1 & M2).

Table III. Description of histological scores of osteoclasts.

Score	Evaluation
0	Normal (no osteoclasts).
1	Few osteoclasts (lining < 5% of most affected alveolar bone surface).
2	Some osteoclasts (lining 5 - 25% of most affected alveolar bone surface).
3	Many osteoclasts (lining 25 - 50% of most affected alveolar bone surface).

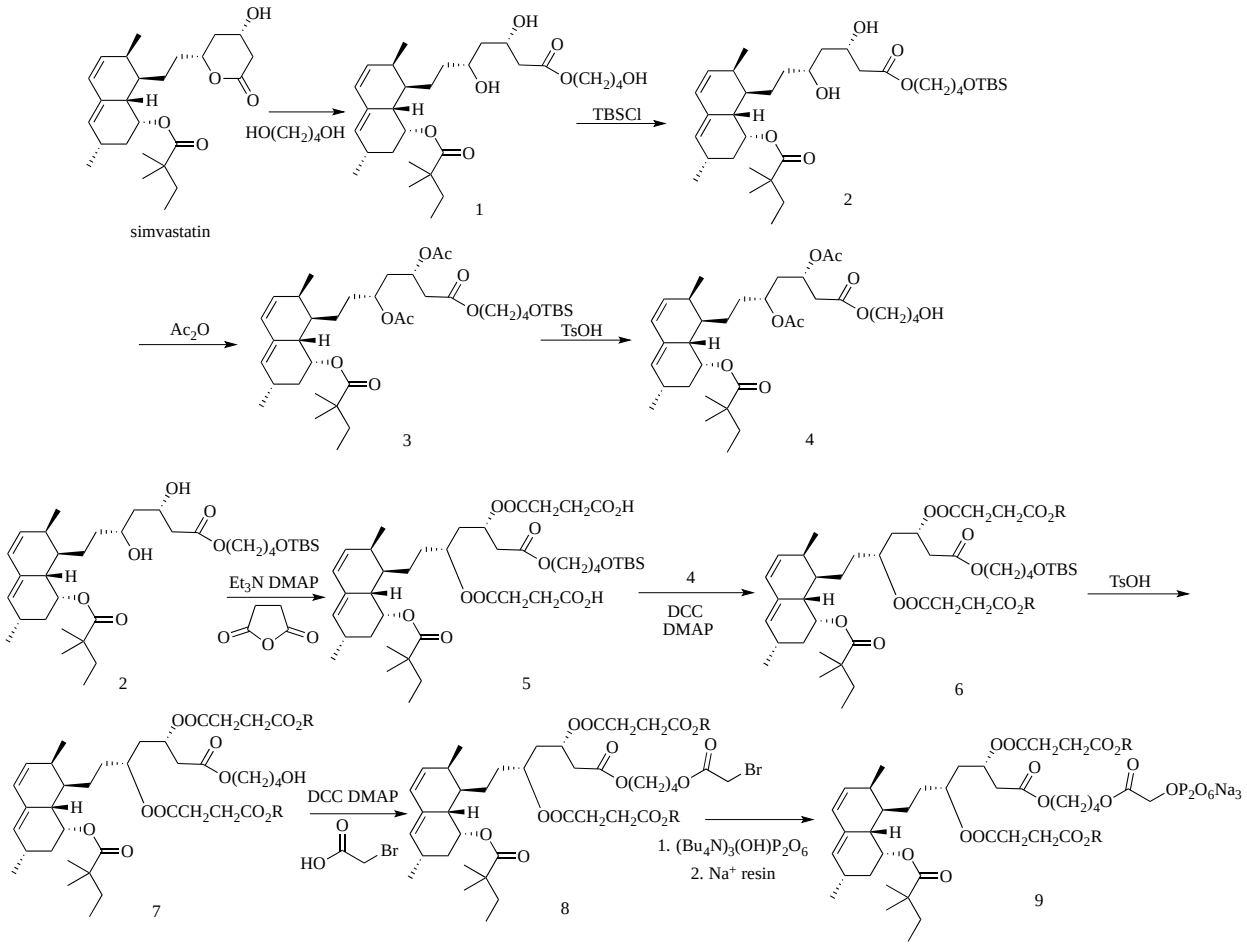

Scheme 1. The synthesis of simvastatin pyrophosphate prodrug (SIM-PPi).

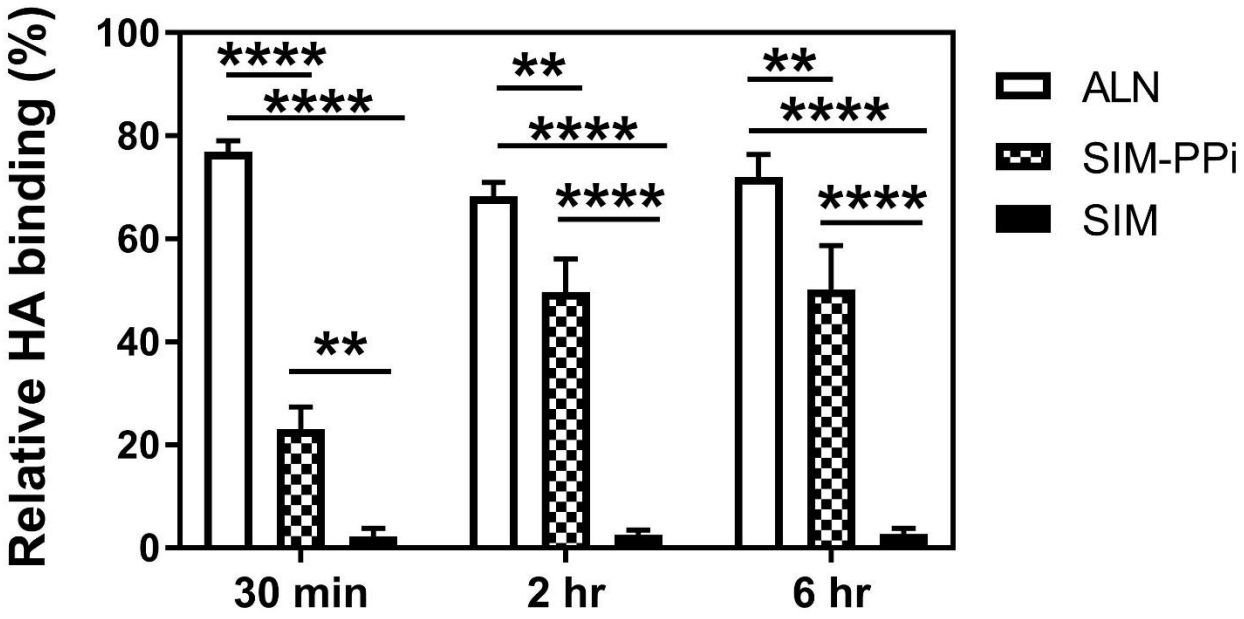

Figure 1. Quantitative assessment of hydroxyapatite (HA) binding of SIM-PPi with varying length of incubation time: 0.5, 2, and 6 hr. Alendronate (ALN) and free simvastatin (SIM) were used as a positive and negative controls, respectively. $^{*}p<0.05$, $^{**}p< 0.01$, and $^{****}p<0.0001$ (two-way ANOVA with Tukey's multiple comparisons).

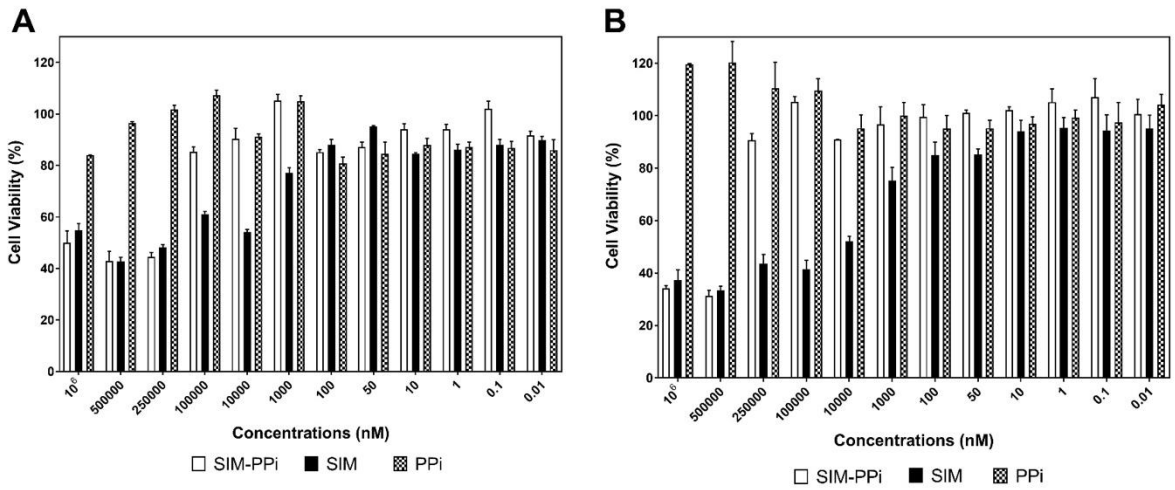

Figure 2. Effect of different concentrations of SIM-PPi, SIM, and PPi on growth of (A) Raw 264.7 cells and (B) MC3T3-E1 cells measured by MTT assay following 72-hour exposure. Data are shown as the mean ± SD.

.

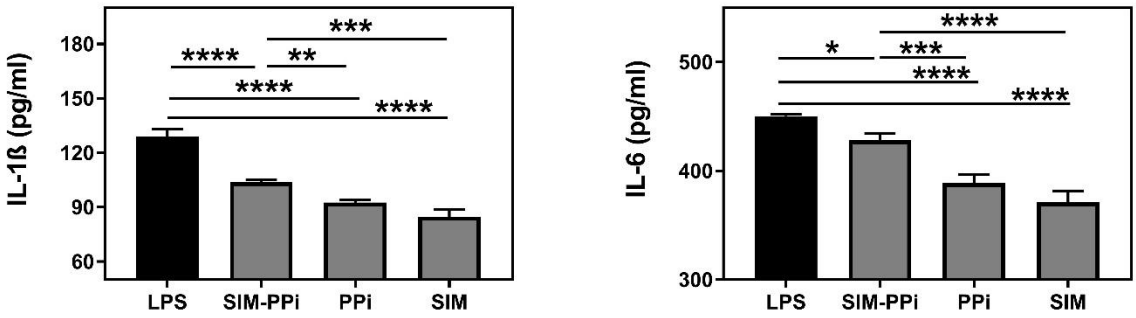

Figure 3. The impact of SIM (100 nM), PPi, and SIM-PPi (equivalent dose) on LPS-induced IL-1β and IL-6 secretion in RAW 264.7 cells. Mean cytokine concentrations are shown ± SD. $^{*}p< 0.05$, $^{**}p< 0.01$, $^{***}p<0.001$, and $^{****}p< 0.0001$ (one-way ANOVA with Tukey's multiple comparisons).

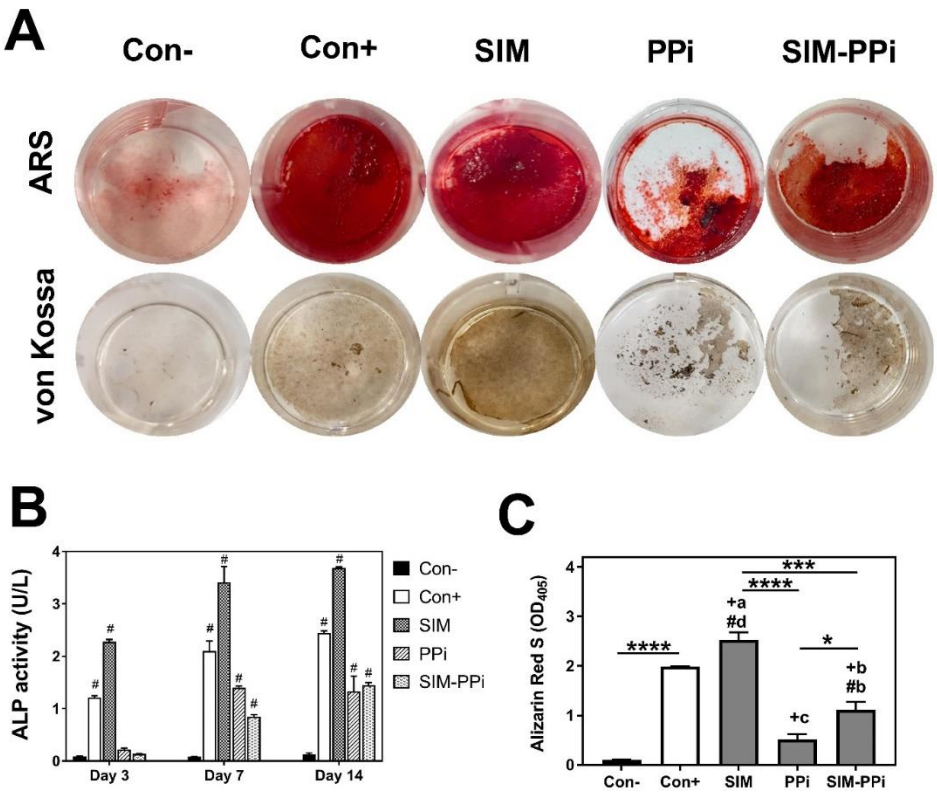

Figure 4. The in vitro evaluation of SIM-PPi's osteogenic efficacy using MC3T3-E1 cell line. **(A)** Representative images of Alizarin Red S **(**ARS) and von Kossa stained wells after 28 days of culture in a 24-well plate with SIM, PPi, and SIM-PPi treatments. **(B)** Alkaline phosphatase (ALP) activity of MC3T3-E1 cell line treated with 100 nM dose equivalent of SIM, PPi, and SIM-PPi. ALP was measured after 3, 7, and 14 days of culture. The values are shown as mean ± SD. $^{\#}p< 0.0001$ when compared to negative control (two-way ANOVA with Dunnett's multiple comparisons). **(C)** ARS quantification measured at 405 nm. $^{*}p<0.05$, $^{***}p<0.001$, $^{****}p<0.0001$. $^{\#b}p<0.01$ and $^{\#d}p<0.0001$ when compared to negative control group. $^{+a}p<0.05$, $^{+b}p<0.01$, and $^{+c}p<0.001$ when compared to positive control group (one-way ANOVA with Tukey's multiple comparisons).

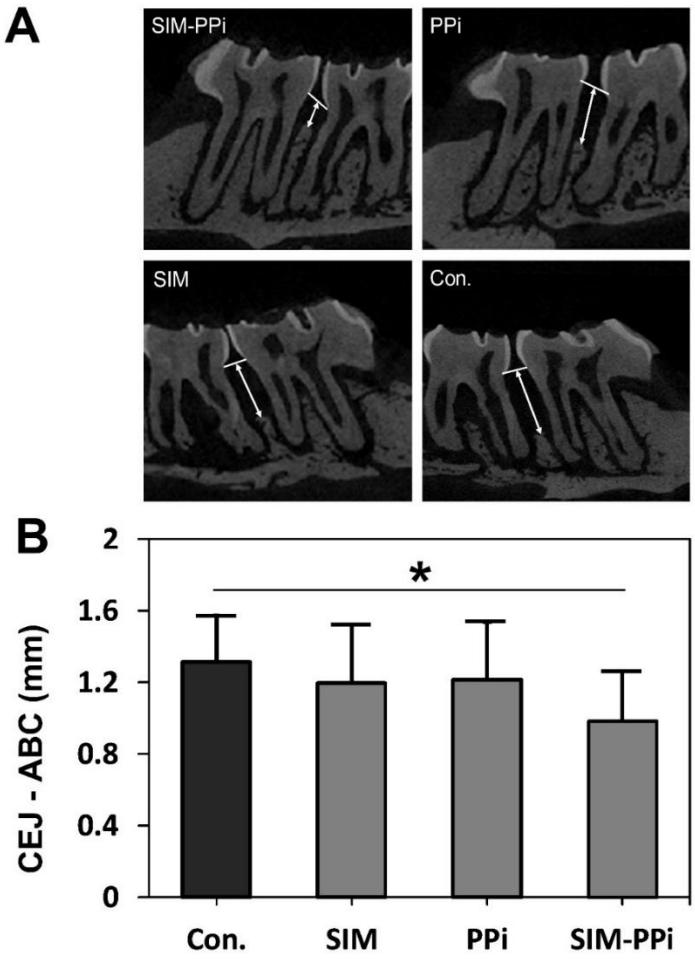

Figure 5. The in vivo evaluation of SIM-PPi efficacy in experimental periodontitis rat model. **(A)** Micro-CT sagittal images showing the effect of different treatments on the maxilla of cementoenamel junction (CEJ) to alveolar bone crest (ABC). White arrows indicate ABC-CEJ distance. **(B)** Measurement of the linear distance between cementoenamel junction (CEJ) and alveolar bone crest (ABC). Values are presented as the mean ± SD. $^{*}p < 0.05$ (one-way ANOVA with Tukey's multiple comparisons).

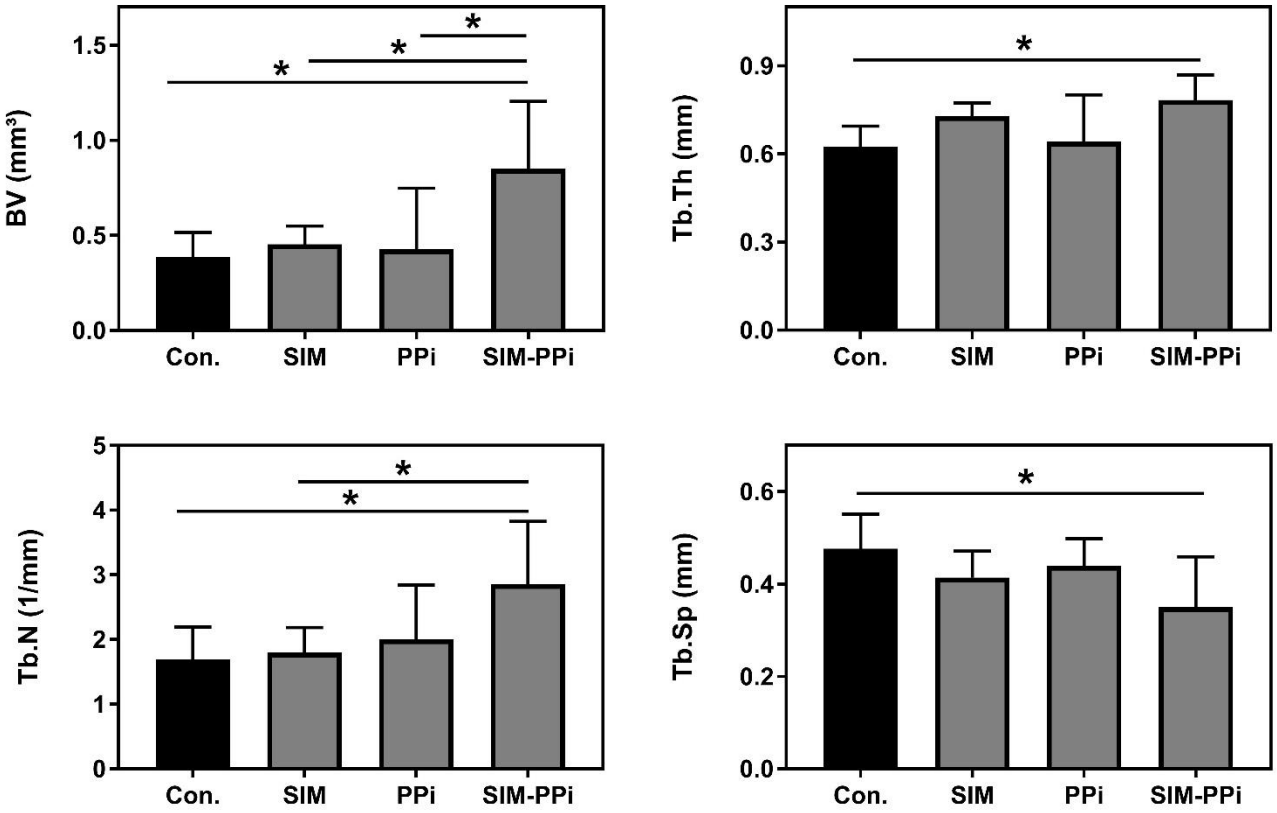

Figure 6. Micro-CT analysis of alveolar bone quality after different treatments. Bone volume (BV), trabecular thickness (Tb.Th), trabecular number (Th.N), and trabecular separation (Tb.Sp). Values are presented as the mean ± SD. $^{*}p < 0.05$ (one-way ANOVA with Tukey's multiple comparisons).

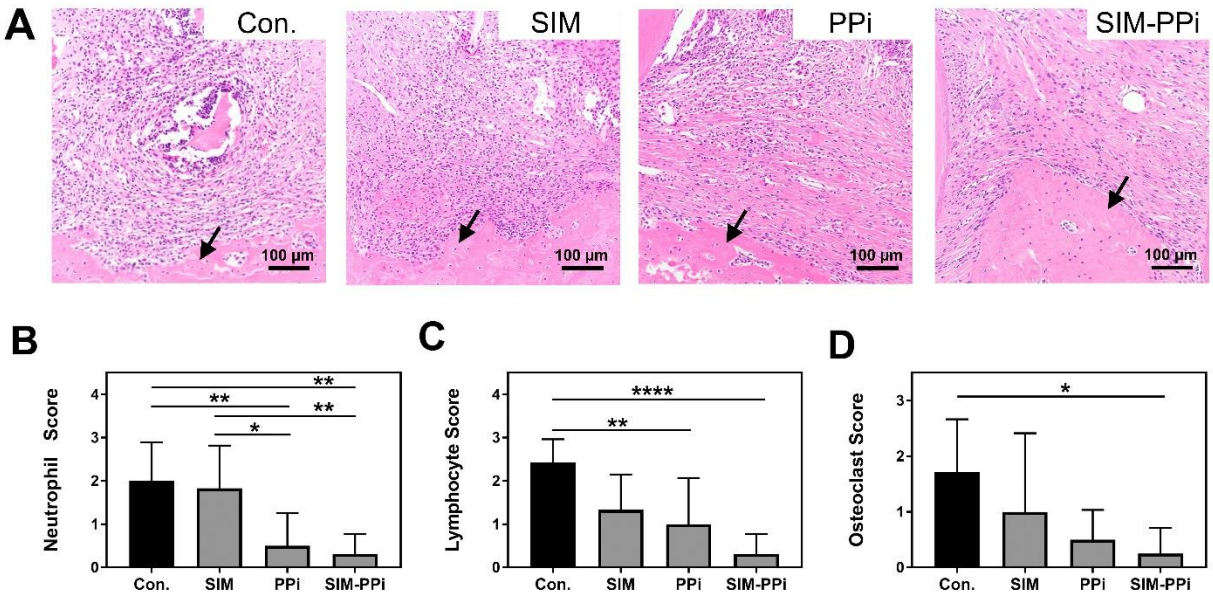

Figure 7. Histological analysis of papillary connective tissue and alveolar bone between first molar (M1) and second molar (M2) after 3 weeks of different treatments. **(A)** Representative images from different treatment groups of H&E stained sections of connective tissue above the alveolar bone crest (ABC) and between first molar (M1) and second molar (M2). Black arrows indicate alveolar bone crest. **(B-C)** Qualitative assessment of neutrophil and lymphocytic infiltrate interproximally between first molar (M1) and second molar (M2). Scoring criteria is shown in Table II, $^{*}p< 0.05$, $^{**}p< 0.01$, and $^{****}p<0.0001$ (one-way ANOVA). **(D)** Qualitative assessment of osteoclasts lining the surface of alveolar bone crest. Scoring criteria is shown in Table III, $*p< 0.05$ (one-way ANOVA with Tukey's multiple comparisons).

REFERENCES

1. Pihlstrom BL, Michalowicz BS, Johnson NW. Periodontal diseases. Lancet [Internet]. 2005 Nov 19 [cited 2017 Nov 6];366(9499):1809–20. Available from: http://www.ncbi.nlm.nih.gov/pubmed/16298220
2. Krayer JW, Leite RS, Kirkwood KL. Non-surgical chemotherapeutic treatment strategies for the management of periodontal diseases. Dent Clin North Am [Internet]. 2010 Jan [cited 2017 Aug 23];54(1):13–33. Available from: http://www.ncbi.nlm.nih.gov/pubmed/20103470
3. Herrera D, Sanz M, Jepsen S, Needleman I, Roldán S. A systematic review on the effect of systemic antimicrobials as an adjunct to scaling and root planing in periodontitis patients. J Clin Periodontol [Internet]. 2002 [cited 2017 Aug 23];29 Suppl 3:136-59; discussion 160-2. Available from: http://www.ncbi.nlm.nih.gov/pubmed/12787214
4. Greenstein G. Local drug delivery in the treatment of periodontal diseases: assessing the clinical significance of the results. J Periodontol [Internet]. 2006 Apr [cited 2017 Aug 23];77(4):565–78. Available from: http://www.joponline.org/doi/10.1902/jop.2006.050140
5. Williams RC, Jeffcoat MK, Howell TH, Reddy MS, Johnson HG, Hall CM, et al. Ibuprofen: An inhibitor of alveolar bone resorption in beagles. J Periodontal Res [Internet]. 1988 Jul 1 [cited 2017 Aug 23];23(4):225–9. Available from: http://doi.wiley.com/10.1111/j.1600-0765.1988.tb01363.x
6. Raja S, Byakod G, Pudakalkatti P. Growth factors in periodontal

regeneration. Int J Dent Hyg [Internet]. 2009 May [cited 2017 Aug 23];7(2):82–9. Available from: http://www.ncbi.nlm.nih.gov/pubmed/19413545

7. Mundy G, Garrett R, Harris S, Chan J, Chen D, Rossini G, et al. Stimulation of bone formation in vitro and in rodents by statins. Science [Internet]. 1999;286(5446):1946–9. Available from: http://www.ncbi.nlm.nih.gov/pubmed/10583956
8. Garrett IR, Mundy GR. The role of statins as potential targets for bone formation. Arthritis Res [Internet]. 2002 [cited 2017 Aug 23];4(4):237. Available from: http://www.ncbi.nlm.nih.gov/pubmed/12106493
9. Bradley AD, Zhang Y, Jia Z, Zhao G, Wang X, Pranke L, et al. Effect of Simvastatin Prodrug on Experimental Periodontitis. J Periodontol [Internet]. 2016 May [cited 2017 Apr 2];87(5):577–82. Available from: http://www.ncbi.nlm.nih.gov/pubmed/26799395
10. Price U, Le HOT, Powell SE, Schmid MJ, Marx DB, Zhang Y, et al. Effects of local simvastatin-alendronate conjugate in preventing periodontitis bone loss. J Periodontal Res. 2013;48(5):541–8.
11. He Y, Ho C, Yang D, Chen J, Orton E. Measurement and Accurate Interpretation of the Solubility of Pharmaceutical Salts. J Pharm Sci [Internet]. 2017 May [cited 2018 Jan 15];106(5):1190–6. Available from: http://linkinghub.elsevier.com/retrieve/pii/S0022354917300266
12. Serajuddin AT, Ranadive SA, Mahoney EM. Relative lipophilicities, solubilities, and structure-pharmacological considerations of 3-hydroxy-3-

methylglutaryl-coenzyme A (HMG-CoA) reductase inhibitors pravastatin, lovastatin, mevastatin, and simvastatin. J Pharm Sci [Internet]. 1991 Sep [cited 2018 Jan 17];80(9):830–4. Available from: http://www.ncbi.nlm.nih.gov/pubmed/1800703

13. Taha EA, Youssef NF. Spectrophotometric determination of some drugs for osteoporosis. Chem Pharm Bull (Tokyo) [Internet]. 2003 Dec [cited 2018 May 25];51(12):1444–7. Available from: http://www.ncbi.nlm.nih.gov/pubmed/14646329
14. Gregory CA, Gunn WG, Peister A, Prockop DJ. An Alizarin red-based assay of mineralization by adherent cells in culture: comparison with cetylpyridinium chloride extraction. Anal Biochem [Internet]. 2004 Jun 1 [cited 2017 Nov 16];329(1):77–84. Available from: http://linkinghub.elsevier.com/retrieve/pii/S0003269704001332
15. Stein D, Lee Y, Schmid MJ, Killpack B, Genrich MA, Narayana N, et al. Local simvastatin effects on mandibular bone growth and inflammation. J Periodontol [Internet]. 2005 Nov [cited 2018 Jun 1];76(11):1861–70. Available from: http://www.ncbi.nlm.nih.gov/pubmed/16274305
16. Lee Y, Schmid MJ, Marx DB, Beatty MW, Cullen DM, Collins ME, et al. The effect of local simvastatin delivery strategies on mandibular bone formation in vivo. Biomaterials [Internet]. 2008 Apr [cited 2018 Jun 1];29(12):1940–9. Available from: http://www.ncbi.nlm.nih.gov/pubmed/18255137
17. Nunes NLT, Messora MR, Oliveira LF, Lisboa M, Barcellos Garcia MC, Rêgo ROCC, et al. Effects of Local Administration of Tiludronic Acid on

Experimental Periodontitis in Diabetic Rats. J Periodontol [Internet]. 2017 Sep 15 [cited 2018 May 25];1–19. Available from: http://www.ncbi.nlm.nih.gov/pubmed/28914593

18. Camacho-Alonso F, Davia-Peña RS, Vilaplana-Vivo C, Tudela-Mulero MR, Merino JJ, Martínez-Beneyto Y. Synergistic effect of photodynamic therapy and alendronate on alveolar bone loss in rats with ligature-induced periodontitis. J Periodontal Res [Internet]. 2018 Jun [cited 2018 May 25];53(3):306–14. Available from: http://www.ncbi.nlm.nih.gov/pubmed/29086417
19. Wada-Mihara C, Seto H, Ohba H, Tokunaga K, Kido J, Nagata T, et al. Local administration of calcitonin inhibits alveolar bone loss in an experimental periodontitis in rats. Biomed Pharmacother [Internet]. 2018 Jan [cited 2018 May 25];97:765–70. Available from: http://www.ncbi.nlm.nih.gov/pubmed/29107933
20. Gibson-Corley KN, Olivier AK, Meyerholz DK. Principles for Valid Histopathologic Scoring in Research. Vet Pathol [Internet]. 2013 Nov 4 [cited 2018 May 23];50(6):1007–15. Available from: http://www.ncbi.nlm.nih.gov/pubmed/23558974
21. Schett G, Stolina M, Bolon B, Middleton S, Adlam M, Brown H, et al. Analysis of the Kinetics of Osteoclastogenesis in Arthritic Rats. ARTHRITIS Rheum [Internet]. 2005 [cited 2018 May 25];52(10):3192–201. Available from: https://onlinelibrary.wiley.com/doi/pdf/10.1002/art.21343
22. Bolon B, Morony S, Cheng Y, Hu Y-L, Feige U. Osteoclast Numbers in

Lewis Rats with Adjuvant-induced Arthritis: Identification of Preferred Sites and Parameters for Rapid Quantitative Analysis 1. Vet Pathol [Internet]. 2004 [cited 2018 May 25];41:30–6. Available from: http://journals.sagepub.com/doi/pdf/10.1354/vp.41-1-30

23. Lazzerini PE, Lorenzini S, Selvi E, Capecchi PL, Chindamo D, Bisogno S, et al. Simvastatin inhibits cytokine production and nuclear factor-kB activation in interleukin 1??-stimulated synoviocytes from rheumatoid arthritis patients. Clin Exp Rheumatol. 2007;25(5):696–700.
24. Pereira MC, Cardoso PRG, Da Rocha LF, Rêgo MJBM, Gonçalves SMC, Santos FA, et al. Simvastatin inhibits cytokines in a dose response in patients with rheumatoid arthritis. Inflamm Res. 2014;63(4):309–15.
25. Pradeep AR, Thorat MS. Clinical Effect of Subgingivally Delivered Simvastatin in the Treatment of Patients With Chronic Periodontitis: A Randomized Clinical Trial. J Periodontol [Internet]. 2010 Feb [cited 2017 Nov 6];81(2):214–22. Available from: http://www.ncbi.nlm.nih.gov/pubmed/20151799
26. Vaziri H, Naserhojjati-Roodsari R, Tahsili-Fahadan N, Khojasteh A, Mashhadi-Abbas F, Eslami B, et al. Effect of Simvastatin Administration on Periodontitis-Associated Bone Loss in Ovariectomized Rats. J Periodontol [Internet]. 2007 Aug [cited 2017 Nov 6];78(8):1561–7. Available from: http://www.ncbi.nlm.nih.gov/pubmed/17668976
27. Xu X-C, Chen H, Zhang X, Zhai Z-J, Liu X-Q, Qin A, et al. Simvastatin prevents alveolar bone loss in an experimental rat model of periodontitis

after ovariectomy. J Transl Med [Internet]. 2014;12:284. Available from: http://www.pubmedcentral.nih.gov/articlerender.fcgi?artid=4192445&tool=pmcentrez&rendertype=abstract

28. Elavarasu S, Suthanthiran TK, Naveen D. Statins: A new era in local drug delivery. J Pharm Bioallied Sci [Internet]. 2012 Aug [cited 2017 Nov 6];4(Suppl 2):S248-51. Available from: http://www.ncbi.nlm.nih.gov/pubmed/23066263
29. Durie BGM, Katz M, Crowley J. Osteonecrosis of the Jaw and Bisphosphonates. N Engl J Med [Internet]. 2005 Jul 7 [cited 2017 Nov 6];353(1):99–102. Available from: http://www.ncbi.nlm.nih.gov/pubmed/16000365
30. Kennel KA, Drake MT. Adverse effects of bisphosphonates: implications for osteoporosis management. Mayo Clin Proc [Internet]. 2009 Jul [cited 2017 Nov 6];84(7):632–7; quiz 638. Available from: http://www.ncbi.nlm.nih.gov/pubmed/19567717
31. Shellis RP, Addy M, Rees GD. In vitro studies on the effect of sodium tripolyphosphate on the interactions of stain and salivary protein with hydroxyapatite. J Dent [Internet]. 2005 Apr [cited 2017 Nov 6];33(4):313–24. Available from: http://www.ncbi.nlm.nih.gov/pubmed/15781139
32. Hefferren JJ. Historical view of dentifrice functionality methods. J Clin Dent [Internet]. 1998 [cited 2017 Nov 6];9(3):53–6. Available from: http://www.ncbi.nlm.nih.gov/pubmed/10518861
33. Joiner A. Whitening toothpastes: A review of the literature. J Dent

[Internet]. 2010 Jan [cited 2017 Nov 6];38:e17–24. Available from: http://www.ncbi.nlm.nih.gov/pubmed/20562012

34. Yankell SL, Emling RC, Petrone ME, Rustogi K, Volpe AR, DeVizio W, et al. A six-week clinical efficacy study of four commercially available dentifrices for the removal of extrinsic tooth stain. J Clin Dent [Internet]. 1999 [cited 2017 Nov 6];10(3 Spec No):115–8. Available from: http://www.ncbi.nlm.nih.gov/pubmed/10825858

35. Yucel-Lindberg T, Båge T. Inflammatory mediators in the pathogenesis of periodontitis. Expert Rev Mol Med [Internet]. 2013;15(August):e7. Available from: http://www.ncbi.nlm.nih.gov/pubmed/23915822

36. Pagkalos J, Cha JM, Kang Y, Heliotis M, Tsiridis E, Mantalaris A. Simvastatin induces osteogenic differentiation of murine embryonic stem cells. J Bone Miner Res [Internet]. 2010 Nov [cited 2017 Nov 16];25(11):2470–8. Available from: http://doi.wiley.com/10.1002/jbmr.163

CHAPTER 3.

GSK3 Inhibitor- Loaded Modified Pluronic Hydrogel Prevents Experimental Periodontitis

3.1 INTRODUCTION

As mentioned in Chapters 1&2, simultaneous anti-inflammatory and osteogenic intervention is essential for periodontitis management. In this chapter, glycogen synthase kinase 3 beta (GSK3β), a multi-tasking serine/threonine kinase with crucial roles in several physiological processes including inflammation and bone homeostasis, was selected. It has been shown to have a critical role in host inflammatory response(1–3) and bone homeostasis(4) as a negative regulator, suggesting that inhibitors of GSK3β may provide therapeutic effects for inflammatory and bone metabolic diseases(5). Particularly, a GSK3β inhibitor (SB216763) has been studied in periodontal disease and data confirmed its therapeutic benefits in preventing alveolar bone loss associated with periodontal disease(6). During the last decade, several selective GSK-3β inhibitors have been synthesized and tested in clinical trials at various phases(7,8). In particular, 6-bromoindirubin-3'-oxime (BIO), a potent GSK3β inhibitor with an enzymatic IC_{50} of 5 nM, has exhibited anti-inflammatory and strong bone and teeth anabolic effects(2,3,9–15). However, due to the involvement of GSK3 in many other physiological processes, systemic administration may cause serious adverse side

effects(16–18). Hence, it is necessary to limit and restrict its biological action primarily at the intended site of action. Local delivery of BIO into the periodontal pocket allows to directly target periodontal tissue, achieving high local concentrations along with minimizing systemic toxicities. However, BIO's poor aqueous solubility and rapid clearance from periodontal pockets are major challenges.

Thermoresponsive hydrogel formulations injected into the periodontal pocket would be a promising option for the local delivery of BIO to augment the bony defect associated with periodontitis. Poloxamer 407 (Pluronic F127), an excipient of various formulations that is approved by U.S. FDA for pharmaceutical applications, is a triblock amphiphilic copolymer consisting of blocks of ethylene oxide and propylene oxide (PEO101 PPO56 POE101)(19–22). It has been used extensively in controlled drug and cell delivery (23). Its unique thermal reversible gelation property in aqueous solutions (in the range of 20–35% w/v) makes it an attractive biomaterial for regenerative applications in dentistry and other areas(24,25). The amphiphilic F127 polymer enhances the solubility of hydrophobic drugs at room temperature by forming micelles. When exposed to physiological temperature, the polymer solution forms hydrogel, holding encapsulated drugs in its collapsed micellar structure to provide sustained release kinetics. F127 is also known to be non-toxic and biocompatible (25). The constant flow of crevicular fluid, the poor bone-adhesion and mechanical properties of F127

hydrogel, however, would significantly limit the bioavailability of the payload drug in the periodontal pocket.

Therefore, to improve binding of F127 hydrogel to the hard tissues, we here report the development of a novel thermosensitive pyrophosphorolated F127 hydrogel system (PF127) for the delivery of BIO. After detailed characterization, the therapeutic potential of the BIO-loaded PF127 delivery system was evaluated on experimental periodontitis rat model.

3.2 METHODS AND MATERIALS

3.2.1 Materials and Reagents

Pluronic F127 and pyrophosphate were obtained from Sigma-Aldrich (St. Louis, MO, USA). BIO was synthesized according to literature(26) Dense Ceramic Hydroxyapatite discs (0.5" diameter and .08" Thick) were purchased from Clarkson Chromatography Products, Inc. (South Williamsport, PA USA). Mouse osteoblast MC3T3-L1 cells were originally purchased from ATCC (Manassas, VA, USA). Minimum Essential Media (alpha-MEM) and trypsin-EDTA were purchased from Gibco (Grand Island, NY, USA). Fetal bovine serum (FBS) was obtained from Gemini BenchMark (West Sacramento, CA). Cell Counting Kit-8 (CCK-8) was purchased from Dojindo Molecular Technologies, Inc. (Rockville, MD USA). All other reagents and solvents, if not specified, were obtained from either Fisher Scientific (Pittsburgh, PA, USA) or Acros Organics (Morris Plains, NJ, USA).

3.2.2 Synthesis of Pyrophosphorolated Pluronic F127 (F127-PPi)

Synthesis of Tosylated Pluronic F127

Pluronic F127 (1.0 g, 0.079 mmol) and 4-toluenesulfonyl chloride (151 mg, 0.79 mmol) were dissolved in dry dichloromethane, followed by the addition of pyridine (62 µL, 0.79 mmol) and the solution was stirred for 24 hours. Dichloromethane (100 mL) was then added. The resulting solution was washed with HCl solution (1 M, 20 mL), brine (100 mL × 2) and water (100 mL × 2). The organic phase was separated and dried over $MgSO_4$. After removal of the solvent, the residue was purified on a LH-20 column to give 922 mg of the desired product, yield: 90%. ^{1}HNMR ($CDCl_3$, 500 MHz) δ ppm 7.78 (d, J = 3.0 Hz, 1H), 7.33 (d, J = 3.0 Hz 1H), 4.14 (t, J = 5.0 Hz, 2H), 3.77 (t, J = 4.5 Hz, 8H), 3.59-3.55 (m, 872 H), 3.50-3.44 (m, 142 H), 3.38 (m, 65H), 2.44 (s, 3H), 1.12 (t, J = 5.0 Hz, 195H); ^{13}C NMR ($CDCl_3$, 125 MHz) δ ppm 144.7, 133.0, 129.8, 127.9 , 75.5, 75.4, 75.1, 73.4, 73.0, 72.9, 72.7, 69.2, 68.7, 21.6, 17.5, 17.3.

Synthesis of Pyrophosphorolated Pluronic F127

The tosylated Pluronic F127 (1.0 g, 0.077 mmol) and tris(tetra-n-butylammonium) hydrogen diphosphate [(n-$Bu_4N)_3(HO)P_2O_6$] (0.31 mmol, 280 mg)were dissolved in dry acetonitrile, the solution was stirring at room temperature for 3 hours until the starting materials completely disappeared (monitored by TLC). After evaporation of the solvents, the residue was dissolved in water (10 mL). The solution was dialyzed (MWCO = 10 kDa) against NaCl solution (0.1 mol/L) overnight to exchange tetrabutyl ammonium to sodium, after which the solution

was further dialyzed against distilled water to remove the excessive NaCl. The final aqueous solution was lyophilized to obtain 859 mg of final pyrophosphorolated Pluronic F127 product, yield: 85%. ^{1}HNMR ($CDCl_3$, 500 MHz) δ ppm 4.16 (t, J = 5.0 Hz, 2H), 3.78 (t, J = 4.5 Hz, 8H), 3.59-3.54 (m, 872H), 3.50-3.44 (m, 142 H), 3.39-3.36 (m, 65H), 2.44 (s, 3H), 1.13 (t, J = 5.0 Hz, 195H); ^{13}C NMR ($CDCl_3$, 125 MHz) δ ppm 75.5, 75.4, 75.1, 73.4, 73.0, 72.9, 72.8, 72.7, 70.6, 17.5, 17.3; ^{31}P NMR (202.5MHz, $CDCl_3$): δ (ppm) = -7.70 (d, J = 20.2Hz), -7.91 (d, J = 20.2Hz).

3.2.3 Preparation of BIO-loaded Thermoresponsive Hydrogel

PF127 hydrogel formulations with predetermined polymer concentrations (20, 25 and 30% w/v) were prepared by mixing F127-PPi and F127 at different ratio (0:100, 25:75, 50:50, 75:25, 100:0% w/w). In brief, the desired amount of F127-PPi and F127 was dissolved in phosphate buffered saline (PBS, pH 7.4) with stirring in an ice-water bath (~ 4 °C, to avoid micellization and/or gelation during solution preparation) until clear solution (PF127) was obtained and then stored at 4 °C overnight. BIO was then dissolved in the polymer solutions by continuous stirring at 4 °C, the obtained solutions were filtered through 0.8 µm filter syringes.

3.2.4 *In vitro* Hydroxyapatite (HA) Binding

To predict the binding of formulated hydrogels to HA, which is the primary inorganic component of natural hard tissues, an *in vitro* binding test was performed using HA discs. Briefly, polymer solutions (25% w/v) were prepared, containing 100 µM of

BIO, with different ratio of F127-PPi and F127 (0:100, 25:75, 50:50, 75:25, and 100:0% w/w) to optimize binding affinity. Hydrogels (1 ml) were formed on HA disc placed in plastic wells at 37 °C, and allow hydrogels to stabilize for 15 min. After that, HA discs, on which hydrogels are formed, were inverted with temperature maintained at 37 °C by keeping the inverted hydrogels inside the bath. The binding time of hydrogel to HA disc was measured. The binding experiment was performed in triplicate. Based on this study, one formulation was selected for all subsequent experiments.

3.2.5 Biocompatibility of PF127 Hydrogel

To measure cell viability of selected PF127 hydrogel formulation (25% w/v of mixed F127-PPi and F127, 50:50% w/w) comparing to F127 hydrogel (25% w/v) with or without BIO (100 nM), Cell Counting Kit-8 (CCK-8) was utilized. Briefly, mouse preosteoblast MC3T3-L1 cell line was cultured in Minimum Essential Media (alpha-MEM) supplemented with 10% fetal bovine serum (FBS) and 1% penicillin/streptomycin (basal growth medium). Cells were incubated at 37 °C in 5% CO_2 to 90% confluence. The hydrogels were extracted in alpha-MEM and then incubated at 37 °C for 24 h, according to the ISO Standard 10993–12(27,28)**.** Cells were then seeded in 96 well plates (1×10^4 cells/well) and incubated for 24 h. Subsequently, cells were treated with either media only, PF127 extract, PF127-BIO extract, F127 extract, F127-BIO extract, or free BIO (100 nM), and then the plates were incubated for 24 and 48 h. Following each time point, 10 µL of CCK-8 reagent was then added to each well and further incubated for 4 h at 37 °C. The

absorbance of each well was recorded at 450 nm using a microplate reader (SpectraMaxM2, Molecular Devices, Sunnyvale, CA, USA).

3.2.6 Comparing Aqueous Solubility of BIO in PF127 vs F127

This experiment was conducted to measure the aqueous solubility of BIO in PF127 solutions comparing to F127. The solubility values of BIO were obtained by measuring equilibrium solubility after adding the analyte to the testing medium for a predetermined period of time as reported previously(29). Briefly, an excessive amount of BIO was added to different concentrations of either PF127 or F127 solutions in microcentrifuge tubes. The suspensions were agitated on a rotor at 4 °C for 48 h to reach the equilibrium. The mixtures were then centrifuged (2,000 rpm, 5 min, at 4 °C) to settle the undissolved drug. The supernatants (saturated solutions) were obtained by filtering through 0.2 µm syringe filters, and then the BIO concentrations were measured using a UV spectrophotometer (SpectraMax M2, Molecular Devices, Sunnyvale, CA, USA) at 260 nm.

3.2.7 Gelation and Viscosity Studies

To investigate sol-gel-sol phase transition behavior of PF127 solutions with or without BIO comparing to F127 solutions, phase transition diagrams were constructed using the tube inverting method(25,30,31). Each solution at a given concentration ranging between 20 and 40% w/v was prepared as described above.

A sample volume of 1 mL was transferred into an Eppendorf tube and then subjected to a controlled temperature increase from 4 to 80 °C. Each 1 °C increase was followed by isothermal maintenance for 5 minutes and then inverting the tube for visual inspection of the occurrence of phase transition. The sol and gel phases were identified as “flowing” and “non-flowing”, respectively. The gelation time of PF127 and F127 solutions at physiological temperature was also determined by incubation at 37 °C followed by tube inversion every 5s. The viscous properties of gel phase were also investigated at constant temperature by means of flow curves(25) (37 °C, shear rate from 1 to 100 s^{-1}) using a rheometer (TA Instruments AR1500ex). Samples were poured on the rheometer lower plate at 0 °C, heated to 37°C and maintained for 15 minutes to reach the thermal stability before isothermally tested.

3.2.8 *In vitro* Release of BIO from Hydrogel

The release rate of the physically entrapped BIO from PF127 hydrogels (20, 25, and 30% w/v), was studied by a membrane-less experiment, as reported previously(27,28,32). Briefly, samples of 1 mL of polymer solutions containing 0.5 mg of BIO were transferred into screw cap-tubes and incubated in a water bath at 37 °C until the gels were formed. After gelation, 2 mL of phosphate buffered saline (PBS; pH 7.4) containing 0.5 % tween 80 pre-equilibrated at 37 °C was gently laid over the surface of the hydrogels and incubated in a water bath at 37 °C with continuous gentle shaking. To measure the release of BIO, release medium (2 mL) were taken at regular time intervals and replaced with an equal volume of pre-

equilibrated fresh release buffer. The concentration of BIO was determined by measuring the absorbance at 260 nm using a UV spectrophotometer (SpectraMax M2, Molecular Devices, Sunnyvale, CA, USA). Release study was performed in triplicate.

3.2.9 *In vitro* Hydrogel Erosion

The erosion time of PF127 hydrogel formulations (20, 25, and 30% w/v) was determined by performing the weight remaining (%) experiment, as reported by other studies(27,28,32). Briefly, samples of 1 mL of polymer solutions were transferred into screw cap-tubes and incubated in a water bath at 37 °C until the gels were formed. After gelation, the original weight of the hydrogel samples was measured as (W_0). Subsequently, 2 mL of PBS (pH 7.4) pre-equilibrated at 37 °C was gently laid over the surface of the hydrogels and incubated in a water bath at 37 °C with continuous gentle shaking. The weight of remaining hydrogels (W_t) was measured at regular time intervals after completely blotting off the buffer. Erosion study was performed in triplicate. Weight remaining (%) was calculated as:

$$\text{Weight remaining } (\%) = \frac{(W_0 - W_t)}{W_0} \times 100$$

3.2.10 Evaluation of BIO Hydrogel's Therapeutic Efficacy on an Experimental Periodontitis Rat Model

Sprague Dawley rats (female, 10-month-old, retired breeders) were purchased from Envigo. The animals were acclimated for one week prior to any experimental procedure. Rats were divided randomly into six groups: Healthy control, experimental periodontitis (EP) treated with saline, EP treated with 25% w/v of mixed F127-PPi and F127 hydrogel (50:50% w/w, containing 100 µM of BIO) (PF127-BIO), EP treated with 25% w/v of F127 hydrogel (containing 100 µM of BIO) (F127-BIO), EP treated with 25% w/v of PF127 hydrogel, and EP treated with free BIO (100 µM). Silk ligatures were used to induce the experimental periodontitis as previously described(29,33). Briefly, each rat was anesthetized using a chamber attached to isoflurane vaporizer (1- 4% isoflurane and 100% oxygen), followed by body weight measurement. To maintain anesthesia during experimental procedures, a nose cone (0.5% - 2% isoflurane and 100% oxygen) was applied throughout the entire experimental procedure. Experimental periodontitis was induced in all groups by gently tightening a 4-0 silk ligature around the maxillary 2nd molars on both sides. After one week, ligatures were removed. Treatments were locally injected (10µL) into the palatal gingiva between the maxillary first molar (M1) and second molar (M2) on the first day of week 1, 2 and 3 after ligature placement. At week 4, all animals were euthanized using CO_2 asphyxiation, followed by dissecting the entire palate including all three molars and fixation in 10% formalin for µ-CT and histological evaluations. All animal procedures were approved by the Institutional Animal Care and Use Committee (IACUC) of the University of Nebraska Medical Center (UNMC).

3.2.11 Micro-computed Tomography (μ-CT) Analysis

All palate samples (including all three molars) were scanned using a micro-CT imaging system (Bruker SkyScan1172, Kontich, Belgium), as described in previous studies (34). The voltage and current of X-ray source were set at 70 kV and 141 μA, respectively, with a pixel size of 12.9 μm and a 0.5 mm-thick aluminum filter was used. The exposure time was 1880 ms, and X-ray projections were obtained at 0.7° intervals with a scanning angular rotation of 180°, and 5 frames were averaged for each rotation. To generate three-dimensional (3D) images, scans were reconstructed using the system-reconstruction software (NRecon; Skyscan). Sagittal sections were obtained using the Skyscan DataViewer software, then the linear distance from the cementoenamel junction (CEJ) to the alveolar bone crest (ABC) was measured s using the Skyscan CT-Analyzer software. For each sample, the linear distance was measured from two points: distopalatal of M1 and mesiopalatal of M2. Longer distance means more bone loss and vice versa. Coronal sections obtained using the Skyscan DataViewer were used to measure bone volume (BV) and trabecular thickness (Tb.Th) using the CT Analyzer. A rectangular region of interest between M1 and M2 was selected, with its length extended from the distopalatal of M1 to the mesiopalatal of M2, width from the palatal side to the buccal side of M1 and M2, and height 130 slices below CEJ of M1 and M2. Femurs were also collected and scanned to evaluate the systemic effect of BIO. The scanning parameters were set as follows: voltage 70 kV, current 141 μA, exposure time 700 ms, resolution 8.6 μm, and aluminum filter 0.5 mm. 3D reconstructions were achieved using the NRecon and

DataViewer software. A consistent polygonal region of interest of trabecular bone at the distal femur, from 20 slices to 100 slices proximal to the growth plate, was selected for bone quality analysis. The mean bone mineral density (BMD), bone volume (BV), bone volume /tissue volume (BV/TV) and trabecular thickness (Tb.Th) were quantified using the CTAn software(35).

3.2.12 Histological Evaluation

After completing the μ-CT analysis, palates were decalcified in 14% ethylenediaminetetraacetic acid (EDTA) solution for two weeks. The decalcification solution was changed every 3 days. After decalcification, samples were embedded in paraffin. Sagittal sections (4μm) were obtained in a mesiodistal direction with roots aligned in one plane and then stained with hematoxylin and eosin for microscopic observation. To evaluate connective tissues between M1 and M2 for inflammatory cells and alveolar crest for osteoclasts, a pathologist (SML) who was blind to experimental groups, semi-quantitatively assessed samples using a light microscope (Olympus System Microscope Model BX53) under 200× magnification. The inflammatory cells were evaluated semi-quantitatively in the gingival tissues above the alveolar crest using a scoring system(29,36,37), where 0 is negative, 1 is a few inflammatory cells lining less than 30 % of the affected tissues, 2 is some inflammatory cells (30 - 60 %), and 3 is many inflammatory cells (>60 %). Osteoclasts lining the surface of alveolar crest were also semi-quantitative assessed using a scoring system(29,38) where 0 is negative, 1 is a few osteoclasts lining less than 5% of most affected alveolar bone

surface, 2 is some osteoclasts (5 - 25%), and 3 is many osteoclasts (25 - 50%). Immunohistochemical staining of β-catenin was also performed using primary antibody (rabbit monoclonal anti-β-catenin antibody, Abcam, ab32572; 1:400 dilution). After deparaffinization and rehydration, sections were incubated in citrate buffer (pH 6.0, 0.1 M) for antigen retrieval, washed, and then incubated in hydrogen peroxide. Sections were then blocked and incubated with the primary antibody, followed by incubation with the secondary antibody. The antibody complexes were visualized using the DAB chromogen. Hematoxylin was used for counterstaining. The staining intensity was independently evaluated by a pathologist (S.M.L.) using a scale of from 0 to 3, where 0 is negative, 1 is weak staining, 2 is moderate staining, and 3 is strong staining(14,39). To calibrate SML's scoring, another researcher (YA) independently scored a stack of slides and compared with SML's results before SML proceeded with all the analyses.

3.2.13 Statistical Analysis

All the obtained data were presented as the mean ± standard deviation (SD). Statistical analysis was performed using Prism 8.0 software (GraphPad, San Diego, CA). Continuous outcomes among more than three groups were compared using the Analysis of Variance (ANOVA). Tukey's post hoc t-test for multiple comparisons was used for the pairwise comparison. *P*-value < 0.05 was considered statistically significant.

3.3 RESULTS

3.3.1 *In vitro* Hydroxyapatite (HA) Binding

HA binding study was performed to predict the bone affinity of the 25% w/v PF127 hydrogel composed of different ratio of F127-PPi and F127 (Fig. 9a). The binding time increased as the F127-PPi content was increased in the hydrogel. Among different ratios of F127-PPi, 50, 75, and 100 (w/w %) showed the longest binding time to HA disc (24.6, 25.6, and 28.2 min), respectively. Their binding time was statistically significant when compared to F127 hydrogel ($P < 0.0001$). Also, the ratio of 25 (w/w %) exhibited considerable binding time (18.2 min) which was significantly higher than F127 hydrogel ($P < 0.0017$). F127 hydrogel had the lowest binding time (8.5 min) among all the formulations. Based on this observation, the formulation of 50:50% w/w ratio of PF127 and F127 was used in the subsequent experiments as showed strong binding affinity with relatively low PPi content.

3.3.2 Biocompatibility of PF127-based Hydrogel

To evaluate the *in vitro* safety of PF127 hydrogel comparing to F127 which is known to be biocompatible, MC3T3-L1 cells were treated with extracted PF127, PF127-BIO, F127, F127-BIO, or free BIO (100 nM) for 24 and 48 h, and the cell viability was determined using the CCK-8 assay (Fig. 8a-b). The viability percentage of MC3T3-L1 cells treated with PF127 25% w/v, when compared to media-treated control, was slightly reduced to 84.5% after 24 h and further decreased to 79.5% after 48 h. Whereas viability with F127 was 87.5% and 83.5%

after 24 and 48 h, respectively. When BIO was added to hydrogels, cell viability was not changed significantly. However, when cells treated with 100 nM of free BIO, the viability was improved to 102% and 104.5% comparing to media-treated control.

3.3.3 Solubility of BIO in PF127 vs F127

The saturated solubility of BIO in different concentrations of PF127 at 4 °C and pH 7 was analyzed and compared to its solubility in F127 (Fig. 9b). The solubility of BIO appears to be proportionally dependent on polymer concentration. In 20% PF127, its solubility was determined to be 0.5 mg/mL versus 0.1 mg/mL in 20% F127. However, when polymer concentration was increased to 25%, BIO's solubility in PF127 was improved significantly to 2 mg/mL, while in F127 improved only to 0.3 mg/mL. When concentration further increased to 30%, solubility in PF127 was continued to increase to 3 mg/mL, while in F127 improved to 0.6 mg/mL. Clearly, PF127 has greatly improved BIO's aqueous solubility.

3.3.4 Gelation and Viscosity Analysis of the PF127 Hydrogel

Tube-inverting test was performed on PF127 solutions with or without BIO to determine their phase transition temperatures, in comparison to F127 solutions. Figure 10a shows the phase diagram of PF127. Overall, lower critical gelation temperature (LCGT) of PF127 was lower than that of the F127 hydrogels, and upper critical gelation temperature (UCGT) of PF127 was higher than that of F127.

The addition of BIO into both PF127 and F127 hydrogels will not affect LCGT, but slightly increase UCGT. Though all formulations underwent gelation within less than 2 minutes at 37 °C, PF127 formulations gelled faster than F127 with or without drug loading. Rheological tests were also performed on PF127 and F127 hydrogels with and without BIO at 37 °C to study the effect of the pyrophosphorolation and drug content on their viscous property (Fig. 10b-c). All hydrogels showed a typical shear-thinning behavior (non-Newtonian) and the viscosity was decreased as a function of shear rate. No notable differences in viscosity were observed between PF127 and F127 hydrogels within the same concentration, except 20% w/v PF127 which showed low viscosity and a very weak hydrogel. BIO addition seemed to have no significant impact on hydrogels' viscous property.

3.3.5 *In vitro* Release of BIO from PF127 Hydrogel

BIO was physically entrapped inside the hydrogel matrix, and its release at 37 °C from PF127 hydrogels (20, 25, and 30% w/v) was studied. As shown in Figure 9c, the release profiles of BIO from the hydrogels were shown to be a function of the concentration of hydrogel: the higher the hydrogel concentration, the slower the release rate. The total release (~ 99 %) of BIO from 20% w/v hydrogel occurred in 24 h with burst release (~ 50%) in the first 3 h. BIO release from 25% w/v hydrogel was shown with a burst release in the first 12 h followed by a sustained

release in the next 48 h. While 30% w/v hydrogel exhibited sustained release of BIO over 48 h.

3.3.6 *In vitro* Hydrogel Erosion

The PF127 hydrogels erosion behavior was characterized by measuring weight remaining (%) at regular incubation time intervals. The results correlate with the release study and shown to be a function of the concentration of hydrogel. As shown in Figure 9d, 20% w/v hydrogel was completed eroded in 24 h, ~50% was eroded in the first 3 h. While 25% w/v hydrogel was completed eroded in 48 h, ~60% weight loss was observed in the first 6 h (burst erosion) followed by sustained erosion. 30% w/v hydrogel was completely eroded in 48 h in a sustained erosion manner.

3.3.7 Micro-computed Tomography (μ-CT) Analysis

As shown in Figure 11a, it is obvious that the PF127-BIO hydrogel treated group preserved alveolar bone crest compared to other treated groups. The linear distance of CEJ to ABC, representing alveolar crest height, indicated that the PF127-BIO hydrogel treated group had a significantly shorter distance when compared to all other treated groups. While F127-BIO treated group exhibited statistically significant difference only when compared to the saline-treated group; free BIO treated group did not show a statistically significant difference when

compared to the saline-treated group as presented in Figure 11b. For further validation of alveolar bone loss, bone volume (BV, Figure 11c) and trabecular thickness (Tb.Th, Figure 11d) were quantified. The value of BV for the PF127-BIO treated group was significant when compared to all the other treated groups. In contrast, F127-BIO treated group exhibited a statistically significant difference only when compared to the saline-treated group. The values of Th.Th for the PF127-BIO and F127-BIO treated groups were significant when compared only to the saline-treated group. Free BIO treated group when compared to the saline group, none of the above parameters produced a statistically significant difference. Femur analyses data did not show any significant difference between all groups.

3.3.8 Histological Evaluation

To evaluate the effect of the different treatments on inflammatory cells, osteoclasts, and β-catenin, stained sections were assessed semi-quantitatively. Histology scores of inflammatory cells were shown in Figure 12c. PF127-BIO hydrogel-treated group has the lowest score of inflammatory cells when compared to all other treated groups ($P < 0.0001$ compared to saline, $P < 0.01$ compared to F127-BIO and free BIO trated groups), while F127-BIO and free BIO treated groups exhibited a statistically significant difference ($P < 0.01$) only when compared to the saline-treated group. Osteoclast score of the PF127-BIO hydrogel treated group was the lowest among all the treatment groups and was significantly ($P < 0.001$) lower than the saline-treated group (Fig. 12d). Scores of F127-BIO and free BIO treated groups were significant when compared to the

saline-treated group. β-catenin positive cell score of the PF127 hydrogel-treated group was the highest among all the treatment groups (Fig. 12e, $P < 0.0001$ compared to saline, $P < 0.05$ compared to F127-BIO and free BIO trated groups). Scores of F127-BIO and free BIO-treated groups were not significant ($P > 0.05$) when compared to the saline-treated group.

3.4 DISCUSSION

Inflammation-induced alveolar bone loss in response to periodontal infection has long been the focus in clinical management of periodontal disease. To prevent disease progression, simultaneous anti-inflammatory and osteogenic interventions are considered to be essential. Glycogen synthase kinase 3 (GSK3) plays a substantial role in regulating the production of pro- and anti-inflammatory cytokines in innate and adaptive immune cells(1). It acts as a downstream effector molecule in the PI3K pathway that stimulates the production of proinflammatory cytokines including TNF, IL-6, IL-12, and IL-1β, known to promote osteoclastogenesis and promote alveolar bone loss(6). GSK3 is also a cytosolic Wnt signaling inhibitor that induces β-catenin degradation and thus suppresses osteoblast differentiation(4,9,12,40). Hence, there is a strong rationale for considering GSK3 as an attractive therapeutic target for periodontal disease. Pharmacological inhibition of GSK3 using 6-bromoindirubin-3'-oxime (BIO) has been found to alleviate different inflammatory diseases by positively regulating inflammatory cytokines(6,13,14,41–43). Additionally, BIO has also been exhibited to promote

robust osteoblast differentiation, potent bone anabolism(9,40), natural tooth repair(15) and to prevent mandibular cartilage pathological changes(14). Hence, BIO was proposed in this study to prevent periodontal disease progression because of its potency as an anti-inflammatory and an osteoinductive agent. However, in addition to its poor water solubility and lack of osteotropicity, oncogenic concerns(17), have limited BIO's clinical applications.

To overcome these limitations, we have developed a novel osteotropic hydrogel for local delivery of BIO with better water solubility and direct access to periodontal tissues and thus minimize potential long-term side effects associated with Wnt/β-catenin signaling agonists(17,18). In this study, the osteointegration or ionic bonding of Pluronic F127 hydrogel was improved through a straightforward two-step reaction, optimizing this delivery system for bone regeneration(44). The chain termini of Pluronic F127 were modified with pyrophosphate (PPi) without compromising gelation and viscous properties of F127. In addition to the unique thermoresponsive characteristics of F127 hydrogel, this design was also built upon our previous studies in which Pluronic copolymers were modified with biomineral-binding moiety (PPi) to develop dentotropic micelle formulations as an effective and safe delivery tool for antimicrobials to improve dental plaque prevention and treatment(45). This novel thermoresponsive pyrophosphorolated hydrogel (PF127) should be capable of interacting with the periodontal hard tissues and achieving the ultimate goal of sustained local delivery to assist the clinical

management of periodontal disease. The findings of the present study validate this design objective and confirm the superior anti-inflammatory and periodontal bone preservation/regeneration capacity of the BIO loaded-PF127 hydrogel comparing to F127 hydrogel on experimental periodontitis rat model.

The binding experiment (Fig. 9a) showed that pyrophosphorolated hydrogels have stronger binding to HA discs than F127 hydrogel, confirming that PF127 hydrogel is a viable strategy for drug delivery to hard tissues. Interestingly, BIO's solubility in PF127 solution comparing to F127 was greatly improved and proportionally to the increase of the polymer concentration. This observation could be explained partly by the better aqueous solubility of PF127 polymers as a function of the PPi content. The cell viability data indicated that PF127 design retains the good biocompatibility of Pluronic F127 for 48 h(25) even after loading the drug. Similarly, it was shown that PF127 hydrogels with or without drug loading preserved the thermoresponsive properties of F127 hydrogels and were found to be dependent upon aqueous solubility of the polymer. As the temperature increases, solubility decreases and thus micelle formation is promoted, leading to the tangling of micelles' coronas and hence gel formation(46). It is noted that the 20% w/v PF127 exhibited low viscosity and formed weak hydrogel which might be due to the higher aqueous solubility of PF127 polymers, increasing the critical micellar concentration (CMC). *In vitro* release of BIO through the PF127 hydrogels and erosion profile was affected by the amount of polymer in the hydrogel. The viscosity of the hydrogel increases as a function of polymer concentration which ultimately reduces the drug release rate, diffusion coefficient,

and surface erosion process, indicating that BIO release was mainly driven by a combination of diffusion and concurrent hydrogel erosion. Though the relatively fast BIO release and gel erosion profile within 48 h might be disadvantageous for some applications where longer retention is desirable, its application for Wnt/β-catenin agonists delivery may be advantageous as it may help to prevent sustained activation of Wnt/β-catenin signaling, which is associated with oncogenic activities (17,18). Hence, PF127-BIO hydrogel seems to be an optimized and promising periodontal delivery system for such potent therapeutic agent (BIO) that would achieve the desired outcomes and avoid possible serious side effects associated with the inhibition of GSK3 and the overexpression of *β*-catenin. Taken together, these *in vitro* data confirm that comparing to F127 hydrogel, PF127 hydrogel has stronger ionic bonding and interaction with bone-like materials as well as higher drug loading (solubility) with similar biocompatibility, rheological, release and gel erosion profiles.

When evaluated *in vivo* using a ligature-induced periodontitis rat model, micro-CT analysis of alveolar bone showed that the PF127-BIO hydrogel treatment was the most effective treatment among all groups in preserving alveolar bone integrity (Fig. 11). It prevented alveolar crest loss and maintained bone volume (BV) when compared to all other groups. Also, in accordance with the micro-CT findings, the histological evaluation revealed superior osteogenic and anti-inflammatory effects of PF127-BIO hydrogel. It significantly increased β-catenin positive cell score and reduced inflammatory cell score when compared to all other groups. It also has a lower osteoclast score when compared to saline control (Fig. 12), suggesting

reduced erosion of the mineralized tissue within the periodontium. These observations could be attributed to the osteogenic(9,40,47) and anti-inflammatory effects of BIO(2,13,42,43), respectively. PF127 hydrogel itself did not show any significant protective effects against bone loss indicating that it did not contribute to preserving alveolar bone integrity. As an important consideration for the effect Wnt/β-catenin agonists, they may be drained into the circulation after the local release. Therefore, the femoral bone quality was analyzed to identify potential systemic osteogenic effects of BIO. All treatment groups did not show any significant changes in the femoral bone quality when compared to control, suggesting that the effect of BIO was locally restricted to periodontal tissues. In addition, we believe that the small localized doses of Wnt/β-catenin agonists used in animal studies are substantially lower than those used in clinical trials, indicative of a low potential to produce a systemic response(15)

Overall, the weekly administration of PF127-BIO hydrogel was found to be more effective in preventing periodontitis-induced alveolar bone loss when compared to F127-BIO hydrogel and free BIO treatments. We believe that after local administration, PF127-BIO hydrogel's interaction with periodontal hard tissues enhances the retention of the hydrogel, thus ensuring the gradual release of BIO at the desired site. This mechanism might provide a rational explanation of the superior therapeutic effect of PF127-BIO hydrogel than F127-BIO and dose equivalent free BIO in prevention of alveolar bone loss associated with periodontitis. Clinically, local treatment for periodontal bone loss should be given when periodontitis lesions are identified. Therefore, the treatment was initiated at

the time of ligature placement to make it more clinically relevant. Furthermore, the weekly administration schedule would be easily adapted into current clinical dental practice, indicative of a high clinical translation potential.

3.5 CONCLUSION

In this study, we report the development and preparation of a novel osteotropic thermosensitive hydrogel delivery system by conjugating pyrophosphates (PPi) to the chain termini of Pluronic F127. This hydrogel system not only enhanced drug loading but also exhibited affinity to hydroxyapatite (HA), with retained unique thermoresponsive properties of Pluronic F127. When tested on an experimental periodontitis rat model, PF127-BIO hydrogel was found to be effective in preserving periodontium tissues and preventing disease progression. As suggested by the results and upon further optimization, we believe this novel hydrogel as a local delivery system may have a great potential to be further developed into a novel clinical treatment of periodontal disease.

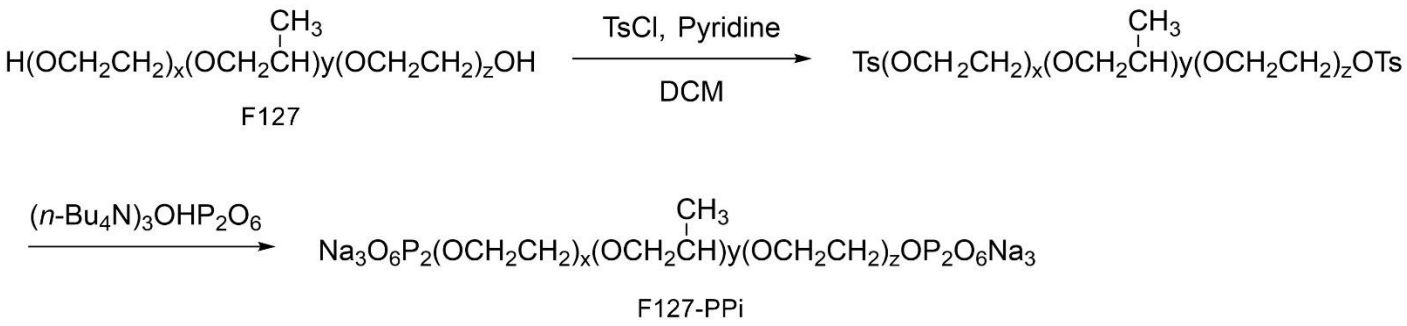

Scheme 2**.** The synthesis of Pyrophosphorolated Pluronic F127 (F127-PPi).

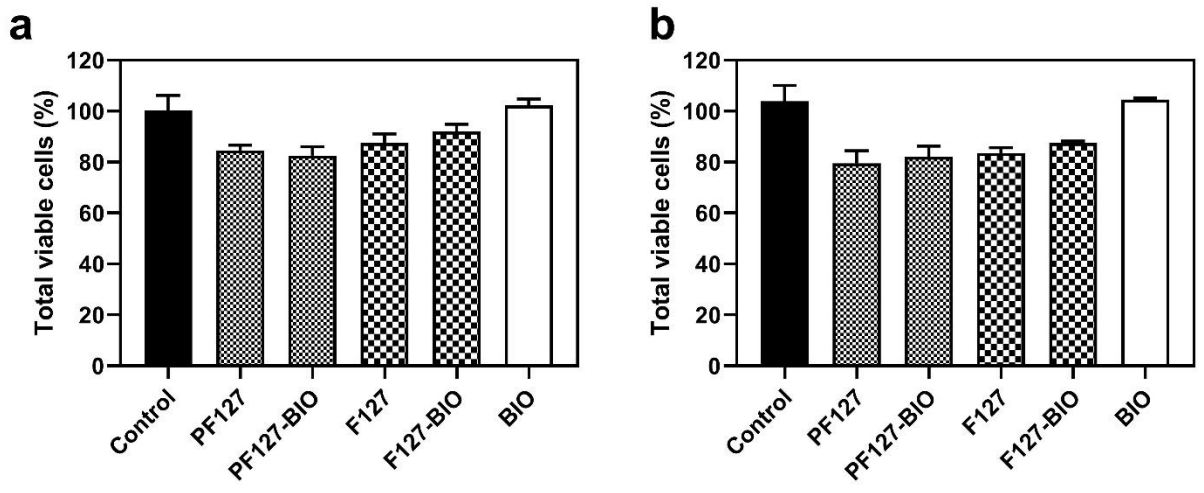

Figure 8. Effect of different treatments on growth of MC3T3-E1 cells measured by CCK-8 assay following (a) 24 and (b) 48-hour exposure. Data are shown as the mean ± SD.

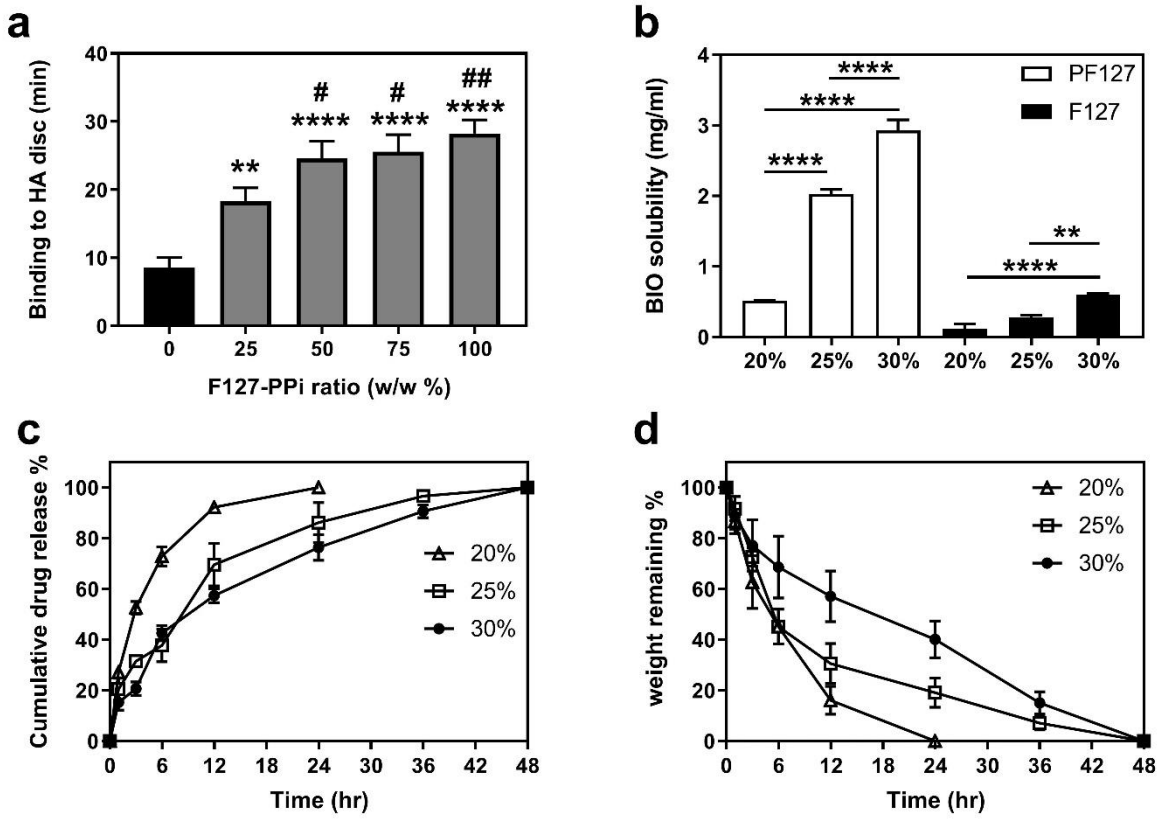

Figure 9. In vitro characterization of PF127 hydrogels. **(a)** Assessment of hydroxyapatite (HA) binding of 25% w/v PF127 hydrogels prepared with different ratios of F127-PPi and F127. $^{**}p< 0.01$, and $^{****}p<0.0001$ when compared to F127 hydrogel (ratio of 0); $^{\#}p<0.05$ and $^{\#\#}p< 0.01$ when compared to ratio of 25 (one-way ANOVA with Tukey's multiple comparisons). **(b)** Saturated solubility of BIO in PF127 vs F127 solutions at 4 °C. $^{**}p< 0.01$ and $^{****}p<0.0001$ (one-way ANOVA with Tukey's multiple comparisons). **(c)** Cumulative BIO release from PF127 hydrogels at 37 °C. **(d)** Erosion time of PF127 hydrogels incubated at 37 °C measured by weight remaining (%). Values are presented as the mean ± SD, n=3.

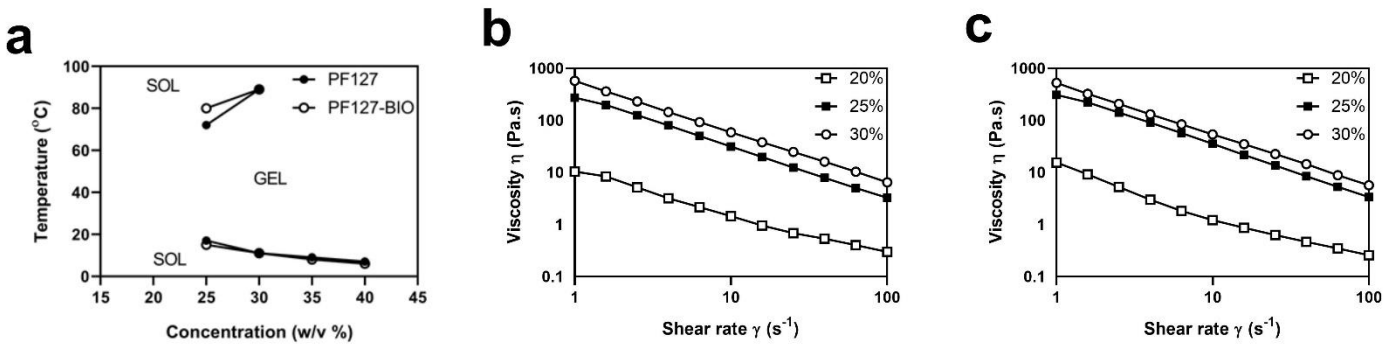

Figure 10. (a) Sol-gel-sol phase diagram for PF127 and PF127-BIO hydrogels. (b-c) The viscosity of (b) PF127 and (c) PF127-BIO hydrogels at different shear rate.

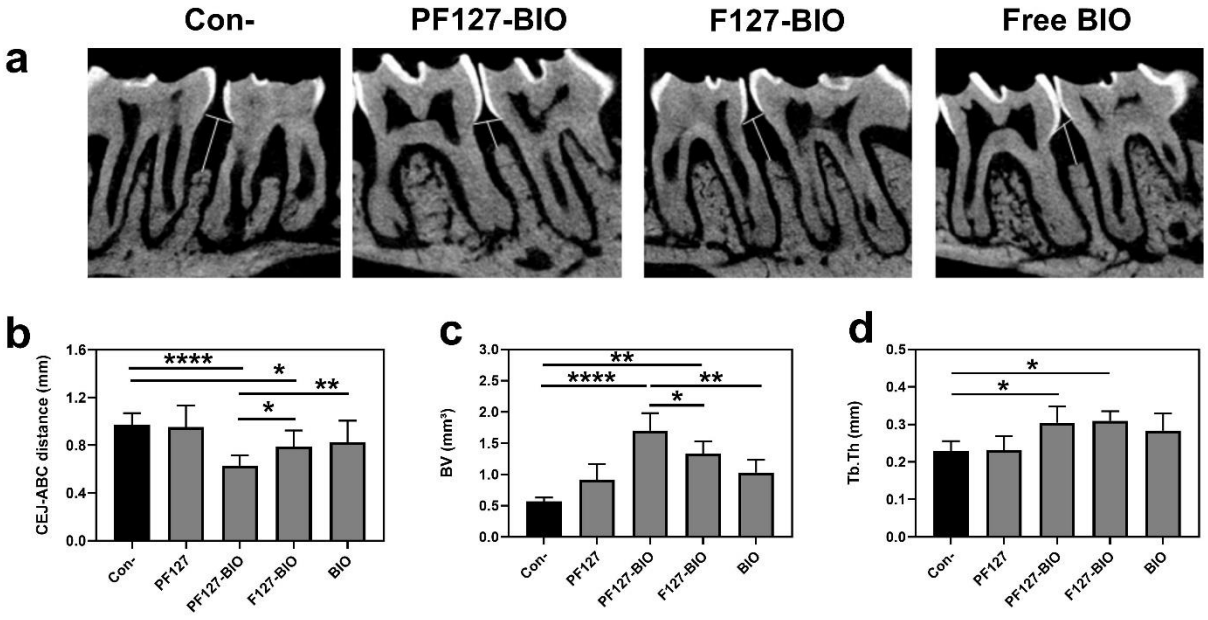

Figure 11. The in vivo evaluation of PF127-BIO hydrogel efficacy in an experimental periodontitis rat model. **(a)** Micro-CT sagittal images showing the effect of different treatments on the maxilla of cementoenamel junction (CEJ) to alveolar bone crest (ABC). White vertical lines indicate ABC-CEJ distance. **(b)** Measurement of the linear distance between CEJ and ABC. **(c-d)** Quantitative analysis of alveolar bone quality after different treatments. Bone volume (BV), trabecular thickness (Tb.Th). Values are presented as the mean ± SD. $^{*}p<0.05$, $^{**}p< 0.01$, and $^{****}p<0.0001$ (one-way ANOVA with Tukey's multiple comparisons).

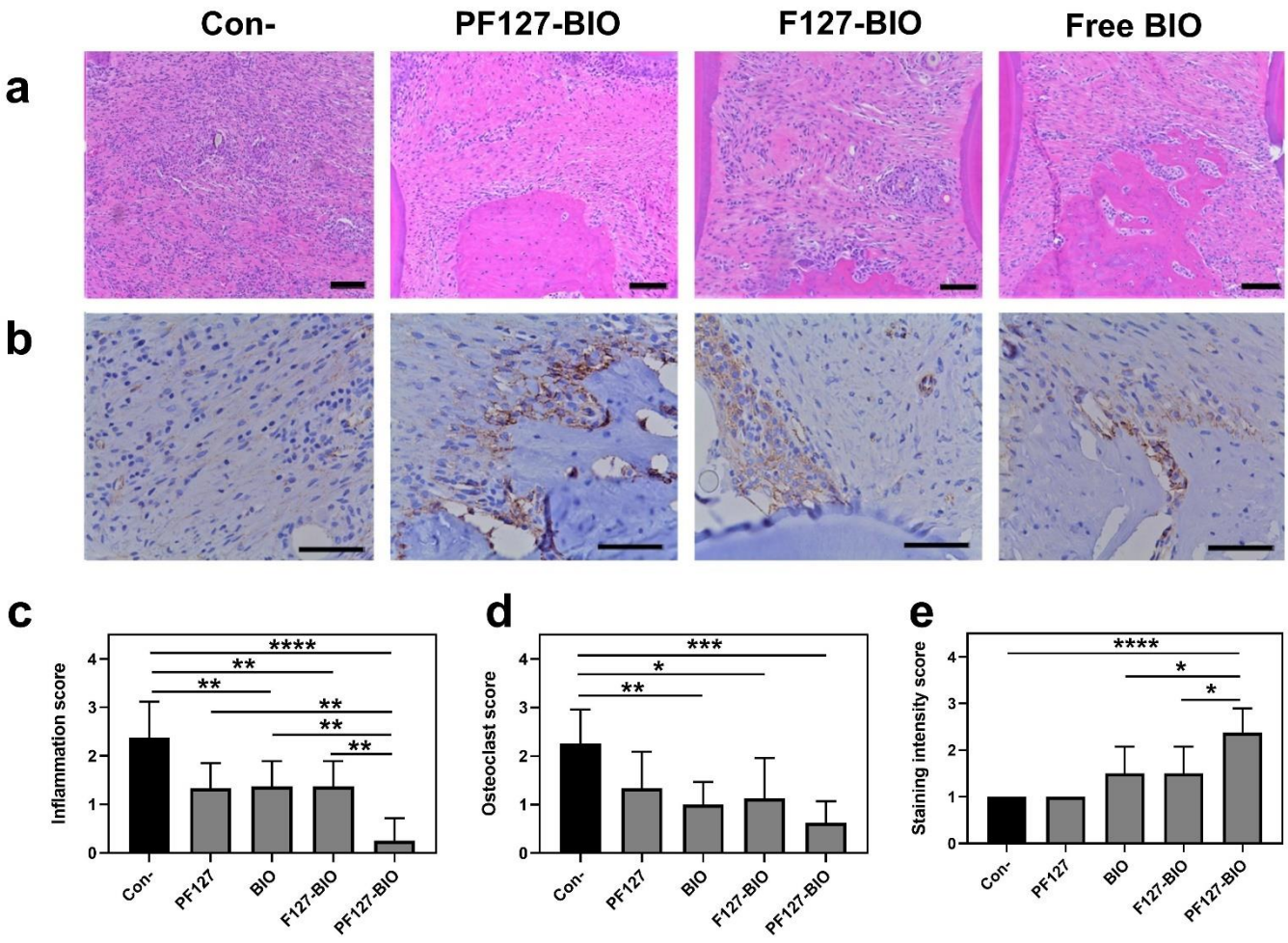

Figure 12. Histological analysis of papillary connective tissue and alveolar bone between first molar (M1) and second molar (M2) after 3 weeks of different treatments. **(a-b)** Representative images from different treatment groups of **(a)** H&E stained tissues and **(b)** IHC staining of β-catenin of connective tissue above the alveolar bone crest (ABC) and between first molar (M1) and second molar (M2). Scale bar = 100 μm. **(c-e)** Semi-quantitative assessment of **(c)** inflammatory cells, **(d)** osteoclasts, and **(e)** β-catenin positive cells interproximally between first molar (M1) and second molar (M2). Values are presented as the mean ± SD. $^{*}p<0.05$, $^{**}p<0.01$, $^{***}p<0.001$, and $^{****}p<0.0001$ (one-way ANOVA).

REFERENCE

1. Wang H, Brown J, Martin M. Glycogen synthase kinase 3: A point of convergence for the host inflammatory response. Cytokine. 2011.

2. Huang WC, Lin YS, Wang CY, Tsai CC, Tseng HC, Chen CL, et al. Glycogen synthase kinase-3 negatively regulates anti-inflammatory interleukin-10 for lipopolysaccharide-induced iNOS/NO biosynthesis and RANTES production in microglial cells. Immunology. 2009;128(1 PART 2):275–86.

3. Whittle BJR, Varga C, Pósa A, Molnár A, Collin M, Thiemermann C. Reduction of experimental colitis in the rat by inhibitors of glycogen synthase kinase-3β. Br J Pharmacol. 2006;147(5):575–82.

4. Arioka M, Takahashi-Yanaga F, Sasaki M, Yoshihara T, Morimoto S, Hirata M, et al. Acceleration of bone regeneration by local application of lithium: Wnt signal-mediated osteoblastogenesis and Wnt signal-independent suppression of osteoclastogenesis. Biochem Pharmacol. 2014;

5. Martinez A, Castro A, Dorronsoro I, Alonso M. Glycogen synthase kinase 3 (GSK-3) inhibitors as new promising drugs for diabetes, neurodegeneration, cancer, and inflammation. Medicinal Research Reviews. 2002.

6. Adamowicz K, Wang H, Jotwani R, Zeller I, Potempa J, Scott D a. Inhibition of GSK3 abolishes bacterial-induced periodontal bone loss in

mice. Mol Med. 2012;

7. Xie J, Méndez JD, Méndez-Valenzuela V, Aguilar-Hernández MM. Cellular signalling of the receptor for advanced glycation end products (RAGE). Cell Signal [Internet]. 2013 Nov [cited 2018 Apr 19];25(11):2185–97. Available from: http://www.ncbi.nlm.nih.gov/pubmed/23838007

8. Sanguineti R, Storace D, Monacelli F, Federici A, Odetti P. *Pentosidine Effects on Human Osteoblasts* in Vitro. Ann N Y Acad Sci [Internet]. 2008 Apr [cited 2018 Apr 19];1126(1):166–72. Available from: http://www.ncbi.nlm.nih.gov/pubmed/18448811

9. Wang F-S, Ko J-Y, Weng L-H, Yeh D-W, Ke H-J, Wu S-L. Inhibition of glycogen synthase kinase-3β attenuates glucocorticoid-induced bone loss. Life Sci [Internet]. 2009 Nov 4 [cited 2018 Apr 19];85(19–20):685–92. Available from: http://www.ncbi.nlm.nih.gov/pubmed/19782693

10. Krause U, Harris S, Green A, Ylostalo J, Zeitouni S, Lee N, et al. Pharmaceutical modulation of canonical Wnt signaling in multipotent stromal cells for improved osteoinductive therapy. Proc Natl Acad Sci U S A [Internet]. 2010 Mar 2 [cited 2018 Apr 19];107(9):4147–52. Available from: http://www.ncbi.nlm.nih.gov/pubmed/20150512

11. Fukuda T, Kokabu S, Ohte S, Sasanuma H, Kanomata K, Yoneyama K, et al. Canonical Wnts and BMPs cooperatively induce osteoblastic differentiation through a GSK3B-dependent and B-catenin-independent mechanism. Differentiation. 2010;

12. E. P, E. B, W. VH. Wnt signaling: A win for bone. Arch Biochem Biophys. 2008;

13. Kwon YJ, Yoon CH, Lee SW, Park YB, Lee SK, Park MC. Inhibition of glycogen synthase kinase-3β suppresses inflammatory responses in rheumatoid arthritis fibroblast-like synoviocytes and collagen-induced arthritis. Jt Bone Spine. 2014;

14. Jiang YY, Wen J, Gong C, Lin S, Zhang CX, Chen S, et al. BIO alleviated compressive mechanical force-mediated mandibular cartilage pathological changes through Wnt/β-catenin signaling activation. J Orthop Res. 2018;36(4):1228–37.

15. Neves VCM, Babb R, Chandrasekaran D, Sharpe PT. Promotion of natural tooth repair by small molecule GSK3 antagonists. Sci Rep [Internet]. 2017;7(September 2016):1–7. Available from: http://dx.doi.org/10.1038/srep39654

16. Takahashi-Yanaga F. Activator or inhibitor? GSK-3 as a new drug target. Biochem Pharmacol. 2013;86(2):191–9.

17. Kahn M. Can we safely target the WNT pathway? Nat Rev Drug Discov [Internet]. 2014 Jul 1 [cited 2019 Apr 4];13(7):513–32. Available from: http://www.ncbi.nlm.nih.gov/pubmed/24981364

18. Huang P, Yan R, Zhang X, Wang L, Ke X, Qu Y. Activating Wnt/β-catenin signaling pathway for disease therapy: Challenges and opportunities. Pharmacol Ther. 2018;

19. Giuliano E, Paolino D, Fresta M, Cosco D. Mucosal Applications of Poloxamer 407-Based Hydrogels: An Overview. Pharmaceutics. 2018;10(3):159.

20. Dumortier G, Grossiord JL, Agnely F, Chaumeil JC. A review of poloxamer 407 pharmaceutical and pharmacological characteristics. Pharmaceutical Research. 2006.

21. Fakhar-ud-Din, Khan GM. Development and characterisation of levosulpiride-loaded suppositories with improved bioavailability in vivo. Pharm Dev Technol. 2019;

22. Monti D, Burgalassi S, Rossato MS, Albertini B, Passerini N, Rodriguez L, et al. Poloxamer 407 microspheres for orotransmucosal drug delivery. Part II: In vitro/in vivo evaluation. Int J Pharm. 2010;

23. Rangabhatla ASL, Tantishaiyakul V, Boonrat O, Hirun N, Ouiyangkul P. Novel in situ mucoadhesive gels based on Pluronic F127 and xyloglucan containing metronidazole for treatment of periodontal disease. Iran Polym J (English Ed. 2017;26(11):851–9.

24. Akash MSH, Rehman K, Li N, Gao JQ, Sun H, Chen S. Sustained delivery of IL-1Ra from pluronic F127-based thermosensitive gel prolongs its therapeutic potentials. Pharm Res. 2012;29(12):3475–85.

25. Diniz IMA, Chen C, Xu X, Ansari S, Zadeh HH, Marques MM, et al. Pluronic F-127 hydrogel as a promising scaffold for encapsulation of dental-derived mesenchymal stem cells. J Mater Sci Mater Med.

2015;26(3):1–10.

26. Polychronopoulos P, Magiatis P, Skaltsounis AL, Myrianthopoulos V, Mikros E, Tarricone A, et al. Structural Basis for the Synthesis of Indirubins as Potent and Selective Inhibitors of Glycogen Synthase Kinase-3 and Cyclin-Dependent Kinases. J Med Chem. 2004;

27. Li Y, Cao J, Han S, Liang Y, Zhang T, Zhao H, et al. ECM based injectable thermo-sensitive hydrogel on the recovery of injured cartilage induced by osteoarthritis. Artif Cells, Nanomedicine Biotechnol [Internet]. 2018;46(sup2):152–60. Available from: https://doi.org/10.1080/21691401.2018.1452752

28. Ma X, He Z, Han F, Zhong Z, Chen L, Li B. Preparation of collagen/hydroxyapatite/alendronate hybrid hydrogels as potential scaffolds for bone regeneration. Colloids Surfaces B Biointerfaces [Internet]. 2016;143:81–7. Available from: http://dx.doi.org/10.1016/j.colsurfb.2016.03.025

29. Wang X, Jia Z, Almoshari Y, Lele SM, Reinhardt RA, Wang D. Local Application of Pyrophosphorylated Simvastatin Prevents Experimental Periodontitis. Pharm Res. 2018;

30. Gong CY, Shi S, Dong PW, Kan B, Gou ML, Wang XH, et al. Synthesis and characterization of PEG-PCL-PEG thermosensitive hydrogel. Int J Pharm. 2009;365(1–2):89–99.

31. Gong CY, Shi S, Dong PW, Zheng XL, Fu SZ, Guo G, et al. In vitro drug

release behavior from a novel thermosensitive composite hydrogel based on Pluronic f127 and poly(ethylene glycol)-poly(ε-caprolactone)-poly(ethylene glycol) copolymer. BMC Biotechnol. 2009;9:1–13.

32. Deshmukh M, Singh Y, Gunaseelan S, Gao D, Stein S, Sinko PJ. Biodegradable poly(ethylene glycol) hydrogels based on a self-elimination degradation mechanism. Biomaterials. 2010;

33. Bradley AD, Zhang Y, Jia Z, Zhao G, Wang X, Pranke L, et al. Effect of Simvastatin Prodrug on Experimental Periodontitis. J Periodontol [Internet]. 2016 May [cited 2017 Apr 2];87(5):577–82. Available from: http://www.ncbi.nlm.nih.gov/pubmed/26799395

34. Gregory CA, Gunn WG, Peister A, Prockop DJ. An Alizarin red-based assay of mineralization by adherent cells in culture: comparison with cetylpyridinium chloride extraction. Anal Biochem [Internet]. 2004 Jun 1 [cited 2017 Nov 16];329(1):77–84. Available from: http://linkinghub.elsevier.com/retrieve/pii/S0003269704001332

35. Jia Z, Wang X, Wei X, Zhao G, Foster KW, Qiu F, et al. Micelle-forming dexamethasone prodrug attenuates nephritis in lupus-prone mice without apparent glucocorticoid side effects. ACS Nano. 2018;

36. Gibson-Corley KN, Olivier AK, Meyerholz DK. Principles for Valid Histopathologic Scoring in Research. Vet Pathol [Internet]. 2013 Nov 4 [cited 2018 May 23];50(6):1007–15. Available from: http://www.ncbi.nlm.nih.gov/pubmed/23558974

37. Schett G, Stolina M, Bolon B, Middleton S, Adlam M, Brown H, et al. Analysis of the Kinetics of Osteoclastogenesis in Arthritic Rats. ARTHRITIS Rheum [Internet]. 2005 [cited 2018 May 25];52(10):3192–201. Available from: https://onlinelibrary.wiley.com/doi/pdf/10.1002/art.21343

38. Bolon B, Morony S, Cheng Y, Hu Y-L, Feige U. Osteoclast Numbers in Lewis Rats with Adjuvant-induced Arthritis: Identification of Preferred Sites and Parameters for Rapid Quantitative Analysis 1. Vet Pathol [Internet]. 2004 [cited 2018 May 25];41:30–6. Available from: http://journals.sagepub.com/doi/pdf/10.1354/vp.41-1-30

39. Song S, Ajani JA, Honjo S, Maru DM, Chen Q, Scott AW, et al. Hippo coactivator YAP1 upregulates SOX9 and endows esophageal Cancer cells with stem-like properties. Cancer Res. 2014;

40. Georgiou KR, King TJ, Scherer MA, Zhou H, Foster BK, Xian CJ. Attenuated Wnt/β-catenin signalling mediates methotrexate chemotherapy-induced bone loss and marrow adiposity in rats. Bone [Internet]. 2012 Jun [cited 2018 Apr 19];50(6):1223–33. Available from: http://www.ncbi.nlm.nih.gov/pubmed/22484100

41. Park DW, Jiang S, Liu Y, Siegal GP, Inoki K, Abraham E, et al. GSK3β-dependent inhibition of AMPK potentiates activation of neutrophils and macrophages and enhances severity of acute lung injury. Am J Physiol Cell Mol Physiol. 2014;307(10):L735–45.

42. Wang Y, Huang WC, Wang CY, Tsai CC, Chen CL, Chang YT, et al.

Inhibiting glycogen synthase kinase-3 reduces endotoxaemic acute renal failure by down-regulating inflammation and renal cell apoptosis. Br J Pharmacol. 2009;157(6):1004–13.

43. Klamer G, Shen S, Song E, Rice AM, Knight R, Lindeman R, et al. GSK3 inhibition prevents lethal GVHD in mice. Exp Hematol [Internet]. 2013;41(1):39–55.e10. Available from: http://dx.doi.org/10.1016/j.exphem.2012.09.005

44. Bai X, Gao M, Syed S, Zhuang J, Xu X, Zhang XQ. Bioactive hydrogels for bone regeneration. Bioact Mater. 2018;3(4):401–17.

45. Chen F, Jia Z, Rice KC, Reinhardt RA, Bayles KW, Wang D. The development of dentotropic micelles with biodegradable tooth-binding moieties. Pharm Res. 2013;30(11):2808–17.

46. Callan M, 1 J, Kelly J, Nguyen K, Marmorat C, Rafailovich M. Characterization of Pluronic F127 for the Controlled Drug Release Vancomycin in the Spinal Column. Available from: https://cpb-us-e1.wpmucdn.com/you.stonybrook.edu/dist/f/2071/files/2017/04/1-Kim-F127-Pg-9-19-y289nt.pdf

47. Low SA, Galliford C V., Yang J, Low PS, Kopeček J. Biodistribution of Fracture-Targeted GSK3β Inhibitor-Loaded Micelles for Improved Fracture Healing. Biomacromolecules. 2015;

Chapter 4.

Summary

Periodontal disease is a prevalent and chronic inflammatory disease that affects the supporting structures of the teeth including gingiva, periodontal ligament, and alveolar bone resulting in pocket formation, mobility, bone loss, and eventually may lead to tooth loss. In addition to direct bacterial degradation of periodontal tissue, the host immune response, which aims at protecting host tissues from bacterial aggression, also acts as a mediator of the periodontal damage(1). Current treatment strategies are aimed at reducing bacterial load by mechanical therapy and administration of antimicrobial agents(2,3). Additionally, host modulation agents have been utilized to ameliorate host response and reduce disease progression(4,5). However, these agents usually are given orally with large doses, causing antibiotic resistance, adverse drug reaction, and side effects, and subsequently reducing patient compliance(6,7). Additionally, oral drugs distribute to other organs of the body that may reduce drug concentration inside periodontal pocket(8). Alternatively, due to the nature of the local periodontal defect, local drug delivery in the form of intra-pocket administration prove to be more promising than oral administration(7,9). With local delivery strategies, a high concentration of drug inside the periodontal pocket can be attained with reduced systemic distribution, thereby minimizing side effects. However, rapid drug

clearance from the periodontal pocket requires repeated dosing which could reduce patient compliance.

In Chapter 1, we have reviewed and discussed the local drug delivery systems that have been developed for periodontal disease. These local systems have been successful and shown positive outcomes in many clinical studies in terms of overall periodontal health. However, most of the currently available formulations, which focused only on delivering anti-microbial agents, suffer from several limitations including lack of interaction or bonding with periodontal tissues, need for removal of non-biodegradable delivery systems, lack of penetration into deeper regions of periodontal pocket and poor patient compliance, indicative of a low clinical translation potential and also highlighting the urgent need for the development of effective drug delivery systems that can preserve periodontal tissues.

In Chapter 2, we developed a novel osteotropic simvastatin (SIM) prodrug by conjugating SIM trimer to a pyrophosphate (PPi). This prodrug design has enhanced SIM's solubility and exhibited strong affinity to hydroxyapatite (HA). Also, this prodrug retained bone anabolic and anti-inflammatory properties of SIM. When tested on an experimental periodontitis rat model, SIM-PPi was found to be more effective than free SIM in ameliorating inflammation and preserving periodontal bone. We believe this prodrug would be easily adapted into clinical practice.

In Chapter 3, in an attempt to avoid the complexity of chemical syntheses, we reported and discussed another strategy of local drug delivery for periodontal disease. A novel osteotropic thermosensitive hydrogel delivery system was developed, utilizing unique properties of Pluronic F127. Pyrophosphates (PPi) were conjugated to the chain termini of Pluronic F127. This hydrogel system (PF127) not only enhanced drug loading but also exhibited affinity to hydroxyapatite (HA), with retained unique properties of Pluronic F127. A GSK3 inhibitor (BIO) was used as a drug model that has anti-inflammatory and osteogenic effects. When tested on an experimental periodontitis rat model, PF127-BIO hydrogel was found to be effective in preserving periodontium and preventing disease progression.

In conclusion, these two novel delivery strategies (SIM-PPi prodrug and PF127 hydrogel) were shown to address some of the limitations associated with current local delivery systems for periodontal disease, indicating that they may have the potential to be further developed for better clinical management of periodontitis.

Future studies

1. Evaluate the therapeutic efficacy on diabetic background, as the risk of periodontal disease is increased by approximately threefold in diabetic individuals compared with non-diabetic individuals.
2. Smoking is another major risk factor associated with the severity of periodontitis. Hence, establishing a successful animal model would be of great interest.
3. Several natural products have been identified and studied in the treatment of periodontal disease. PF127 hydrogel could be utilized to address their limitations and augment their therapeutic benefits.

References

1. Pihlstrom BL, Michalowicz BS, Johnson NW. Periodontal diseases. Lancet [Internet]. 2005 Nov 19 [cited 2017 Nov 6];366(9499):1809–20. Available from: http://www.ncbi.nlm.nih.gov/pubmed/16298220

2. Herrera D, Sanz M, Jepsen S, Needleman I, Roldán S. A systematic review on the effect of systemic antimicrobials as an adjunct to scaling and root planing in periodontitis patients. J Clin Periodontol [Internet]. 2002 [cited 2017 Aug 23];29 Suppl 3:136-59; discussion 160-2. Available from: http://www.ncbi.nlm.nih.gov/pubmed/12787214

3. Greenstein G. Local drug delivery in the treatment of periodontal diseases: assessing the clinical significance of the results. J Periodontol [Internet]. 2006 Apr [cited 2017 Aug 23];77(4):565–78. Available from: http://www.joponline.org/doi/10.1902/jop.2006.050140

4. Williams RC, Jeffcoat MK, Howell TH, Reddy MS, Johnson HG, Hall CM, et al. Ibuprofen: An inhibitor of alveolar bone resorption in beagles. J Periodontal Res [Internet]. Blackwell Publishing Ltd; 1988 Jul 1 [cited 2017 Aug 23];23(4):225–9. Available from: http://doi.wiley.com/10.1111/j.1600-0765.1988.tb01363.x

5. Raja S, Byakod G, Pudakalkatti P. Growth factors in periodontal regeneration. Int J Dent Hyg [Internet]. 2009 May [cited 2017 Aug 23];7(2):82–9. Available from:

http://www.ncbi.nlm.nih.gov/pubmed/19413545

6. Walker CB. Selected antimicrobial agents: Mechanisms of action, side effects and drug interactions. Periodontol 2000. 1996;

7. Southard GL, Godowski KC. Subgingival controlled release of antimicrobial agents in the treatment of periodontal disease. Int J Antimicrob Agents. 1998;

8. Goodson JM. Antimicrobial strategies for treatment of periodontal diseases. Periodontol 2000. 1994;

9. Schwach-Abdellaoui K, Vivien-Castioni N, Gurny R. Local delivery of antimicrobial agents for the treatment of periodontal diseases. European Journal of Pharmaceutics and Biopharmaceutics. 2000.